Investigation into the mode of action of the antimicrobial peptide Os on *Candida albicans* (ATCC 90028) biofilm formation

by
Savannah Jade Watson
14004641

Submitted in partial fulfilment of the degree:
MSc Biochemistry

In the Faculty of Natural and Agricultural Sciences
Department of Biochemistry
University of Pretoria
South Africa

Supervisor: Prof ARM Gaspar (Department of Biochemistry, Genetics and Microbiology)
Co-supervisor: Prof MJ Bester (Department of Anatomy)
Co-supervisor: Dr H Taute (Department of Anatomy)

2019

DECLARATION

Submission declaration:

I, Savannah Jade Watson declare that the dissertation, which I hereby submit for the degree MSc Biochemistry at the University of Pretoria, is my own work and has not previously been submitted by me for a degree at this or any other tertiary institution.

3/12/2019

…… ……

SIGNATURE DATE

Plagiarism declaration:

UNIVERSITY OF PRETORIA

FACULTY OF NATURAL AND AGRICULTURAL SCIENCES

DEPARTMENT OF BIOCHEMISTRY

Full name: Savannah Jade Watson Student number: 14004641

Title of the work: Mode of action of the antimicrobial peptide Os on *Candida albicans* (ATCC 90028) biofilm formation

Declaration:

1. I understand what plagiarism is and am aware of the University's policy in this regard.
2. I declare that this **dissertation** is my own original work. Where other people's work has been used (either from a printed source, Internet or any other source), this has been properly acknowledged and referenced in accordance with departmental requirements.
3. I have not used work previously produced by another student or any other person to hand in as my own.
4. I have not allowed, and will not allow, anyone to copy my work with the intention of passing it off as his or her own work.

SIGNIATURE: DATE: 3/12/2019

ACKNOWLEDGEMENTS

Firstly I want to thank God for the life that I have and the opportunities that He has given me. “Whatever you do, do everything for the glory of God”. Throughout this project, I am thankful that He has put the following people in my path:

- My supervisor, Prof A.R.M Gaspar and my co-supervisor Prof M.J Bester, for their continual support and guidance, and for all the encouragement over the years. Thank you for all your words of wisdom and dedication you gave to me and my work.

- My co-supervisor, Dr Helena Taute, for always being willing to help and provide assistance when needed. Thank you for spending countless hours sitting with me in the microscopy unit and still having the patience to answer all of my questions. I truly value your support.

- Dr June Serem, for always lending an ear when I had a question and for having the patience to explain concepts until I understood them. You provided me with more support than was required, for which I am truly grateful.

- Rebecca Mbuayama, for all the long hours spent with me in the laboratory. You taught me to have confidence and courage when it came to research and to relentlessly never stop seeking answers. Thank you for making my MSc memorable. I will always remember what you have taught me and I will never forget the passion for science that I developed alongside you.

- Members of the group; for all the support and motivation. Thank you for all the long hours we have spent in meetings discussing my results and for giving me advice and guidance. Thank you for all the laughs and memories we have made along the way. I am proud to be a part of this research group.

- Callan Moore, for your endless love and support. Thank you for all your patience, and encouragement. I am so grateful to have had you along for this journey. To my number one fan. I love you.

- Lastly, I want to thank my mother, Tammy Watson. Thank you for all that you have sacrificed for me to be where I am today. None of this would have been possible if it were not for you. Thank you for all the support, motivation, encouragement, and love you have given me. Thank you for supporting my dreams and for driving me to accomplish them. “PHIL 4:13”.

SUMMARY

Antimicrobial resistance is one of the biggest risks to global health, with an increasing number of infections becoming harder to treat. These include fungal infections, especially *Candida albicans* biofilms. Fungal biofilms are microbial communities composed of various cell types, bound to a substrate surface that produces a protective extracellular matrix, which makes treatment challenging. Increasing resistance, and the lag in the development of novel antifungal agents, has created a need for novel and alternative anti-mycotic agents, of which antifungal peptides (AFPs) show promise. In a preliminary study, Os, a tick derived AFP was shown to possess anti-biofilm activity against *C. albicans*. In this study, the ability of the antimicrobial peptide Os to inhibit biofilm formation was further investigated and its mode of action was explored, and compared to a shorter, amidated analogue of Os, Os(11-22)NH_2, which previously has been shown to inhibit planktonic *C. albicans* cells and biofilms.

Os displayed no antifungal activity against planktonic *C. albicans* cells at the tested concentrations (0.78 µM to 100 µM) in RPMI-1640. In a 24h established *C. albicans* biofilm, Os exhibited a 50% biofilm inhibitory concentration (BIC_{50}) value of 46 µM, which was approximately 2 fold better than reported for Os(11-22)NH_2. At the BIC_{50}, the mode of action was further investigated. Inverted light microscopy of crystal violet stained Os treated biofilms indicated that Os targets the growth and development of adhered yeast cells. Using the dichloro-dihydro-fluorescein diacetate assay, it was determined that treatment of *C. albicans* biofilms with Os induced reactive oxygen species (ROS) formation. However, the addition of the antioxidant ascorbic acid (AA) significantly ($p < 0.0001$) decreased the presence of endogenous ROS in treated cells, but this did not lead to a decrease in the biofilm inhibitiory activity of Os. Instead, addition of AA significantly ($p < 0.05$) enhanced the activity of Os. In contrast to Os(11-22)NH_2, Os did not disrupt membrane structure, evaluated using propidium iodide staining. Using 5FAM-labelled Os and confocal laser scanning microscopy, Os was located to the plasma membrane or cell wall, bound to intracellular structures and accumulated in the cytoplasm. The effects of Os on the ultrastructure of yeast, pseudohyphae and hyphae in *C. albicans* biofilms was evaluated with scanning electron microscopy. Os caused cell shrinkage in yeast and pseudohyphal cells, as well as cell wall or plasma membrane cracks/tears in yeast and hyphal cells. The formation of pits was also observed in pseduohyphal cells. Surface protuberances were apparent on the surface of Os treated hyphal cells.

In conclusion, although Os negatively affects the structures of the various cell types found within a *C. albicans* biofilm by associating with membranes and translocation into cells, its biofilm inhibitory activity is not due to membrane permeabilisation or endogenous ROS production. More investigation into the mode of action of this peptide is required.

LIST OF ABBREVIATIONS

A	
AA	Ascorbic acid
ABC	ATP-binding cassette
Abs	Absorbance
AFP(s)	Antifungal peptides(s)
Als3	Agglutin-like sequence 3
AmpB	Amphotericin B
AMP(s)	Antimicrobial peptides(s)
ANOVA	One-way analysis of variance
APD	Antimicrobial Peptide Database
ATCC	American Type Culture Collection
ATP	Adenosine triphosphate
Au	Gold
AuNP(s)	Gold nanoparticle(s)
AVC	Apical vesicle cluster
B	
BIC_{50}	Biofilm inhibitory concentration at 50%
BSE	Back-scattered electrons
C	
c	Concentration
CA	Citric acid
CAS	Caspofungin
CFU/mL	Colony-forming units per mL
CLSM	Confocal laser scanning microscopy
CPP	Cell penetrating peptide
CRAMP	Cathelicidin-related antimicrobial peptide
CTB	CellTiter-Blue
CV	Crystal violet
CYP51A1	Cytochrome p-450 lanosterol 14α-demethylase
D	
DAPI	4’,6’-Diamidino-2-phenylindole
DCFH-DA	2’,7’-Dichlorodihydrofluorescein diacetate
DCFH	2’,7’-Dichlorodihydrofluorescein
DCF	2’,7’-Dichlorofluorescein
ddH_2O	Double distilled water
df	Dilution factor
dsDNA	Double stranded DNA
DMSO	Dimethyl sulfoxide
E	
ε	Extinction coefficient
ECM	Extracellular matrix
EUCAST	European Committee on Antimicrobial Susceptibility Testing
F	
5FAM	5-Carboxyfluorescein
FEG	Field emission gun

G

g	Gravity
GI	Gastrointestinal
Glc	Glucose
GlcCer	Glucosylceramide
GPL(s)	Glycerphospholipid(s)
GSL(s)	Glycosphingolipid(s)

H

h	Hours
HMDS	Hexamethyl disilazane
Hwp1	Hyphal wall protein 1

M

M	Molar
MDR	Multi-drug resistance
MF	Major facilitator
MIC	Minimum inhibitory concentration
MIC_{50}	Minimum inhibitory concentration at 50%
$M(IP_2)C$	Manosyldiinositol phosphorylceramide
mM	Millimolar
MOPS	Morpholinopropanesulfonic acid
MRSA	Methicillin resistant *Staphylococcus aureus*
MS	Mass spectrometry
MW	Molecular weight

N

NA	No activity
NaPB	Sodium phosphate buffer
NIH	National Institute of Health
nm	Nanometer
NP(s)	Nanoparticles(s)

O

OD	Optical density
OD_{280}	Optical density at 280 nm
OD_{530}	Optical density at 530 nm
OD_{620}	Optical density at 620 nm
OsDef2	*Ornithodoros savignyi* defensin isoform 2

P

PA	Phosphatidic acid
PBS	Phosphate buffered saline
PC	Phosphatidylcholine
PDB	Protein Data Bank
PG	Phosphatidylglycerol
PI	Phosphatidylinositol
PI	Propidium iodide
$(PI(4,5)P_2)$	Phosphatidylinositol (4,5)-bisphosphate
PIA	Polysaccharide-intercellular-adhesion
PS	Phosphatidylserine

R

RP-HPLC	Reversed-Phase High Performance Liquid Chromatography
RPMI-1640	Roswell Park Memorial Institute-1640
Rs	*Raphanus sativus*

S

s	Seconds
SA	South Africa
SE	Secondary electrons
SEM	Scanning electron microscopy
SEM	Standard error of the mean
SOD	Superoxide dismutase

T

TEM	Transmission electron microscopy
TLR	Toll-like receptor
Trp	Tryptophan
Tyr	Tyrosine

U

µL	Microlitre
µm	Micrometer
µM	Micromolar
Uv-vis	Ultraviolet-visible

W

WHO	World Health Organisation

Y

YPD	Yeast Peptone Dextrose

TABLE OF CONTENTS

LIST OF FIGURES

LIST OF TABLES

CHAPTER 1: Literature Review

1.1 Introduction

Invasive fungal infections are an important contributor to morbidity and mortality worldwide (De Pauw *et al.*, 2008). Fungal infections are capable of forming complex microbial communities embedded within an extracellular matrix (ECM), commonly known as biofilms. *Candida* biofilms may occur on mucosal surfaces as well as on indwelling medical devices. Moreover, *Candida* biofilms on medical devices have the potential to initiate candidemia infections which may lead to invasive systemic infections (Nobile & Johnson, 2015). As such, fungal biofilms play a pivotal role in clinical infections. A certain study indicated a mortality rate of 40% of catheter associated candidemia (Fesharaki *et al.*, 2018). Furthermore, 40% of hospital patients with biofilm infected intravenous catheters, developed occult fungemia with consequences such as severe sepsis and death (Nguyen *et al.*, 1995). In the United States alone, biofilm infections occur in more than 50% of the 5 million central venous catheters that are placed (Fox & Nobile, 2013), leading to approximately 10 000 deaths annually (Nobile & Johnson, 2015). Moreover, more than 3 million US dollars has been spent on biofilm related infections. The degree to which *Candida* biofilms infect indwelling medical devices, requires their removal as the current standard of treatment (Chandra *et al.*, 2001). Removal may require surgery and is often accompanied by treatment with high concentrations of antifungal agents (Coste, 2015), posing even more danger to the patient. Hospitalised immune compromised patients, including those with cancer, HIV and neonates with immature immune systems are more vulnerable. *Candida* species are among the main cause of hospital-acquired infections (Sardi *et al.*, 2013b).

Hospital-acquired infections are 75% more prevalent in developing countries, (Obiero *et al.*, 2015). According to the World Health Organisation (WHO), in Sub-Saharan Africa, more than 40% of hospitalisations resulted in hospital-acquired infections. Immune-compromised patients, living with HIV which, according to Statistics South Africa, are 6.9 million people in 2015, are at high risk of contracting invasive fungal infections, especially those that are hospital patients (Schwartz *et al.*, 2019). Antibiotic resistance is an important contributor to the susceptibility of invasive fungal infections. The overuse of broad-spectrum antibiotics and antifungal agents has contributed to developing resistance in once susceptible fungi (Srinivasan *et al.*, 2014). There are more than 150 *Candida* species, and a total of 95% of infections are caused by 5 different *Candida* species (Pfaller & Diekema, 2007). *C. albicans* species is the most commonly isolated species, from the oral cavities of HIV and cancer patients, with a frequency of 73% and 45%, respectively (Owotade *et al.*, 2013).

There is a limited number of antifungal agents to treat *C. albicans* infections, especially with the emergence of drug resistance, where the yeast has developed resistance to more than 1 class of antifungal agent (Matejuk *et al.*, 2010). This increased antifungal resistance and the lag in the development of new antimicrobial agents, has created a need for the development of novel antifungal

agents. Antimicrobial peptides (AMPs) which serve as a source of novel antifungal agents may be the solution (Matejuk *et al.*, 2010).

1.2 *Candida albicans* infections

Fungi are members of eukaryotic organisms, and include yeasts, moulds and mushrooms under the kingdom fungi. Features shared with animal eukaryotic organisms include membrane bound nuclei containing chromosomes, membrane bound cytoplasmic organelles, 80 S ribosomes, and membranes that contain sterols. Features shared with plant eukaryotic organisms include a cell wall and vacuoles to name a few. Fungi display unique characteristics that distinguish them from other eukaryotic plants and animals, including their cell wall which contains glucans and chitin, making fungi the only organisms to combine these components within their cell walls (Munro, 2013).

Yeasts are unicellular organisms that reproduce asexually by mitosis. Asexual reproduction mostly occurs through the development of an outgrowth, due to the asymmetric division at a particular site of the yeast cell in a process known as budding. In contrast, moulds grow to form multicellular filaments known as hyphae (Riquelme *et al.*, 2018). Fungi that are capable of switching between the yeast and hyphal stage are known as dimorphic fungi (Jacobsen *et al.*, 2012), and *C. albicans* is an example of such a fungus.

C. albicans forms part of the normal human microbiota within the gastrointestinal (GI) tract, oral cavity and mucosal surfaces of its host (Nobile & Johnson, 2015). In a healthy individual, *C. albicans* is harmless, and forms a commensal with its host and exists compatibly with other members of the human microbiota. Changes to the local environment, such as the use of antibiotics as well as alterations to the immune system lead to the rapid growth of *C. albicans* (Douglas, 2003), resulting in candidiasis (Abbott, 1995). Systemic infections can lead to candidemia, and these invasive infections are more severe, and may affect the bloodstream and central nervous system (Laupland *et al.*, 2005). The incidence of invasive infections due to *C. albicans* has increased over the past 50 years (Hobson, 2003).

1.3 Fungal biofilms and their development

Biofilms are the most common and natural state of growth of the majority of microorganisms (Nobile & Johnson, 2015). Biofilm formation occurs on both biotic (plant and mammalian tissue, aquatic habitats) and abiotic (medical devices) environments. Some species form biofilms on solid surfaces, including *Candida sp*, *Streptococcus sp*, and *Staphylococcus sp*, whereas other species form biofilms at the air-liquid interface, including *Mycobacterium sp*, and *Bacillus sp* (Hall-Stoodley *et al.*, 2004). According to the National Institute of Health (NIH), pathogenic biofilms are responsible for more than 80% of all microbial infections (Nobile & Johnson, 2015). Biofilms pose a serious threat in clinical settings. The standard of treatment for biofilm infected medical devices is the removal of the device (Perlin, 2015),

which is very costly and is often performed with surgery, and is usually accompanied with the administration of high doses of antifungal agents. However, some patients are too critical to withstand surgery and the high doses of medication are accompanied with toxic side effects, and pose a threat to the kidneys and liver (Andes *et al.*, 2012).

Candida biofilms can be found on mucosal surfaces, including oral and vaginal epithelia (Gulati & Nobile, 2016), as well as on indwelling medical devices, including catheters (urinary and central venous), dental implants, prosthetics, lenses, and heart valves (Chandra *et al.*, 2001). *C. albicans* biofilms are highly structured, and contain various cell types (Chandra *et al.*, 2001), including round yeast, oval pseudohyphal and elongated hyphal cells, all of which are required for biofilm formation (Finkel & Mitchell, 2011).

Biofilm formation involves 3 developmental phases, involving intricate and sequential growth practices, each of which are identified by an increase in cellular metabolic activity (Ramage *et al.*, 2005). *C. albicans* biofilms are bi-layered, with the bottom layer comprising of tightly attached round yeast cells and the upper layer containing the various hyphal cells. Fungal biofilm development (Figure 1.1) begins with the adherence of round yeast cells to a substrate surface, to form the basal layer of anchoring cells (Gulati & Nobile, 2016) (Figure 1.1 A). The adhered cells display characteristics distinct from planktonic cells, including increased adherence properties, with increased potential to form biofilms (Gulati & Nobile, 2016). This step is crucial for normal biofilm development. The high surface hydrophobicity of *C. albicans*, allows this yeast to attach to virtually any surface. The next stage involves the proliferation of round yeast cells over the substrate surface, as well as the early filamentation of the attached cells (Figure 1.1 B). Lastly, biofilm maturation involves the formation of composite layers of hyphal and round yeast cells, as well as the accumulation of the ECM (Gulati & Nobile, 2016) (Figure 1.1 C). Round yeast cells within the matrix may detach from the biofilm and colonise other areas (Landini *et al.*, 2010) (Figure 1.1 D). *In vitro* investigations indicate that round yeast cells are dispersed throughout biofilm formation (Uppuluri *et al.*, 2010).

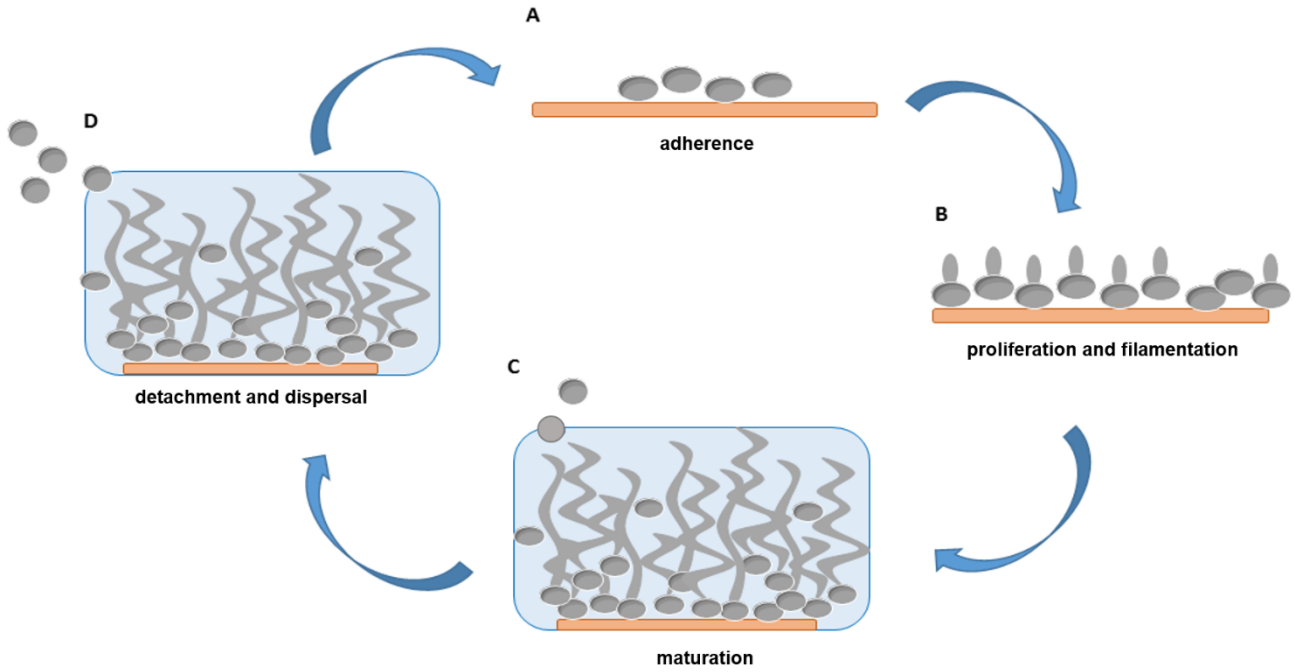

Figure 1.1: Schematic representation of the sequential process of biofilm formation (A) Round yeast cells adhere to the substrate surface **(B)**. The attached round yeast cells proliferate and begin the filamentation process **(C)**. Maturation of the biofilm involves the progression of some cells into the hyphal/filamentous form, as well as the accumulation of the matrix components, to form the ECM **(D)**. Round yeast cells may become detached from the biofilm and disperse to other areas to re-initiate biofilm formation. Redrawn and adapted from Li and Wang (2011).

The ECM has a dynamic composition, which may be affected by changes in environmental conditions (Pierce *et al.*, 2017). However, the overall composition and relative abundance of the dry weight of each component of the matrix includes proteins (55%), carbohydrates (25%), nucleic acids (5%), and lipids (15%), respectively (Zarnowski *et al.*, 2014). This ECM is highly hydrated and self-produced (Sandai *et al.*, 2016). The ECM usually also contains external particulates such as lysed *C. albicans* and host cells including erythrocytes, neutrophils, epithelial and urothelial cells (Nett *et al.*, 2015). Water channels between cells within the biofilm, assist in the diffusion of nutrients from the environment to the anchoring basal cells, and allows for the removal of waste from the biofilm (Ramage *et al.*, 2005).

1.4 Antifungal drugs for the treatment of *C. albicans* biofilm infections

There is a limited number of antifungal drugs available for the treatment of *C. albicans* infections and these drugs target either the cell wall (biosynthesis pathways), plasma membrane (membrane sterols), or various intracellular compartments and molecules (Figure 1.2).

The most abundant polysaccharides in the cell wall are the glucose containing polysaccharides, β-glucans, including β-(1,3)-glucans as well as β-(1,6)-glucans. These polysaccharides provide osmotic stability and are important for cell growth and division (Groll & Walsh, 2001). Elongated mannoproteins (mannose containing proteins), also occur in the cell wall (Varki *et al.*, 2009). These proteins are a

diverse group of proteins, and include structural and cell adhesion proteins, as well as enzymes responsible for cell wall synthesis. As mannoproteins are unique to fungi, they are ideal drug targets. Chitin, a polymer of N-acetylglucosamine in the cell wall, provides rigidity. Although chitin is not as abundant as β-glucans or mannoproteins, it plays a vital role in cell budding and septum formation. Disruption of chitin may lead to a loss of membrane integrity and morphological defects, as well as an indirect intracellular effect on the actin skeleton. The plasma membrane is composed of a lipid bilayer, and the sterol ergosterol, which provides fluidity and support to the cell (Nes, 1974). Ergosterol also has a hormone-like function, which prompts cellular growth and proliferation (Georgopapadakou & Walsh, 1996).

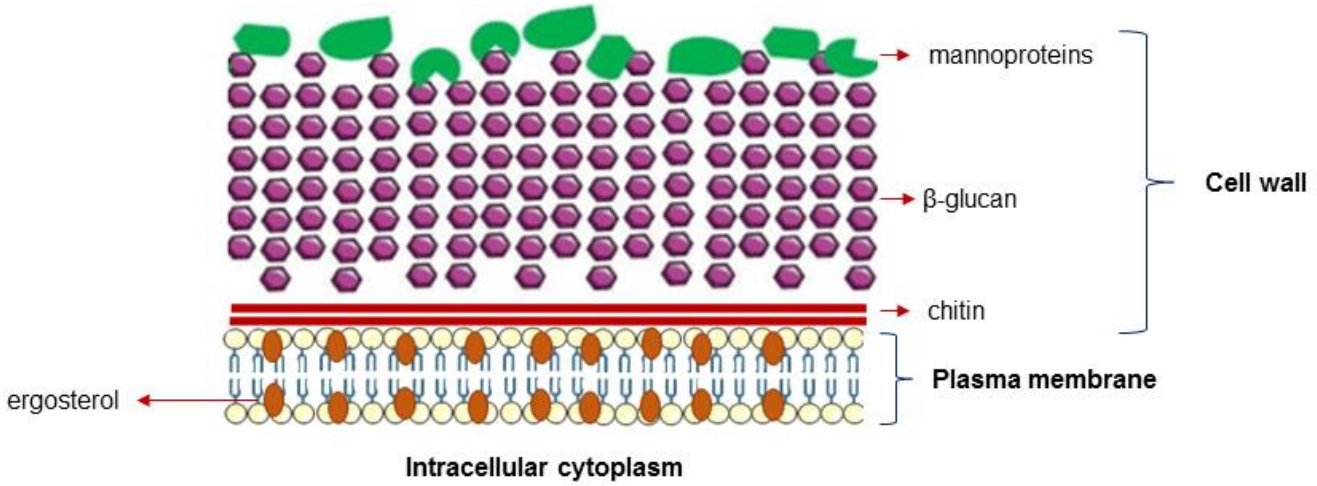

Figure 1.2: Schematic representation of the three main compartments of fungi. The outer cell wall contains mannoproteins, β-glucans, and chitin. The plasma membrane is made up of a lipid bilayer containing various lipids, including the sterol ergosterol. The intracellular cytoplasm contains various membrane bound organelles. Redrawn and adapted from Fesel and Zuccaro (2016).

The 3 main chemical classes of antifungal drugs are the polyenes which interact with sterols in the membrane, the azoles which inhibit the biosynthesis of membrane sterols, and the echinocandins which inhibit the biosynthesis of cell wall components (Figure 1.3).

Polyenes are named after their alternating conjugated bonds associated with their macrolide ring structure (Dixon & Walsh, 1996). Amphotericin B (AmpB), nystatin and natamycin are the most commonly used polyenes (Ghannoum & Elewski, 1999; Vandeputte *et al.*, 2011). Polyenes irreversibly bind to ergosterol, insert themselves into the plasma membrane and form pores, which causes cellular leakage and eventual cell death (Barker & Rogers, 2006) (Figure 1.3). AmpB is the most effective antifungal agent available (Gallis *et al.*, 1990). The affinity of polyenes for the mammalian ergosterol counterpart cholesterol, renders this class of antifungals highly toxic (Chen & Sorrell, 2007). Unfortunately, *C. albicans* has developed resistance to polyenes, through the modification of ergosterol (Ghannoum & Rice, 1999).

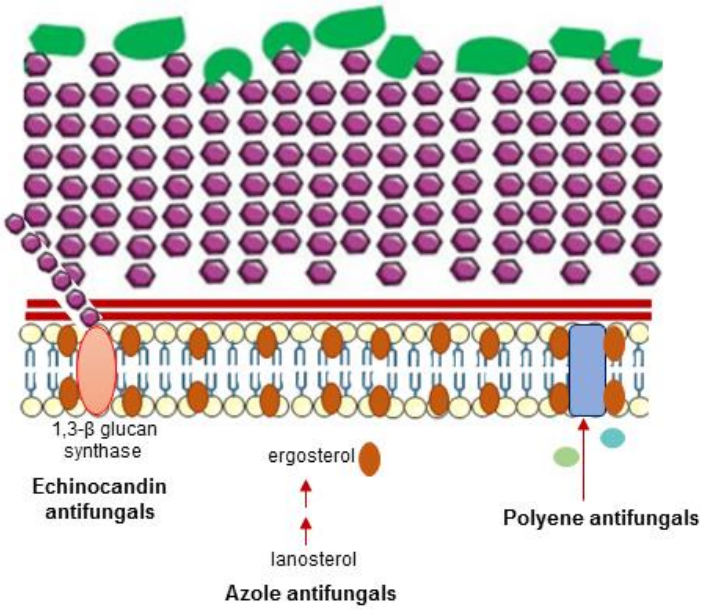

Figure 1.3: Schematic representation of the different modes of action of the three chemical classes of antifungal agents used in the treatment of *C. albicans* and other fungal infections. Echinocandins are non-competitive inhibitors of the enzyme responsible for β-glucan synthesis, and the absence of β-glucans within the cell wall may lead to osmotic instability and cell death. Azoles target ergosterol biosynthesis, causing a reduction in ergosterol, thus disrupting the integrity of the plasma membrane. Polyenes irreversibly bind to ergosterol, insert themselves within the plasma membrane, resulting in cellular leakage of essential ions. Redrawn and adapted from Kathiravan *et al.* (2012).

Azoles have a typical 5 membered organic azole ring, containing either 2 or 3 nitrogen atoms, and as such, are classified as either imidazoles (ketoconazole, miconazole, and clotrimazole) or triazoles (fluconazole and itraconazole), respectively (Sheehan *et al.*, 1999). The cytochrome p-450 lanosterol 14α-demethylase (CYP51A1) enzyme of *C. albicans* is required for the biosynthesis of ergosterol, and is the target of azoles (Lupetti *et al.*, 2002) (Figure 1.3). The depletion of ergosterol within *C. albicans* membranes, not only disrupts the membrane integrity, but also its hormone-like function, thus affecting growth and proliferation of the cell. CYP51A1 is a key enzyme for cholesterol biosynthesis in mammalian cells (Koltin & Hitchcock, 1997), however with a decreased affinity for the human enzyme, thus limiting toxicity (Chen & Sorrell, 2007). The safety profile of azoles has led to their widespread use, resulting in increased azole resistance. A 50% resistance of *C. albicans* to fluconazole, has been reported in South Africa (Dos Santos Abrantes *et al.*, 2014).

Echinocandins are a class of semi-synthetic, cyclic lipopeptides, with an acyl lipid side chain (Grover, 2010). The 3 drugs within this class include caspofungin (CAS), micafungin, and anidulafungin. Echinocandins non-competitively inhibit β-(1,3)-glucan synthase (Figure 1.3). The inability of *C. albicans* to produce β-(1,3)-glucan will affect the integrity of the cell and lead to osmotic instability and eventual cell death (Grover, 2010). CAS is specific for fungal walls, and thus displays low toxicity. Echinocandins are not metabolised by liver P450 cytochromes, as such their drug-drug interaction is minimal, making them ideal to be used in combination treatment (Chen & Sorrell, 2007). This class of

antifungals is relatively new, thus resistance has been rarely reported. The safety profile of echinocandins makes them the popular drug of choice. However the risk of overuse, with the development of resistance is a major concern.

1.5 Fungal biofilm resistance to antifungal drugs

A limited number of antifungal drugs are effective against biofilm related infections (Cools *et al.*, 2017). In addition, biofilms are resistant to several classes of antifungal agents including azoles and echinocandins (Sandai *et al.*, 2016). Resistance of *C. albicans* biofilms to antifungal drugs is complex, and is mostly attributed to the upregulation of efflux pumps, ECM properties and the presence of persister cells (Figure 1.4). The latter are a small subset of metabolically dormant variants, which occur randomly within biofilms, and are highly resistant to antifungal agents (Lewis, 2010).

Efflux pumps are transport proteins responsible for drug extrusion from within a cell. These pumps may be substrate specific, or may transport a range of compounds such as different antibiotic classes (Webber & Piddock, 2003). The latter is associated with multi-drug resistance (MDR). The over expression of membrane associated protein transporters, ensures that *C. albicans* cells are unable to intracellularly accumulate drugs to toxic levels (Prasad & Rawal, 2014).

Within planktonic cells, efflux pumps are upregulated upon exposure to an antifungal drug, whereas in biofilms, the efflux pumps are upregulated during the early stages of adherence (Granger, 2012), where they remain upregulated throughout biofilm progression. Thus, biofilm resistance to antifungal agents occurs at an earlier stage. Two major classes of efflux pumps that export drugs in *C. albicans,* include the ATP-binding cassette (ABC) transporter superfamily, and the major facilitator (MF) transporter superfamily. ABC transporters are primary active transporters, and utilise the hydrolysis of adenosine triphosphate (ATP) to remove drugs from within a cell, whereas MF transporters are secondary active transporters, and utilise the electrochemical gradient of protons across the membrane for drug exportation (Cannon *et al.*, 2009). Over expression of the ABC multidrug transporters CDR1 and CDR2, is associated with the decreased susceptibility of *C. albicans* to azoles (Niimi *et al.*, 2006), and is the mechanism responsible for the high-level azole resistance in clinically important *C. albicans* strains (Cannon *et al.*, 2009).

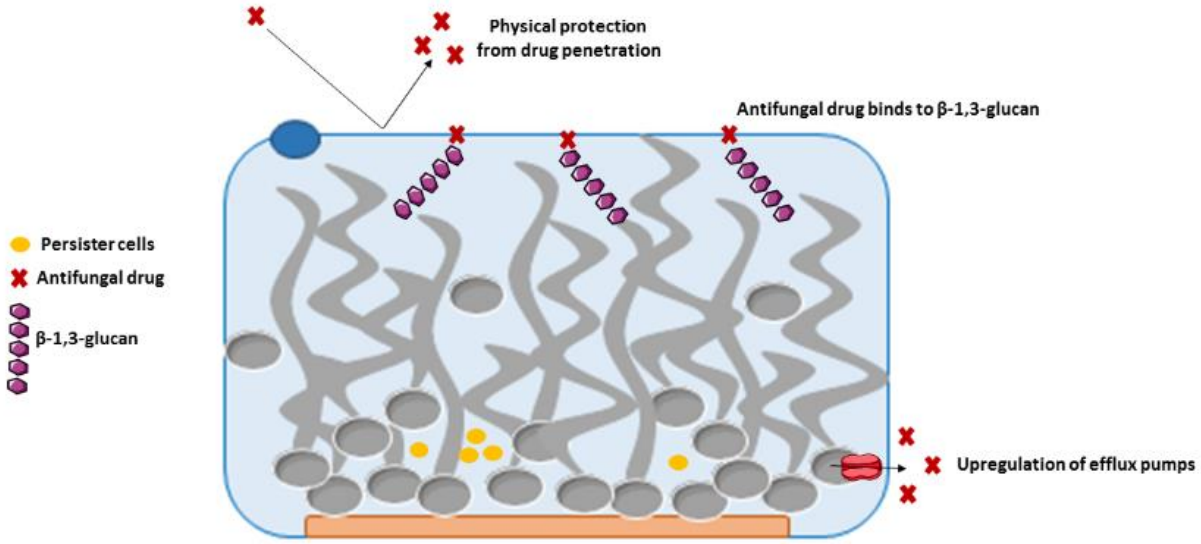

Figure 1.4: Schematic representation of the resistance mechanisms of fungal biofilms to antifungal drugs. The ECM provides physical protection, preventing drug penetration. β-(1,3)-glucans within the matrix bind antifungal drugs, protecting the encased fungal cells. The upregulation of efflux pumps removes antifungal drugs from within cells. A small subset of persister cells are highly resistant to antifungal drugs. Redrawn and adapted from Fox *et al.* (2015).

By acting as a physical barrier, and preventing drug penetration, the ECM can also confer drug resistance. One of the components of the ECM that contributes to antifungal drug resistance is β-(1,3)-glucan (Nett *et al.*, 2007). This polysaccharide binds to antifungal drugs, such as AmpB, and prevents the drug from reaching the cellular components of the biofilm (Vediyappan *et al.*, 2010). Furthermore, the ECM provides mechanical stability, and stabilises the biofilm, contributing to the biofilms resistance. Although the exact role and formation process of persister cells remains unclear, it is known that these cells form following the adherence of round yeast cells to a substrate surface (Taff *et al.*, 2013).

The increased antifungal resistance and the lag in the development of new antifungal agents, has created a need for the development of novel anti-mycotic drugs such as AMPs.

1.6 Antimicrobial peptides

Ubiquitous in nature, AMPs are found in almost all organisms (Bahar & Ren, 2013), and in 2019, the Antimicrobial Peptide Database (APD) contained 3072 AMPs, identified in animals, plants, bacteria, fungi, protists, and archaea, with the majority derived from bacteria. AMPs are relatively short oligopeptides, from 5 to over 100 amino acids in length (Peters *et al.*, 2010). Although anionic AMPs occur, the majority are cationic and are the main focus of AMP research (Oren & Shai, 1997). Cationic AMPs are small, amphipathic molecules, with a considerable portion of hydrophobic residues (30% or more) (Hancock, 2001). In terms of secondary structures, AMPs are classified as either α-helices, β-sheets, extended or mixed α/β. Among the different structural classes, the α-helix and β-sheet structures are more common (Powers & Hancock, 2003). These structural classes form during initial

membrane interaction, or in the presence of membrane-mimicking conditions, since linear AMPs in aqueous solutions are unstable (Hwang & Vogel, 1998). It is widely accepted that AMPs act by non-specifically binding to biological membranes, through the electrostatic interaction with negatively charged membranes. The hydrophobic nature of AMPs allows them to be inserted into the membrane. However, the exact mechanism of interaction remains unclear. Most AMPs display a broad spectrum of activity, with activity against Gram-positive and Gram-negative bacteria, viruses as well as fungi.

In the AMP family, defensins form a diverse group of 25 to 35 long residues, which are cationic, with hydrophobic domains in the folded structure (Alberts *et al.*, 2002). Although unclear on the exact mechanism of action, it is suggested that defensins disrupt their microbial targets by initially inserting their hydrophobic regions into the membrane (Alberts *et al.*, 2002), subsequently interacting with the cell wall and plasma membrane, thereby compromising the integrity of the cell, leading to cellular death.

Within the family of AMPs, peptides with antifungal activity, are known as antifungal peptides (AFPs). Also ubiquitous in nature, AFPs are found in almost all organisms (Bahar & Ren, 2013), including bacteria, insects, plants, fungi, amphibians, and mammals (Table 1.1). AFPs display diversity in terms of their structure, and can be classified as α-helices, β-sheet, mixed α/β, modified cyclic peptides, and lipopeptides to name a few (De Lucca & Walsh, 1999). Although membrane interaction is vital for the antifungal activity of AFPs, additional modes of action have been shown, including the cell wall and various intracellular targets (De Lucca & Walsh, 1999).

Before membrane targeting and interaction, AFPs need to traverse the cell wall, suggesting some type of interaction with cell wall components including mannoproteins, β-glucans and chitin (Cabib & Arroyo, 2013). Cell wall mannoproteins are unique to fungi, and as such are ideal targets for AFPs. Plant defensin *Na*D1 which causes membrane leakage, appeared to loose antifungal activity against proteinase k treated hyphae, indicating that *Na*D1 activity is cell wall dependent, potentially with an initial mannoprotein receptor (Van der Weerden *et al.*, 2010). The saliva peptide histatin-5 binds *C. albicans* cell wall protein Ssa1/2p subsequently leading to increased membrane permebilisation (Li *et al.*, 2003). Additional cell wall targets include the β-(1,3)-glucans, where echinocandins are generally responsible, inhibiting β-(1,3)-glucan synthesis, by targeting β-(1,3)-glucan synthase. Cell wall polysaccharides, such as chitin are also targeted by certain AFPs, including the rabbit defensin NP-1 (Levitz *et al.*, 1986). Interference with chitin has been shown to affect the intracellular cytoskeleton leading to morphological defects (Cabib & Arroyo, 2013) and a loss of membrane integrity (Endo *et al.*, 1997).

Table 1.1 Examples of AFPs from different sources as well as their cell wall and plasma membrane targets

Peptide	Source	Target	Reference
CELL WALL			
*Na*D1	Plant	Mannoprotein	Van der Weerden *et al.* (2010)
Histatin-5	Human	Mannoprotein	Li *et al.* (2003)
CAS	Fungi	B-glucan	Kelly and Kavanagh (2011)
NP-1	Rabbit	Chitin	Levitz *et al.* (1986)
CELL MEMBRANE			
Glycerphospholipids			
Demaseptin S3, S4	Amphibian	PA, PI, PS	De Lucca *et al.* (1998)
Cecropin A, B	Insect	PA, PI, PS	De Lucca *et al.* (1998)
Protegrin-1	Porcine	PG, PC	Ishitsuka *et al.* (2006)
LL-37	Human	PC	Sood *et al.* (2008)
TPP3	Plant	($PI(4,5)P_2$)	Payne *et al.* (2016)
BMAP-28	Human	Unknown	Den Hertog *et al.* (2005)
Sphingolipids and Sterols			
DmAMP1	Plant	$M(IP)_2C$	Thevissen *et al.* (1999)
*Pv*D1	Plant	Ergosterol & GlcCer	Neves de Medeiros *et al.* (2014)
*Rs*AFP2	Plant	GlcCer	Thevissen *et al.* (1999)

PA;phosphatidic acid, **PC;**phosphatidylcholine, **PG;**phosphatidylglycerol, **PI;**phosphatidylinositol, **PS;**phosphatidyl serine, **($PI(4,5)P_2$);** phosphatidylinositol(4,5)bisphosphate,**$M(IP)_2C$;**mannosyldiinositolphosphorylceramide,**GlcCer;**glucosylceramide

Once AFPs have traversed the cell wall, the next potential target is the plasma membrane where the selectivity of membrane acting AFPs, largely depends on the membrane composition (Nguyen *et al.*, 2011). The principal lipids that are found within eukaryotic membranes include glycerophospholipids (GPLs), sphingolipids and sterols (Daum *et al.*, 1998). These lipids have various roles in fungal pathogenicity, host-defense, drug resistance, biofilm formation, structural support, as well as cellular growth and proliferation (Rella *et al.*, 2016).

GPLs contribute between 55% to 75% of membrane lipids (Rautenbach *et al.*, 2016a) and negatively charged GPLs create a more negatively charged fungal membrane, which promotes electrostatic interaction with cationic AFPs. Certain AFPs are known to specifically target negatively charged GPLs (Table 1.1). The cationic amphibian peptides dermaseptin S3 and S4, as well as the *Cecropia* moth peptides cecropin A and B displayed antifungal activity by binding to negatively charged GPLs, resulting in membrane permeabilisation (De Lucca *et al.*, 1998). Human cathelicidins LL-37 and BMAP-28 displayed antifungal activity towards *Candida* spp, primarily targeting membrane GPLs with LL-37 causing substantial membrane damage (Den Hertog *et al.*, 2005) and BMAP-28 causing membrane

permeabilisation. Additional AFP which target negatively charged GPLs include protegrin-1, which caused membrane permeabilisation against various yeast and filamentous fungi (Benincasa *et al.*, 2006), and is currently in phase III of clinical trials for oral mucositis (Rautenbach *et al.*, 2016a). Not all GPLs need to be negatively charged for AFP binding, for example plant defensin TPP3, which preferably binds to phosphatidylinositol ($PI(4,5)P_2$), resulted in membrane permeabilisation and disordered lipids (Payne *et al.*, 2016).

Fungal membranes are distinct from mammalian membranes in terms of the type of sphingolipid and sterol. The main sphingolipid and sterol in fungal membranes include sphingolipids containing inositiol and the sterol ergosterol. Fungal membranes contain glycosphingolipids (GSLs), glycoceramides, and glucosylceramide (GlcCer) which are different from their mammalian counterparts. In addition, the sterol ergosterol is unique to fungi. Lipid rafts containing GSLs and ergosterol occur at the growth tip of hyphae and budding yeast, and serve as important AFP targets since GSLs play a role in signal transduction and protein delivery of membrane proteins (Thevissen *et al.*, 2004) (Table 1.1). Plant defensin DmAMP1 interacts with the sphingolipid $M(IP)_2C$ of *S. cerevisiae* resulting in membrane permeabilisation (Thevissen *et al.*, 1999). Radish plant defensin *Raphanus sativus* AFP2 (*Rs*AFP2) targets *C. albicans* GlcCer, resulting in an altered morphology (Thevissen *et al.*, 1999). Furthermore, plant defensin *Pv*D1 also binds to GlcCer as well as ergosterol (Neves de Medeiros *et al.*, 2014).

The proposed main mode of action of cationic AFPs is the disruption of the membrane integrity, resulting in the leakage of cellular ions and molecules (Yeaman & Yount, 2003). Proposed models for the disruption of membrane integrity include the barrel-stave, carpet and toroidal model. In the barrel-stave model, AFPs reach a threshold concentration, then in order to penetrate the membrane, form a peptide-lined pore within the membrane. The carpet model describes the accumulation of AFPs on the membrane surface, which disrupts the membrane and forms micellar-like structures. The toroidal model differs from the barrel-stave model, in that the inserted AFPs interact with the phospholipid head groups to form a peptide-lipid-lined pore. However, most models are based on model membranes that mimic bacterial membranes, therefore the mode of membrane interaction of a specific peptide with a fungal membrane may be different (Sevcsik *et al.*, 2007).

Although the cell wall and plasma membrane are of particular importance for antifungal drug development, other targets should be considered. It is likely that once AFPs translocate these outer barriers, the mitochondria, nucleic acids, protein synthesis molecules, enzymes and proteins should be accessible to the translocated AFP (Rautenbach *et al.*, 2016a). The activity of certain AFPs are linked to the formation of reactive oxygen species (ROS). ROS are naturally produced during energy metabolism, and play important roles in cell signalling and gene expression. Moreover, ROS are also formed during non-physiological stress conditions including ionizing radiation, inflammation and exposure to AMPs. Environmental stress substantially increases ROS levels that may cause damage to the phospholipids of cell membranes (Lee *et al.*, 2007). Various tyrocidines have been shown to

induce ROS formation within *C. albicans* (Troskie *et al.*, 2014), however not as a direct mode of action. The induced ROS was not linked to antifungal activity, as activity was enhanced instead of inhibited in the presence of ascorbic acid (AA), a known ROS scavenger. The observed ROS could be as a result of osmotic stress or from the binding to GlcCer ergosterol lipid rafts (Rautenbach *et al.*, 2016b). Plant defensin *Pv*D1 was shown to bind GlcCer which leads to ROS production, which subsequently causes disruption of the cytoplasm and plasma membrane (Neves de Medeiros *et al.*, 2014). Furthermore, binding of *Rs*AFP2 to GlcCer also induced ROS formation, which was linked to membrane leakage (Aerts *et al.*, 2007).

1.7 Therapeutic applications of AMPs

For therapeutic applications, AMPs are beneficial due to their broad-spectrum of activity, low toxicity, swift initiation of activity and, most notably, their low susceptibility to resistance (Seo *et al.*, 2012). The latter is attributed to the fact that AMPs have generalised targets, decreasing the likelihood of the development of genetic resistance (Nguyen *et al.*, 2011). In the case of fungi, cell membranes evolve slower compared to the rest of the organism, making AMPs attractive antifungal agents, since most target the cell membrane. Certain AMPs have been shown to be active against antibiotic resistant bacteria. Methicillin-resistant *Staphylococcus aureus* (MRSA) is resistant to the antibiotic vancomycin, but susceptible to the AMP nisin, both of which block cell wall biosynthesis. Most attention has been given to the use of AMPs as a single antimicrobial agent, rather than in combination with other drugs. Advantages of combination therapy include the use of lower drug dosages, fewer side effects, rapid response and slower development of resistance.

There are several pitfalls to the use of AMPs, and these include their sensitivity to protease degradation and high cost of production. These limitations can be overcome by introducing specific peptide modifications (John *et al.*, 2008), using drug delivery systems to enhance AMP stability, and reduce its size (Khaksa *et al.*, 2000). Of the many natural and synthetic AMPs that show potential as antimicrobial agents, very few have actually made it to clinical trials (Koo & Seo, 2019). However, in 2018 alone, approximately 50 peptide drugs were available commercially, with over hundreds of peptides in clinical trials (Lau & Dunn, 2018).

Further therapeutic applications of AMPs includes their use in biofilm control, especially for the inhibition of biofilms. Several peptides from different sources have been identified to have activity against *C. albicans* biofilms (Table 1.2) and have the potential to be developed as novel anti-biofilm agents.

Table 1.2 AMPs with *C. albicans* anti-biofilm activity and their respective sources

AMP	Species/Source	Reference
hLF1-11	Lactoferricin	Morici *et al.* (2016)
VLL-28	Archaeal transcription factor Stf76	Roscetto *et al.* (2018)
HsLin06_18	*Heuchera sanguinea*	Cools *et al.* (2017)
OSIP108	*Arabidopsis thaliana*	De Brucker *et al.* (2014)
P318	Cathelicidn-related AMP (CRAMP)	De Brucker *et al.* (2014)
AuNPs-indolicidin	Indolicidin	De Alteriis *et al.* (2018)

Au; gold, **NPs;** nanoparticles, **AuNPs-indolicidin;** indolicidin coated gold nanoparticles, **CRAMP;** cathelicidin-related AMP

Synthetic peptide hLF1-11 displayed a dose-dependent inhibitory effect on *C. albicans* biofilms and effects include reduced activity of adhered cells and the reduction of hyphal formation compared to the untreated control (Morici *et al.*, 2016). VLL-28, an AFP isolated from an archaeal transcription factor displayed anti-biofilm activity against *C. albicans.* VLL-28 was localised to the fungal surface and inhibited biofilm formation by reducing the viability of adhered cells. In addition, VLL-28 caused the death of most cells within a preformed biofilm, indicating, biofilm eradicating activity (Roscetto *et al.*, 2018). Plant defensin HsAFP1 was shown to have anti-biofilm activity, while HsLin06_18, the truncated peptide derived from the C-terminus of HsAFP1 was investigated for its anti-biofilm activity against *C. albicans*, in combination with CAS. The combination was able to significantly reduce biofilm formation in *C. albicans*, with CAS facilitating the internalisation of HsLin06_18 (Cools *et al.*, 2017). Decapeptide OSIP108, identified in the model plant *Arabidopsis thaliana*, also displayed anti-biofilm activity against *C. albicans*. Overall, this peptide impeded on cell-wall processes, thus hindering biofilm formation. Furthermore, OSIP108 was also able to potentiate the antifungal activity of AmpB and CAS (Delattin *et al.*, 2014). CRAMP isolated from the pancreas of mice was used to derive a 26 residue peptide P318. This peptide was biofilm specific, and did not affect planktonic cells at the tested concentration (De Brucker *et al.*, 2014). Other studies have investigated the use of AuNPs-indolicidin, to combat *C. albicans* biofilms. The nano-complex was able to significantly reduce biofilm formation, as well as affect preformed biofilms (De Alteriis *et al.*, 2018).

1.8 Background to the study

Approximately 50 defensins have been identified in more than 20 different tick species (Tonk *et al.*, 2015). Defensin and defensin-derived peptides display potential as promising pharmaceutical agents (Winter & Wenghoefer, 2012). Several display antifungal activity with reduced toxicity (Thomma *et al.*, 2003). Midgut defensin *Ornithodoros savignyi* defensin isoform 2 (OsDef2) was previously identified in the soft tick *O. savignyi.* OsDef2 was used as a template to derive the carboxy-terminal peptide fragment Os (Table 1.3). Os displayed anti-bacterial (Prinsloo, 2013) as well as antifungal activity against planktonic *C. albicans* cells (Mbuayama, 2016). Likewise, a shorter, amidated derivative Os(11-

22)NH_2 was found to possess antifungal activity against planktonic *C. albicans* cells (Mbuayama, 2016) as well as biofilms (Chiramba, 2018). A preliminary study has also found Os to inhibit *C. albicans* biofilm formation (Mwiria, 2017).

Table 1.3 Physicochemical properties of OsDef2 and derivatives

Peptide	Sequence	Length	Net charge*	MW (g/mol)#
OsDef2	GYGCPFNQYQCHSHC **KGIRGYKGGYCKGAFKQTCKCY**[1]	37	+6	4185.90
Os	**KGIRGYKGGYCKGAFKQTCKCY**[2]	22	+6	2459.92
Os(11-22)NH_2	_____**CKGAFKQTCKCY**-NH_2[3]	12	+4	1378.70

*Net charge at pH 7.#Data obtained from ProtParam available at [http://web.expasy.org/protparam].[1]The carboxy-terminal end of OsDef2 is highlighted in bold.[2]Os is the carboxy-terminal end of OsDef2 including the cysteine residues indicated in red.
[3] Os(11-22)NH_2 is the 12 residues at the carboxy-terminal end of Os, including the cysteine residues indicated in red. This peptide includes an amidation at the carboxy-terminal end, indicated in blue. Obtained from Prinsloo (2013) with modifications.

1.9 Aim of this study

The aim of this study was to investigate the mode of action of the antimicrobial peptide Os on *Candida albicans* (ATCC 90028) biofilm formation.

The specific objectives to achieve the above aim were to:

1. Determine the anti-planktonic activity of Os.
2. Perform a time course study of *C. albicans* biofilm formation.
3. Evaluate the biofilm inhibitory activity of Os.
4. Evaluate the effects of Os on biofilm cell morphology.
5. Determine whether Os induces endogenous ROS production.
6. Investigate the relationship of endogenous ROS generation and biofilm inhibitory activity.
7. Determine if Os leads to permeabilisation of *C. albicans* biofilm plasma membrane.
8. Investigate whether Os enters *C. albicans* biofilm cells.
9. Observe changes to biofilm cell ultrastructure after treatment with Os.

CHAPTER 2: Materials and Methods

2.1 Materials

2.1.1 Strains and media

American Type Culture Collection (ATCC) supplied *C. albicans* strain 90028 (ATCC® 90028™), that was used as the model organism in this study. *C. albicans* stock solutions were stored at -80ºC in 30% (*v/v*) glycerol. Overnight cultures were grown in Yeast Peptone Dextrose (YPD) broth (1% yeast extract, 2% peptone, and 2% glucose (Glc)) or YPD agar (1% yeast extract, 2% peptone, 2% Glc, and 1.5 % agar), supplied by Sigma-Aldrich (St. Louis, MO, USA). For overnight cultures, 4 colonies from a 24h culture on YPD agar were inoculated into 20 mL of YPD broth, and incubated in an orbital shaker (150 rpm) at 37°C for 18h. *C. albicans* was further grown in Rosewell Park Memorial Institute-1640 (RPMI-1640) buffered to pH 7 using morpholinopropanesulfonic acid (MOPS), containing L-glutamine, phenol red and no bicarbonate. RPMI-1640 and MOPS were purchased from Sigma-Aldrich (St. Louis, MO, USA), while Merck (Davidson Rd. Wadeville, Gauteng, SA) supplied the anhydrous glucose.

2.1.2 Peptides, labelled peptides and controls

Os, 5FAM-Os, 5FAM-penetratin and 5FAM-Os(11-22)NH_2 were purchased from GenScript (New Jersey, USA), while Os(11-22)NH_2 was purchased from LifeTein (New Jersey, USA). Although the focus of this study was on Os, its C-terminal amidated analogue, Os(11-22)NH_2, was included in the mode of action studies for comparative purposes. Peptides purchased from Genscript were synthesised using a FlexPeptide™ technology, while those purchased from LifeTein were synthesised using PeptideSyn™ technology. Purity and mass of the peptides were determined with reversed-phase high-performance liquid chromatography (RP-HPLC), and mass spectrometry (MS). Dithiothreitol (10 nmol) was added to Os prior to lyophilisation to prevent disulphide bond formation between the cysteine residues. Table 2.1 provides sequences and physicochemical properties of all peptides used.

Table 2.1: Sequences and the physicochemical properties of the peptides used in this study

Peptide	Sequence	Length	Net charge*	MW (g/mol)#
Os	_____KGIRGYKGGY**C**KGAFKQT**C**K**C**Y	22	+6	2459.92
Os(11-22)NH_2	_____**C**KGAFKQT**C**K**C**Y-**NH_2**	12	+4	1378.69
5FAM-Os	[1]**5FAM-**KGIRGYKGGY**C**KGAFKQT**C**K**C**Y	22	+5	2818.23
5FAM-Os(11-22)NH_2	_____[1]**5FAM-C**KGAFKQT**C**K**C**Y-**NH_2**	12	+3	1737.00
5FAM-penetratin	[1]**5FAM-**RQIKIWFQNRRMKWKK-**NH_2**	16	+5	2717.20

*Net charge at pH 7. #Data obtained from ProtParam available at [http://web.expasy.org/protparam. [1]5-carboxyfluorescein (5FAM) is the amino-terminal fluorescent label indicated in bold. Cysteine residues are indicated in red, while carboxy-terminal amidations are indicated in blue.

The concentration of Os and Os(11-22)NH_2 were determined by measuring the absorbance (Abs) at 280 nm, using the following equation:

$$c = \frac{MW\ x\ df\ x\ Abs}{no.of\ Tyr\ \&\ Trp\ x\ \varepsilon}$$

where c is the peptide concentration in mg/mL; MW is the molecular weight in g/mol, df is the dilution factor, no represents the number of tyrosine (Tyr) or tryptophan (Trp) residues, and ε is the extinction coefficient. The extinction coefficients of Tyr and Trp are 1200 and 5560 AU/mmol/mL respectively (Lamichhane *et al.*, 2011). The concentration of the fluorescently labelled peptides were determined with the same equation, by measuring the absorbance of 5FAM at a wavelength of 492 nm and an ε of 78000 AU/mmol/mL (Buranasompob, 2005). All spectrometric readings were done using an ultraviolet-visible (UV-Vis) spectrophotometer (Separation Scientific, PA, USA).

Peptide stock solutions of 400 µM were prepared for Os, 5FAM-Os, Os(11-22)NH_2 and 5FAM-Os(11-22)NH_2, whereas the stock solution prepared for 5FAM-penetratin was 34.71 µM. Aliquots of stock solutions were dispensed into polypropylene tubes, and stored at -20°C until required.

The antifungal agent, AmpB, which was used as the positive control, was dissolved in dimethyl sulfoxide (DMSO). Both the control and solvent were supplied by Sigma-Aldrich (St. Louis, MO, USA). AmpB stock solutions of 1 mM (in 100% DMSO) were prepared, aliquots dispersed into polypropylene tubes, and stored at -80°C in the dark. AmpB stock solutions were diluted in RPMI-1640 to contain a final concentration of 0.5% DMSO.

2.1.3 Chemicals and reagents

Crystal violet (CV) supplied by Sigma-Aldrich (Johannesburg, South Africa (SA)) was initially dissolved in 100% (*v/v*) ethanol, and further diluted with ddH_2O to produce a 0.1% CV (*m/v*) solution. The dye was extracted with 30% acetic acid (*v/v*), prepared in ddH_2O. Both solutions were stored at room temperature. A 20% formaldehyde (*v/v*) solution was prepared in ddH_2O, from a 35% (*v/v*) stock solution, supplied by Merck (Davidson Rd. Wadeville, Gauteng, SA), and was stored at room temperature.

Cell-Titer Blue (CTB) supplied by Promega (WI, USA) was stored at 4°C. When required, a working concentration of 10% CTB (*v/v*) was prepared in phosphate buffered saline (PBS; 10 mM, pH 7.4), and kept in the dark.

Both AA, supplied by Sigma-Aldrich (St. Louis, MO, USA) and citric acid monohydrate (CA), supplied by Merck (Davidson Rd. Wadeville, Gauteng, SA) were dissolved in ddH_2O, to prepare 1 M stock solutions. Both AA and CA were protected from light, and stored at room temperature.

Fluoresecent dyes, propidium iodide (PI) and 4',6-diamidino-2-phenylindole (DAPI), were both supplied by Sigma-Aldrich (St. Louis, MO, USA), and dissolved in ddH_2O. Stock solutions of 1 mg/mL were prepared, dispensed into aliquots in polypropylene tubes. PI was stored at 4°C and DAPI at -20°C.

For scanning electron microscopy (SEM) the 2.5% glutaraldehyde (*v/v*) and 2.5% formaldehyde (*v/v*) solutions were prepared from 50% stock solutions, and diluted in 0.075 M PBS (pH 7.4), to a final concentration of 0.046 M PBS (pH 7.4). Hexamethyl disilazane (HMDS) was purchased from Sigma-Aldrich (St. Louis, MO, USA).

2.2 Methods: Anti-planktonic activity studies

2.2.1 Anti-planktonic activity assays

The anti-planktonic activity of Os and the control AmpB was determined using the microbroth dilution assay (Rodriguez-Tudela *et al.*, 2008). This assay is used to determine the lowest concentration of a drug, that causes visible cell death of the test organism, compared to the growth control (Rodriguez-Tudela *et al.*, 2008). This concentration is known as the minimum inhibitory concentration (MIC). The microbroth dilution assay is preferred over the radial diffusion assay, as it allows many samples to be tested, with simple, direct and rapid analysis of data (Steinberg & Lehrer, 1997).

The assay was performed in a 96-well plate, according to the method of the European Committee on Antimicrobial Susceptibility Testing (EUCAST) definitive document, with minor modifications (Rodriguez-Tudela *et al.*, 2008). A total of 5 representative colonies from a 24h culture on YPD agar medium, were suspended in 5 mL of ddH_2O, vortexed for 15s, and the optical density (OD) at 530 nm ($OD_{530\ nm}$) subsequently determined. The cell density of the inoculum was adjusted to obtain an $OD_{530\ nm}$ value within the range 0.12 to 0.15, which correlates to a yeast suspension of 1-5 x 10^6 colony forming units per mL (CFU/mL). An OD_{530} value above the range was adjusted, by diluting the inoculum with ddH_2O. A final 10-fold dilution was performed to yield a final yeast suspension of 1-5 x 10^5 CFU/mL. Upon preparing the inoculum, working solutions of AmpB (concentration range of 0.078 µM to 10 µM) were prepared in RPMI-1640 containing 2% Glc, and 1% DMSO. Each well received 50 µL of inoculum and 50 µL of each AmpB concentration, to obtain a final concentration range of 0.04 µM to 5 µM in RPMI-1640 1% Glc and 0.5% DMSO. Working solutions of Os were prepared in RPMI-1640 containing 2% Glc with a concentration range of 1.56 µM to 200 µM. To each well, 50 µL of inoculum and 50 µL of each Os concentration was added, to obtain a final concentration range of 0.78 µM to 100 µM. Following a 24h incubation, the OD_{530} for each well within the 96-well plate was measured and was

used to calculate the % inhibition of *C. albicans* growth by AmpB and Os relative to the growth control (100%) where no drug/peptide was added. A viable count was performed to ensure that the correct cell concentration was used. The plate for the viable count should contain 5 to 125 colonies to ensure the test wells contain between 0.5 x 10^5 and 2.5 x 10^5 CFU/mL (Hsieh *et al.*, 1993; Rodriguez-Tudela *et al.*, 2008).

2.3 Methods: Anti-biofilm activity studies

2.3.1 Time course study of *C. albicans* biofilm formation

To prepare overnight cultures, 4 colonies from a 24h culture on YPD agar medium were inoculated into 20 mL of YPD broth, and incubated in an orbital shaker (150 rpm) at 37°C for 18h. An aliquot of 1 mL was centrifuged at 200 x *g* for 10 min. Subsequently, the supernatant was discarded, the pellet washed in 1 mL of RPMI-1640 containing 1% Glc and centrifuged at 14100 x *g* for 2 min. Throughout all biofilm related studies, RPMI-1640 containing 1% Glc was used. The supernatant was once again discarded and the pellet re-suspended in 1 mL of RPMI-1640 to produce a cell suspension. The OD of the cell suspension was measured at 620 nm ($OD_{620\ nm}$), and was adjusted using RPMI-1640, to a cell density of 1 x 10^6 CFU/mL. A volume of 100 µL of the final cell suspension was added to the wells of a 96-well polystyrene plate (Greiner Bio-One, Kremsmunster, Austria). The plate was incubated at 37°C for 1.5h to allow the round yeast cells to adhere to the bottom of the plate. Following adherence, the RPMI-1640 was aspirated, and the wells were washed with PBS to remove any non-adhered cells. Subsequently, in 100 µL RPMI-1640 media, a time study of 2, 24, 48 and 72h time points was performed to determine the optimal incubation time for the development of well-established biofilms. The growth medium was aspirated and replenished every 24h.

2.3.2 Biofilm staining and biomass determination

CV is a blue aniline derived dye, used to quantify biofilm biomass within an allocated area. The positively charged amine group of CV (Figure 2.1) interacts with cellular anionic molecules, such as proteins, DNA and polysaccharides. The ability of CV to bind to both live and dead cells, and other materials such as the ECM makes this dye not suitable for viability testing. However, this staining method can be used to determine if biofilm formation has occurred and CV extraction with acetic acid allows for biomass quantification.

Following the time study, the medium was aspirated and the biofilms were washed with PBS, fixed with 100 µL of 20% (*v/v)* formaldehyde and incubated at room temperature for 30 min. The formaldehyde was then removed and the plates were left to dry. Following fixing, the biofilms were stained with 200 µL of 0.1% (*m/v*) CV and incubated at room temperature for 20 min. Excess CV was removed by submerging the plates in a tub of water, before blot drying on paper towels. The wells within the plates were left to dry completely before qualitative analysis was performed.

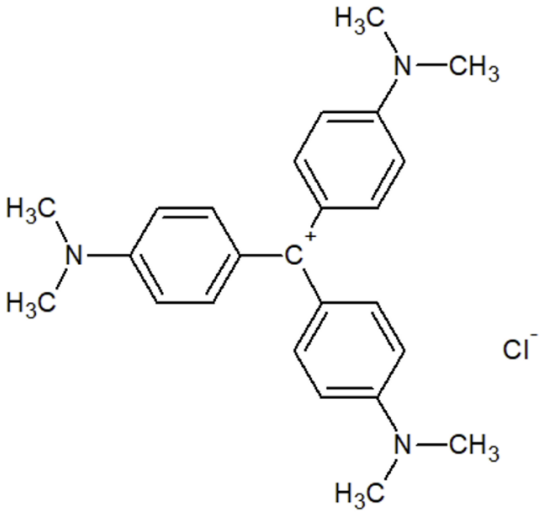

Figure 2.1: Chemical structure of crystal violet. The 3 benzene rings serve as the chromophore group, and provide the dye with its characteristic colour. The central carbon serves as the ionisable auxochrome group which aids in solubilising the dye. Methyl structures serve as the modifying groups, and are responsible for the observed purple colour. Generated using ChemSketch: https://chemsketch.jaleco.com/.

Qualitative evaluation of the biofilm biomass was performed using an inverted light microscope (Optika microscopes, Italy). Quantitative analysis involved solubilising the CV with 125 µL of a 30% (*v/v)* acetic acid solution at room temperature for 15 min. The absorbance of the extracted CV was measured at 550 nm using a plate reader (Molecular devices, USA). Data was expressed as percentage relative to the control not exposed to peptide.

2.3.3 Biofilm inhibition activity assays

CTB is a solution containing the highly purified indicator dye resazurin which is dark blue in colour, and is used as an indicator of cell viability. Viable cells are metabolically active, and are capable of reducing resazurin into the highly fluorescent pink resorufin (Figure 2.2). Reduction of resazurin into resorufin occurs within the mitochondria and cytosol, as a result of various redox enzymes located within these cellular compartments (Gonzalez & Tarloff, 2001). CTB does not damage cells during short exposure times. Although absorbance can be measured, fluorescence is the preferred method, as it is more sensitive. The CTB cell viability assay provides a rapid fluorometric method to establish viability.

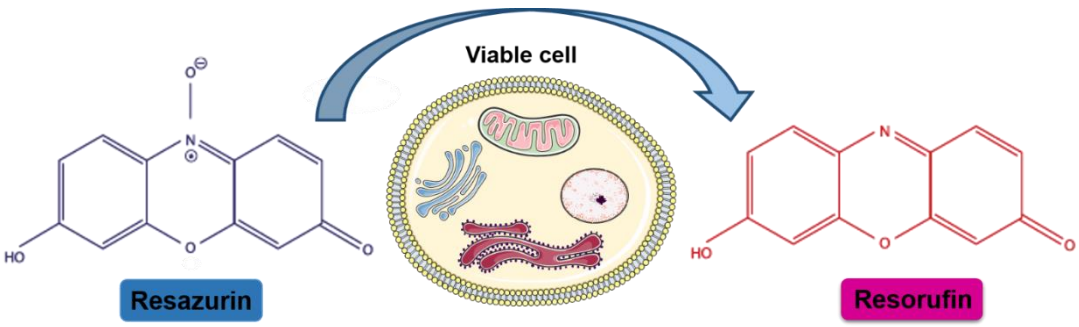

Figure 2.2: Conversion of resazurin to resorufin. CellTiter-Blue contains dark blue resazurin that is metabolically reduced by viable cells to highly pink fluorescent resorufin. Redrawn and adapted from Creative Bioarray: https://www.creative-bioarray.com/support/resazurin-cell-viability-assay.htm.

The minimum concentration required to reduce the biofilm formation by 50% (BIC_{50}) compared to the control (Vriens *et al.*, 2015) was established using the biofilm inhibition assay as described by Vriens *et al.* (2015). AmpB was used as the positive control and was compared to the BIC_{50} of $Os(11\text{-}22)NH_2$ determined by Chiramba (2018).

Adherent cultures of *C. albicans*, were prepared as described in section 2.3.1. Following the wash step, 100 µL of increasing concentrations of AmpB in 0.5% DMSO (concentration range of 0.02 µM to 5 µM) were added to the wells. Likewise for Os, after the wash step, 100 µL of increasing concentrations of Os in RPMI-1640 (concentration range of 0.39 µM to 100 µM) were added. Biofilms were left to grow for 24h at 37°C, and subsequently washed with PBS. Cellular viability was determined by adding 100 µL of 10% (*v/v*) CTB diluted in PBS and after 1h incubation in the dark at 37°C, the fluorescence was measured at an excitation wavelength (λ_{ex}) of 535 nm and an emission wavelength (λ_{em}) of 590 nm using a fluorescence plate reader (Molecular devices, USA).

2.4 Methods: Anti-biofilm mode of action studies

2.4.1 Inverted light microscopy

To determine the effect of Os on biofilm cell morphology, initial adherence of biofilms was performed as described in section 2.3.1. Following the wash step Os and $Os(11\text{-}22)NH_2$ at their respective BIC_{50} values were added. Following 24h exposure, the medium was aspirated, biofilms washed with PBS, fixed with 100 µL of 20% (*v/v*) formaldehyde and incubated at room temperature for 30 min. The formaldehyde was removed and the plates left to dry. Following fixing, the biofilms were stained with 200 µL of 0.1% (*m/v*) CV and incubated at room temperature for 20 min. The excess CV was then removed by submersion in water. The plates were then left to dry completely before qualitative analysis was performed with inverted light microscopy (Optika microscopes, Italy).

2.4.2 DCFH-DA assay for the determination of endogenous ROS

A free radical is any chemical species containing one or more unpaired valence electron (Halliwell & Gutteridge, 2015) and collectively ROS are free radicals derived from oxygen. Normally ROS is produced during oxygen metabolism, and plays important roles in cell signalling and gene expression. During non-physiological conditions such as environmental stress, increased levels of ROS leads to oxidative stress that targets protein, fatty acids and phospholipids of cell membranes (Lee *et al.*, 2007). Other targets are nucleic acids, and adverse effects include base modifications and strand lesions (Cimpan *et al.*, 2005). Increased ROS has been identified as an antifungal mode of action for AFPs.

In the present study ROS levels induced by Os was compared to Os(11-22)NH_2 previously shown to produce ROS (Chiramba, 2018) in *C. albicans* biofilms, and was measured with the 2',7'-dichlorodihydrofluorescein diacetate (DCFH-DA) assay (Figure 2.3).

In this assay, the non-fluorescent, cell permeable probe DFCH-DA enters into the cell where cellular esterases reduce DFCH-DA into 2',7'-dichlorodihydrofluoescein (DCFH). In the presence of ROS, DCFH is converted into the highly fluorescent 2',7'-dichlorofluoescein (DCF). The levels of fluorescence are proportional to cellular ROS production.

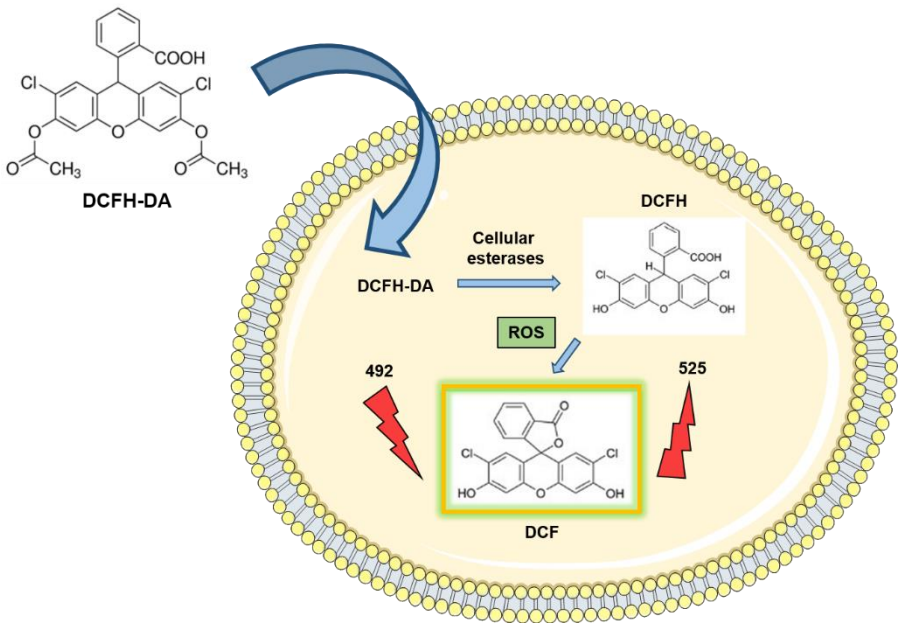

Figure 2.3: Schematic representation of the principle of the DCFH-DA assay. The non-fluorescent DCFH-DA is cell permeable and in the intracellular environment cellular esterases convert DCFH-DA into DCFH. In the presence of cellular ROS, DCFH is reduced to the fluorescent DCF which absorbs light at an excitation wavelength of 492 nm and emits light at an emission wavelength of 525 nm. Redrawn and adapted from bio-protocol: https://bio-protocol.org/e2545.

Initial adherence of biofilms was performed as described in section 2.3.1. The adhered cells were treated with 100 µL of Os(11-22)NH_2 (81 µM), and Os (46 µM) and incubated for 24h at 37°C to allow

biofilm development. To confirm the presence of ROS, Os was additionally incubated with AA (10 mM), a strong ROS scavenger. Since Os(11-22)NH_2 was already shown to produce ROS, it was not further incubated with AA. Following the growth period, the medium was aspirated, biofilms washed with PBS and 100 µL of DCFH-DA (100 µM) was added to each well and incubated in the dark, for 1h at 37°C , with shaking (80 rpm). Fluorescence was measured using a fluorescence plate reader (Molecular devices, USA) at $\lambda_{ex}/\lambda_{em}$: 492/525 (Bink *et al.*, 2011). CA (10 mM) diluted in RPMI-1640, served as a pH control.

To determine whether Os inhibits biofilm formation through the production of ROS, *C. albicans* biofilms were grown in the presence of Os alone, as well as Os combined with AA, and the inhibition (%) quantified using CTB as previously described in section 2.3.3.

2.4.3 Membrane permeability assays

The plasma membrane of *C. albicans* is an important junction for the *Candida*-pathogen relationship (Cabezon *et al.*, 2009). The effect that Os has on the membrane permeability of *C. albicans* biofilms, was established with PI staining. PI is a red fluorescent dye with selective ability to cross cell membranes. PI does not cross the cell membrane of viable cells with an intact plasma membrane, however if the plasma membrane is damaged PI enters the cell and binds double stranded (dsDNA), by intercalating between bases pairs with enhanced fluorescence (Figure 2.4 A). In contrast, DAPI freely crosses the plasma membrane of viable and dead cells where it binds to the minor groove AT regions of dsDNA (Figure 2.4 B) as well as RNA (Tanious *et al.*, 1992). This dual staining is used to distinguish between dead and live cells by first staining with PI to identify dead cells and then DAPI to identify remaining live cells. Staining is evaluated with confocal laser scanning microscopy (CLSM) which isolates fluorescence emission, providing high resolution images of complex structures and helps place cells of interest in their correct morphological context (Zimmer & Roalson, 2005).

To prepare overnight cultures, 4 colonies from a 24h culture on YPD agar medium were inoculated into 20 mL of YPD broth, and incubated in an orbital shaker (150 rpm) at 37°C for 18h. An aliquot of 1 mL was removed and centrifuged at 200 x *g* for 10 min. Subsequently, the supernatant was discarded, the pellet washed in 1 mL of RPMI-1640 and centrifuged at 14100 x *g* for 2 min. The supernatant was once again discarded and the pellet re-suspended in 1 mL of RPMI-1640 to produce a cell suspension. The $OD_{620\,nm}$ of the cell suspension was measured, and was adjusted using RPMI-1640, to a cell density of 1 x 10^6 CFU/mL.

To visualise the biofilms, a volume of 500 µL of the final cell suspension was added to the wells of a 24-well Cellstar polystyrene plate (Greiner Bio-One, Kremsmunster, Austria) with poly-L-lysine coated coverslips at the bottom of the wells.

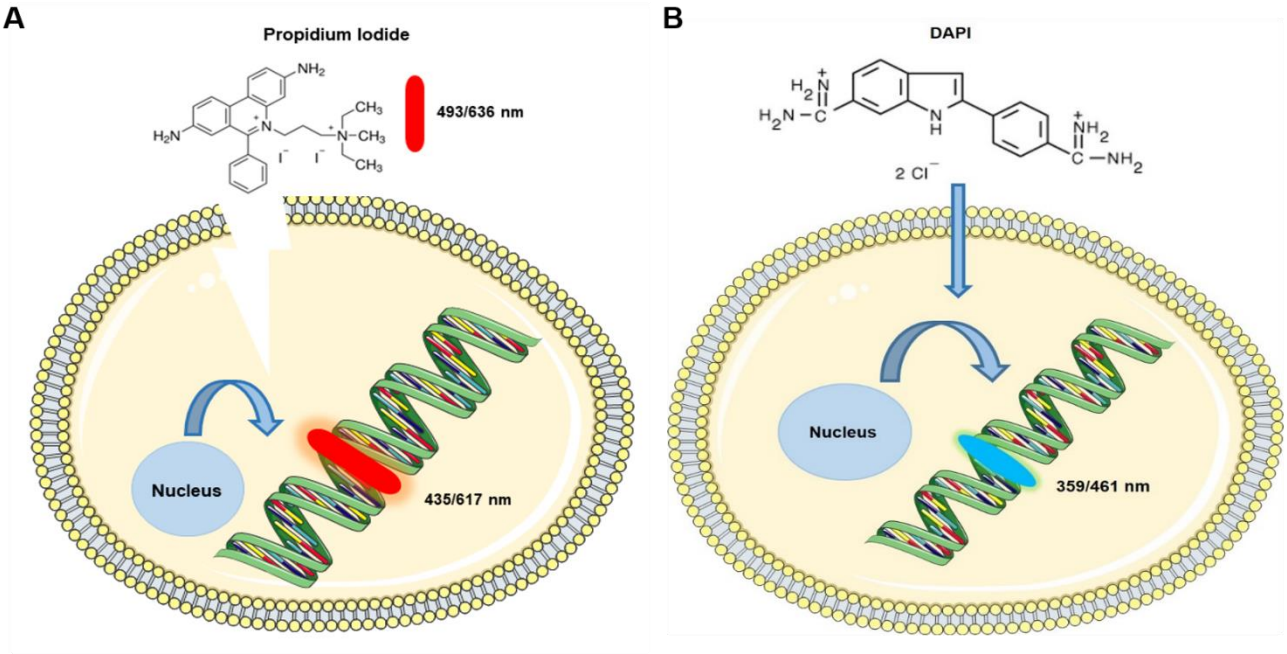

Figure 2.4: Schematic representation of A) propidium iodide (PI) and B) DAPI staining. PI is a red fluorescent dye that stains dead cells but not viable cells. DAPI stains both dead and live cells, and this selectivity is used to distinguish between dead and live cells using confocal laser scanning microscopy. Redrawn and adapted from alpha laboratories: https://www.alphalabs.co.uk/341-07381.

To facilitate the attachment of biofilms to coverslips for microscopy, the coverslips were coated in 0.1% poly-L-lysine (*w/v*). Poly-L-lysine is a positively charged polymer, used to enhance the attachment of cells to solid substrates. Attachment is as a result of the ionic interaction between the anionic cell surface and cationic adhered poly-L-lysine. Round coverslips were supplied by Lasec (Johannesburg, SA). The coverslips were washed with a solution containing 10% NaOH (*w/v*), and 60% ethanol (*v/v*) with shaking for 2h. Following rinsing with ddH_2O, the coverslips were sterilised with 99.9% ethanol (*v/v*) before being transferred to a sterile environment to dry. Subsequently, the dried coverslips were immersed in poly-L-lysine (70000-150000 KDa) supplied by Sigma-Aldrich (Johannesburg, SA) for 2h. Coated coverslips were rinsed with ddH_2O and were allowed to dry for at least 3 days before being stored at room temperture under sterile coditions.

The 24-well plate was incubated at 37°C for 1.5h to allow the round yeast cells to adhere to the cover slips. Following adherence, RPMI-1640 was aspirated, and wells were washed with PBS to remove any non-adhered cells. Subsequently, the adhered cells were further incubated with 500 µL of RPMI-1640, or medium containing Os (46 µM) or Os(11-22)NH_2 (81 µM) for 24h at 37°C. Pre-formed biofilms, grown for 24h and treated for 30 min with anionic detergent Triton-X 100 (1%) were used as the positive control. Following incubation, the biofilms were washed with PBS and stained with 500 µL of 1.5 µg/mL PI for 20 min at 37°C in the dark. After incubation, the solution was removed and biofilms were washed twice in PBS. Biofilms were counterstained with 500 µL of DAPI (10 µg/mL) for 5 min in the dark. DAPI was subsequently removed and the biofilms washed twice with PBS. The coverslips were gently removed from the bottom of the plate, placed onto slides with anti-fading polyvinyl alcohol mounting

medium with DABCO®, and the edges were sealed with clear nail polish. Coverslips were visualised with the Zeiss LSM 880 Meta Confocal Microscope (Carl Zeiss, Oberkochen, Germany). Images were analysed and processed with AXIO VISION 4.8 software (Zeiss, Germany). To view PI the 598-735 nm band pass filter was used together with a 488/405 nm beam splitter. DAPI was observed using a 420-480 nm band pass filter and a 405/488/543 nm beam splitter.

2.4.4 Localisation of peptides

5FAM is a green fluorescent molecule, used to label peptides, nucleotides and proteins. It is a single isomer of carboxyfluorescein, and contains a carboxylic acid that reacts with the primary amines of compounds through carbodiimide activation of the carboxylic acid (Figure 2.5).

Initial adherence of biofilms was performed as described in section 2.4.3. Penetratin, is a peptide known to translocate biological molecules (Madani *et al.*, 2011), as such 5FAM labelled penetratin was used as the positive control. Subsequently, the adhered cells were further incubated with 500 µL of RPMI-1640, 5FAM-penetratin (10 µM), 5FAM-Os(11-22)NH_2 (81 µM), and 5FAM-Os (46 µM), for 24h at 37°C. Following incubation, the biofilms were washed with PBS and stained with 500 µL of 10 µg/mL of DAPI for 5 min in the dark. DAPI was subsequently removed and the biofilms washed twice with PBS. The coverslips were gently removed from the bottom of the plate, placed onto slides with anti-fading polyvinyl alcohol mounting medium with DABCO®, and the edges sealed with clear nail polish. Coverslips were visualised with the Zeiss LSM 510 Meta Confocal Microscope (Carl Zeiss, Oberkochen, Germany). Images were analysed and processed with AXIO VISION 4.8 software (Zeiss, Germany).

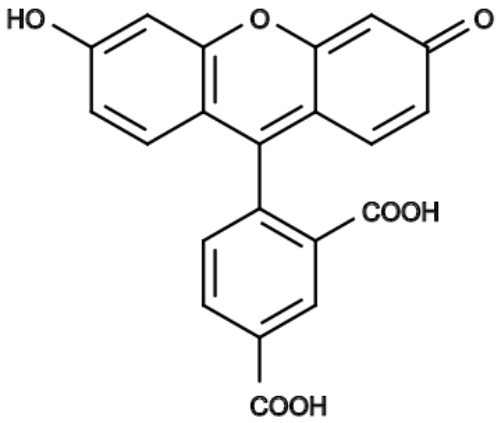

Figure 2.5: Chemical structure of 5-carboxyfluorescein (5FAM). 5FAM is a green fluorescent molecule that binds to the primary amines of peptides through the carboxylic acid of FAM. 5FAM has an excitation and emission wavelength of 495 nm and 520 nm respectively. Obtained from aat bioquest: https://www.aatbio.com/products/5-fam-5-carboxyfluorescein-cas-76823-03-5.

Initial adherence of biofilms was performed as described in section 2.4.3. Penetratin, is a peptide known to translocate biological molecules (Madani *et al.*, 2011), as such 5FAM labelled penetratin was used

as the positive control. Subsequently, the adhered cells were further incubated with 500 µL of RPMI-1640, 5FAM-penetratin (10 µM), 5FAM-Os(11-22)NH_2 (81 µM), and 5FAM-Os (46 µM), for 24h at 37°C. Following incubation, the biofilms were washed with PBS and stained with 500 µL of 10 µg/mL of DAPI for 5 min in the dark. DAPI was subsequently removed and the biofilms washed twice with PBS. The coverslips were gently removed from the bottom of the plate, placed onto slides with anti-fading polyvinyl alcohol mounting medium with DABCO®, and the edges sealed with clear nail polish. Coverslips were visualised with the Zeiss LSM 510 Meta Confocal Microscope (Carl Zeiss, Oberkochen, Germany). Images were analysed and processed with AXIO VISION 4.8 software (Zeiss, Germany). To view 5FAM a 505 nm long pass filter was used together with a 488/515 nm beam splitter. The DAPI settings remained the same as for the membrane permeability assay.

2.4.5 Scanning electron microscopy

To investigate the changes to biofilm cell ultrastructure after treatment with Os, SEM was employed. SEM focuses a high energy electron beam across the surface of the sample being investigated (Figure 2.6). The electrons interact with atoms in the sample, producing various electron signals, including secondary electrons (SE) and backscattered electrons (BSE) which are collected and processed, in order to produce a three dimensional image, conveying information regarding the samples surface morphology (Carter, 2015). Sample preparation for SEM involves coating the sample in a thin layer of conductive material such as Au. Coating reduces the electric charge that develops on samples after bombardment with electrons, which may result in image distortion. Furthermore, the high energy electron beam may cause thermal damage and loss of material from the sample under investigation, and thus coating further improves image quality.

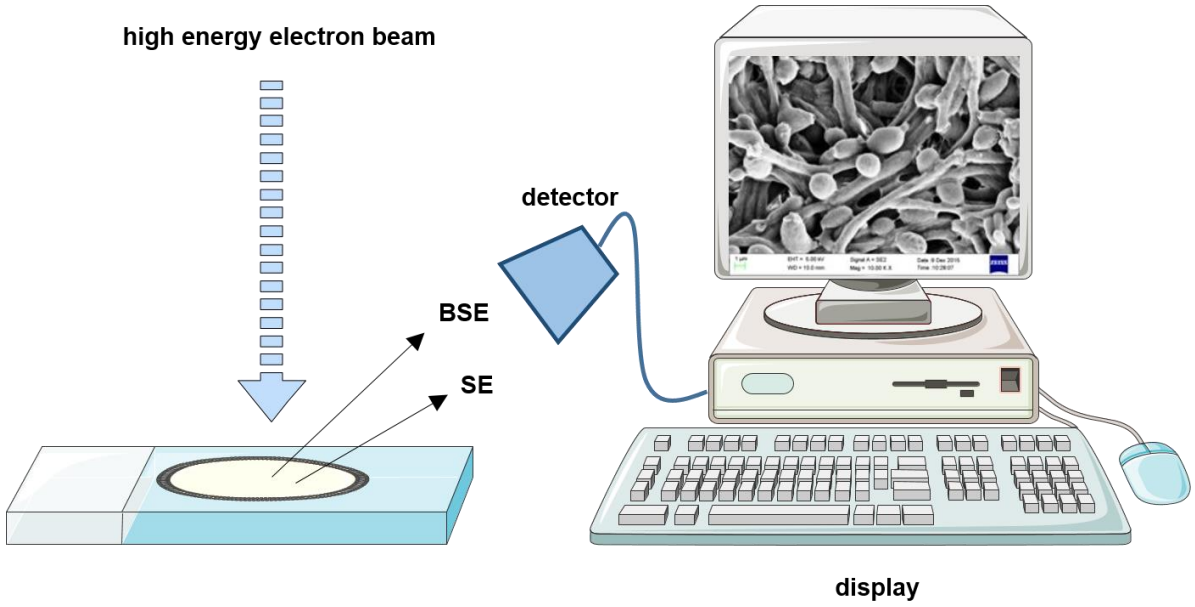

Figure 2.6: Schematic representation of how SEM operates. The surface of the sample is scanned with a high energy electron beam. The electrons interact with atoms in the sample to produce BSE and SE, which are collected by detectors and displayed on a monitor. Redrawn and adapted from (Zhu *et al.*, 2014).

Initial adherence of biofilms was performed as described in section 2.4.3. Subsequently, the adhered cells were further incubated with 500 µL of RPMI-1640, Os(11-22)NH_2 (81 µM), and Os (46 µM) for 24h. Upon incubation, biofilms were washed with PBS to remove non-adherent cells before being fixed with a solution containing 2.5% glutaraldehyde (*v/v*) and 2.5% formaldehyde (*v/v*) in 0.046 M PBS. After 1h of fixing, the biofilms were rinsed 3 times with 0.075 M PBS for 10 min each. The biofilms were then dehydrated with increasing concentrations of ethanol (30%, 50%, 70%, 90%, and 100%), 3 times for 10 min each. The biofilms on the coverslips were dried with HMDS for 1h, in a fume hood. After incubation, the HMDS was removed, and 2 more drops of HMDS was added to the biofilms. Samples were left to completely dry overnight. The dry coverslips were mounted with carbon tape onto aluminium stubs, and coated with carbon using the Q150T ES Turbomolecular pumped coater (Quorum Technologies, UK). Subsequently, samples were viewed using a crossbeam 540 field emission gun (FEG) SEM (Zeiss, Oberkochen Germany).

2.4.6 Data analysis

The BIC_{50} was defined as the lowest concentration required to reduce biofilm formation by 50% (Vriens *et al.*, 2015). Inhibition (%) in the anti-planktonic and anti-biofilm assays were calculated as follows:

$$Inhibition\ (\%) = 100 - [\frac{100\ x\ (a-b)}{c-b}]$$

Where a , is the average fluorescence of biofilms treated with an antifungal agent, b is the average background fluorescence, and c is the average fluorescence of the growth control respectively. Dose-response curves were generated and analysed using GraphPad Prism 7.00 (GraphPad Software, San Diego, CA, USA), using the non-linear and data normalization functions to produce sigmoidal curves. The same software was used for statistical analysis of the data. Analysis included 95% confidence levels, sum of squares, standard error of the mean (SEM), and one-way analysis of variance (ANOVA) for data indicating a normal distribution, using Tukey's multiple-comparison test. For data not indicating a normal distribution, analysis included non-parametric tests using the Kruskal-Wallis and Dunn's multiple comparisons tests. All experiments were obtained from at least 3 independent experiments, and are presented as mean ± SEM.

CHAPTER 3: Results

3.1 Anti-planktonic activity studies

3.1.1 Os is inactive against planktonic *C. albicans* cells

Drugs induce their effect through receptor or non-receptor mediated mechanisms and the intensity of the effect is most often increased, with increasing drug concentrations (Hartung, 1987). Plotting the effect of the drug against the logarithmic concentrations, yields a sigmoidal dose-response curve. Doses nearing the drug's maximum response may yield toxic effects, therefore the MIC of a drug is reported. The MIC is deemed the gold standard for antimicrobial susceptibility testing (Andrews, 2001), however, drugs need to be used at concentrations where their efficacy is not affected, as such the MIC_{50} is most frequently used. The microbroth dilution assay was performed in order to determine the MIC_{50} of Os, where AmpB was used as positive the control (Figure 3.1). The MIC_{50} was established within the inhibition parameters, MIC_{max} and $MIC_{min,}$ respectively, using a concentration range of 0.04 µM to 5 µM. AmpB exhibited antifungal activity against planktonic *C. albicans* cells with an MIC_{50} of 0.49 ± 0.06 µM.

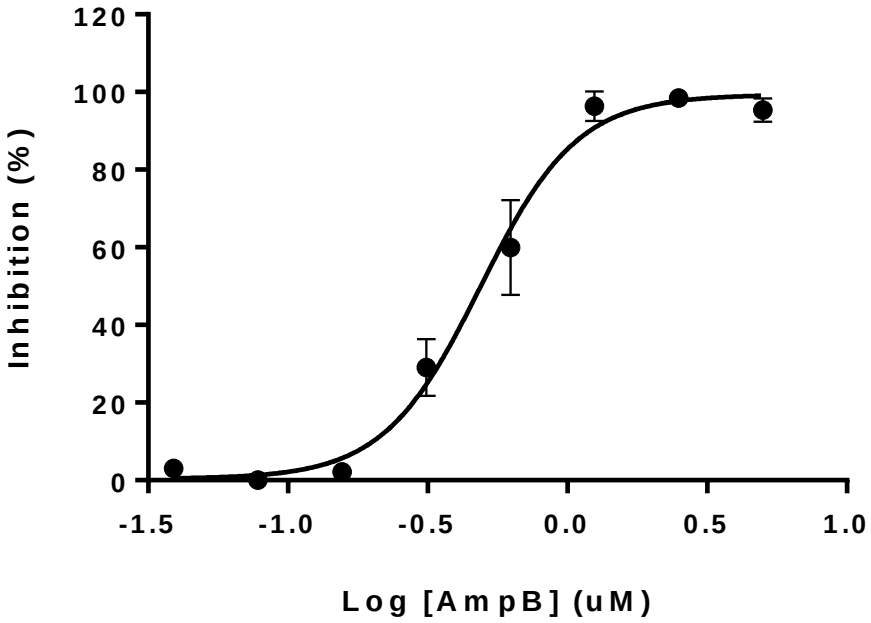

Figure 3.1: Dose-response curve for AmpB inhibition against planktonic *C. albicans* cells. Concentration range is 0.04 µM to 5 µM. Error bars represent mean ± SEM; n=3.

The microbroth dilution assay was performed in order to determine the MIC_{50} of Os. Os exhibited no antifungal activity against planktonic *C. albicans* cells when evaluated at a concentration range of 0.78 µM to 100 µM. The MIC_{50} values are presented in Table 3.1.

Table 3.1: Summary of the MIC_{50} values of AmpB, Os, and Os(11-22)NH_2

Compounds	MIC_{50} ± SEM (μM)
AmpB	0.49 ± 0.06
Os	NA
*Os(11-22)NH_2	*47 ± 0.30

*Included in table for comparative purposes Chiramba (2018). NA; no activity

3.2 Anti-biofilm activity studies

3.2.1 Mature biofilms are present at 24h

To investigate the effects of Os on biofilms it was necessary to determine the time it takes to for a mature *C. albicans* biofilm formation to develop. To achieve this a time course study was undertaken. *C albicans* cells were plated for 1.5h to ensure adherence. Unattached cells were removed by washing, and the adhered cells were allowed to grow for a further 2, 24 and 48h. Biofilm biomass determined with CV staining for the different time intervals is shown in Figure 3.2.

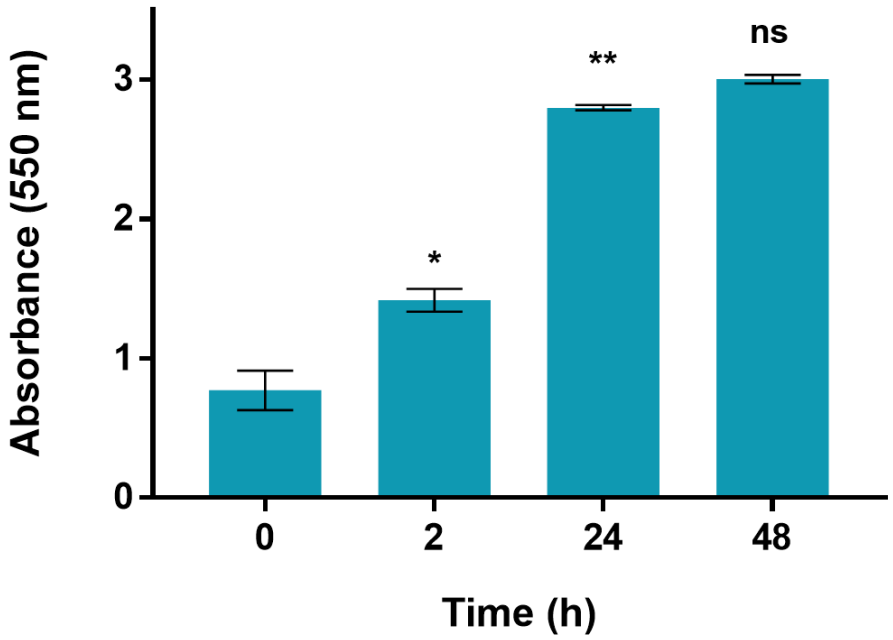

Figure 3.2: Analysis of *C. albicans* biofilm biomass at various points of a time study. *C. albicans* were initially incubated for 1.5h to ensure adherence. Once adhered, indicated as 0h, the biomass was determined after a further 2, 24 and 48h of growth. Error bars represent the mean ± SEM. Statistical differences between 0h vs 2h, 2h vs 24h and 24h vs 48h was determined. Data is generated from 3 independent experiments, each performed in triplicate. Differences * and ** represents $p < 0.05$ and $p < 0.01$ respectively and ns, no significant difference.

In this time study, the biomass of *C. albicans* biofilms increased with time. Statistical analysis indicates there is only a significant difference in biomass between 0h and 2h ($p < 0.05$), as well as between 2h and 24h ($p < 0.01$) of biofilm growth. The difference in biofilm biomass between 24h and 48h was not

significant, indicating that a complete biofilm had formed after 24h. Therefore, all subsequent studies were undertaken using a 24h biofilm.

The presence of a biofilm was further confirmed with light microscopy of CV stained *C. albicans* cultures/biofilms (Figure 3.3). These images indicated that at 0h, *C. albicans* cells had attached to the surface of the plate and grew rapidly (2h) to form well established biofilms at 24h and 48h. No differences in the density of the biofilms were observed between 24h and 48h (Figure 3.3), confirming quantitative findings (Figure 3.2), that a mature biofilm was established at 24h.

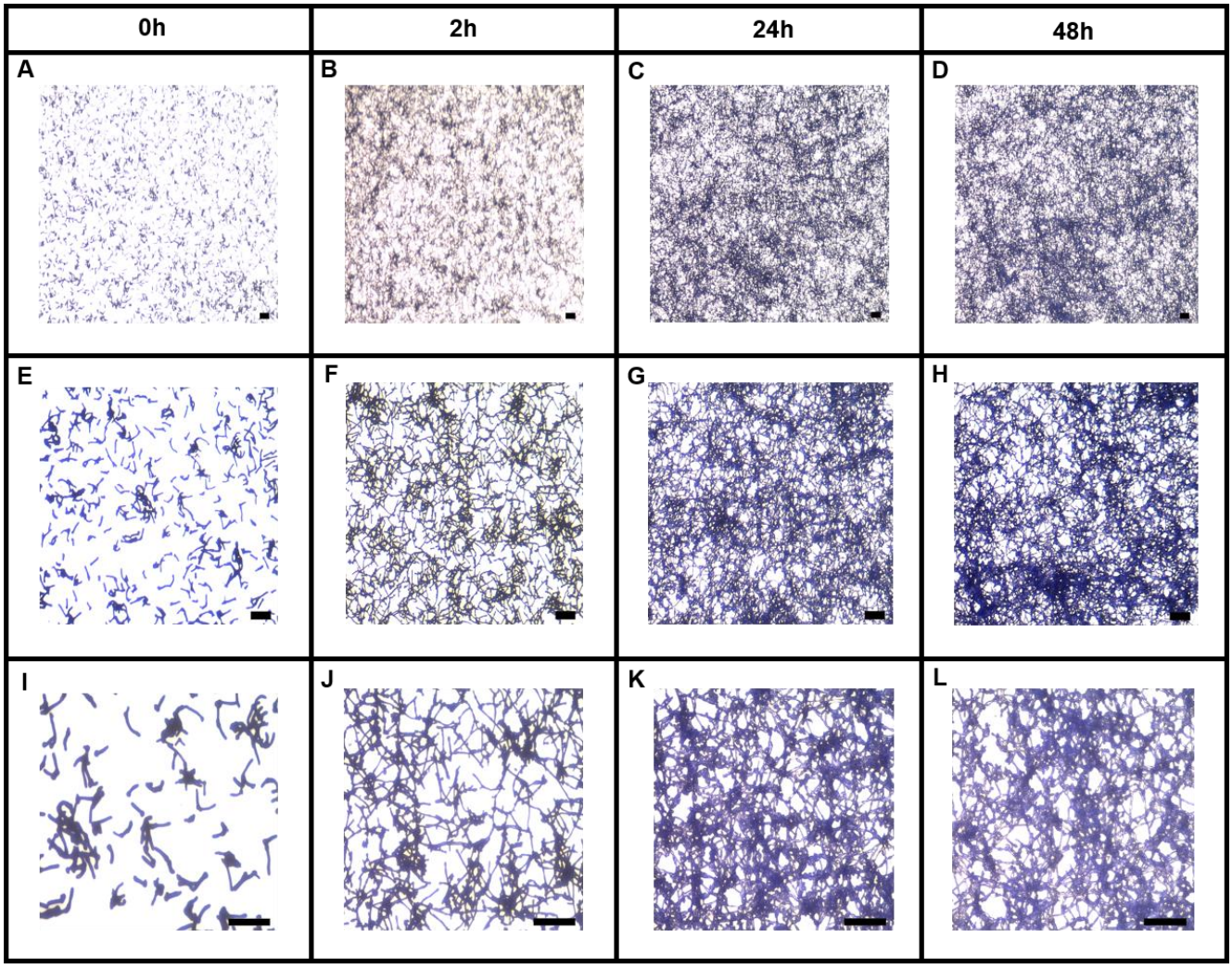

Figure 3.3: *C. albicans* biofilm morphology at various points of a time study. *C. albicans* were initially incubated for 1.5h to ensure adherence. Once adhered, indicated as 0h, the biofilms were grown for a further 2, 24 and 48h before being stained with crystal violet. Scale bars = 50 µm.

3.2.2 Os is able to inhibit biofilm formation

The ability of the control AmpB, and the peptide Os to inhibit *C. albicans* biofilm formation after 24h was then determined. The CTB Cell viability assay was used to determine the BIC_{50} of AmpB and Os. AmpB displayed a sigmoidal dose-response inhibition of *C. albicans* biofilm formation (Figure 3.4). The BIC_{50} for AmpB was determined as 0.28 ± 0.03 µM (Table 3.2).

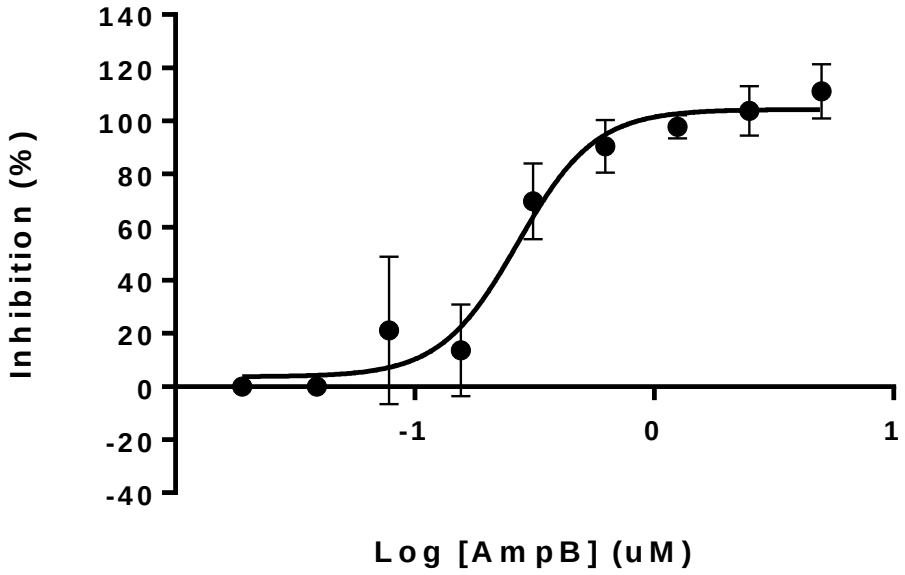

Figure 3.4: Dose-response curve for AmpB inhibition against *C. albicans* biofilms. Concentration range is 0.02 µM to 5 µM. Error bars represent mean ± SEM; n=3.

In contrast to the effects on planktonic *C. albicans* cells, Os displayed a typical sigmoidal dose-response inhibition of *C. albicans* biofilm formation. The BIC_{50} of Os was determined as 46 ± 4.45 µM (Figure 3.5) and is presented in Table 3.2.

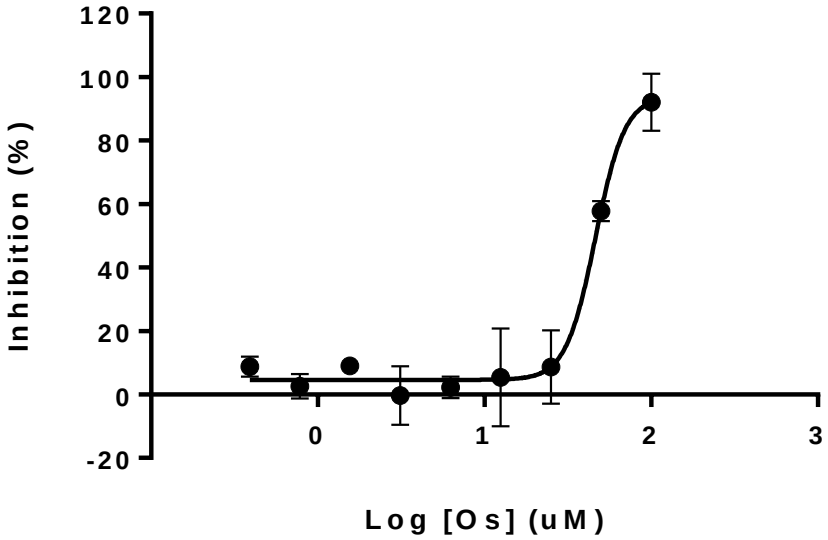

Figure 3.5: Dose-response curve for Os inhibition against *C. albicans* biofilms. Concentration range is 0.39 µM to 100 µM. Error bars represent mean ± SEM; n=3.

Table 3.2: Summary of the BIC_{50} values of AmpB, Os, and Os(11-22)NH_2

Compound(s)	BIC_{50} ± SEM (µM)
AmpB	0.28 ± 0.03
Os	46 ± 4.45
*Os(11-22)NH_2	81 ± 2.71

*Included in table for comparative purposes Chiramba (2018).

AmpB was the most effective in inhibiting *C. albicans* biofilm formation, and the activity of Os was approximately 2 fold greater than Os(11-22)NH_2 (Table 3.2). At these concentrations the mode of action was further investigated.

3.3 Anti-biofilm mode of action studies

3.3.1 Os targets the growth and development of adhered cells

Os(11-22)NH_2, was included in the mode of action studies for comparative purposes. In order to assess the effect that Os and Os(11-22)NH_2 had on *C. albicans* biofilm cell morphology, the biofilms were subsequently grown for 24h in the presence of Os and Os(11-22)NH_2, each at their respective BIC_{50} values, stained with CV and viewed using an inverted light microscope (Figure 3.6).

Compared to the growth control (Figure 3.6 A, D), biofilms treated with Os(11-22)NH_2 (81 µM) and Os (46 µM) appeared sparse and the density was less than the 2h cultures (Figure 3.3). Biofilms treated with Os(11-22)NH_2 appear to contain mostly round yeast cells with long hyphal cells (Figure 3.6 E), whereas Os treated biofilms contain mostly pseudohyphal, shorter hyphal cells, and a few round yeast cells (Figure 3.6 F). This indicates that Os(11-22)NH_2 and Os possibly have different modes of action. Os(11-22)NH_2 appears to be affecting the yeast to hyphal transition, whereas Os appears to be targeting the growth and development of the attached yeast cells.

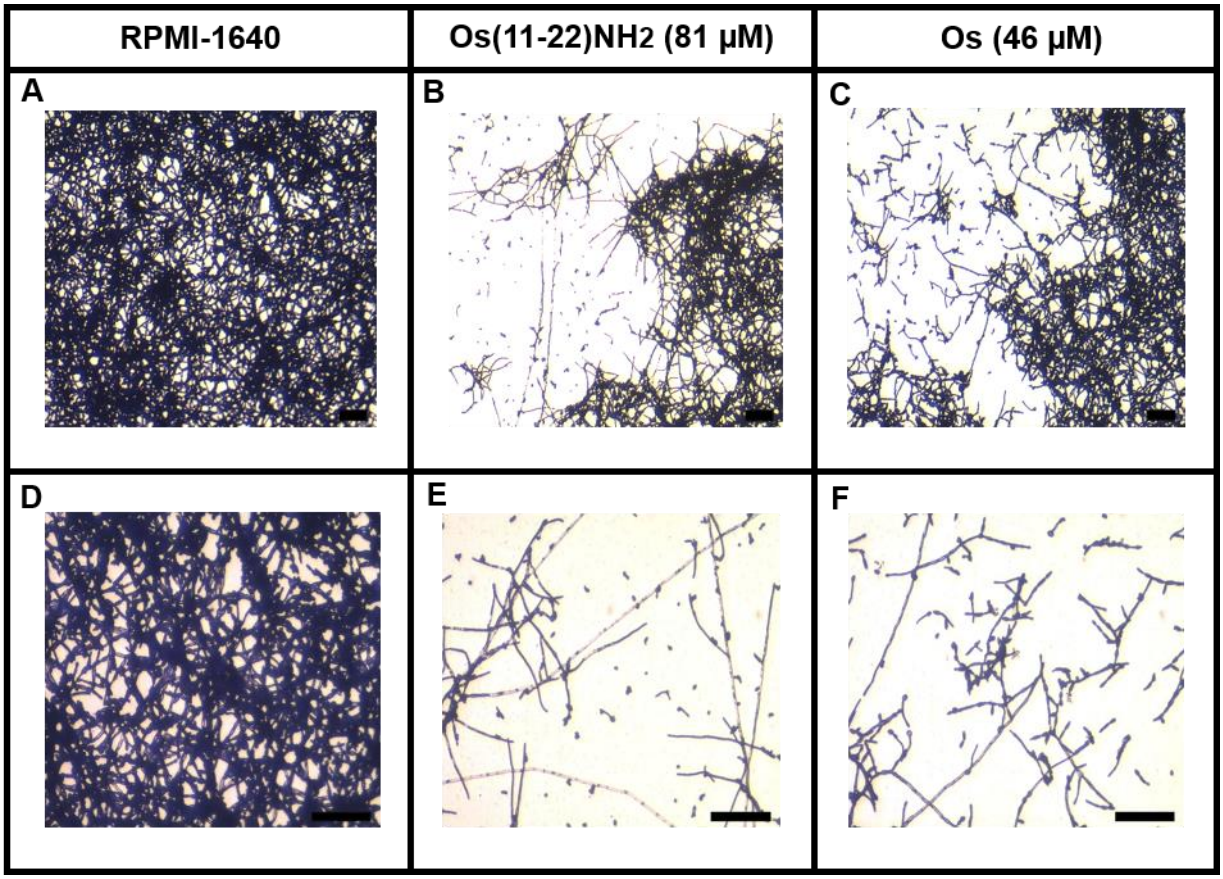

Figure 3.6: *C. albicans* biofilm cell morphology, after treatment with Os(11-22)NH_2 and Os. *C. albicans* were initially incubated for 1.5h to ensure adherence and then the peptides were added and the biofilms allowed to develop for 24h. The biofilms were then stained with crystal violet. **(A, D)** untreated controls, **(B, E)** exposed to 81 µM Os(11-22)NH_2 and **(C, F)** 46 µM Os. Scale bars = 50 µm.

3.3.2 Os induced ROS is not responsible for its biofilm inhibitory activity

The DCFH-DA assay was used to establish whether Os treatment leads to ROS production, in comparison to the untreated biofilms (Figure 3.7). Os(11-22)NH_2 which was previously shown to induce ROS production using the same assay (Chiramba, 2018) was used as a positive control.

Compared to the untreated control, treatment with AA and CA alone did not induce significant levels of ROS. Both Os(11-22)NH_2 and Os produced significantly more ROS ($p < 0.0001$) compared to the untreated control. The addition of AA to Os significantly decreased the presence of endogenous ROS in *C. albicans* biofilm cells ($p < 0.0001$).

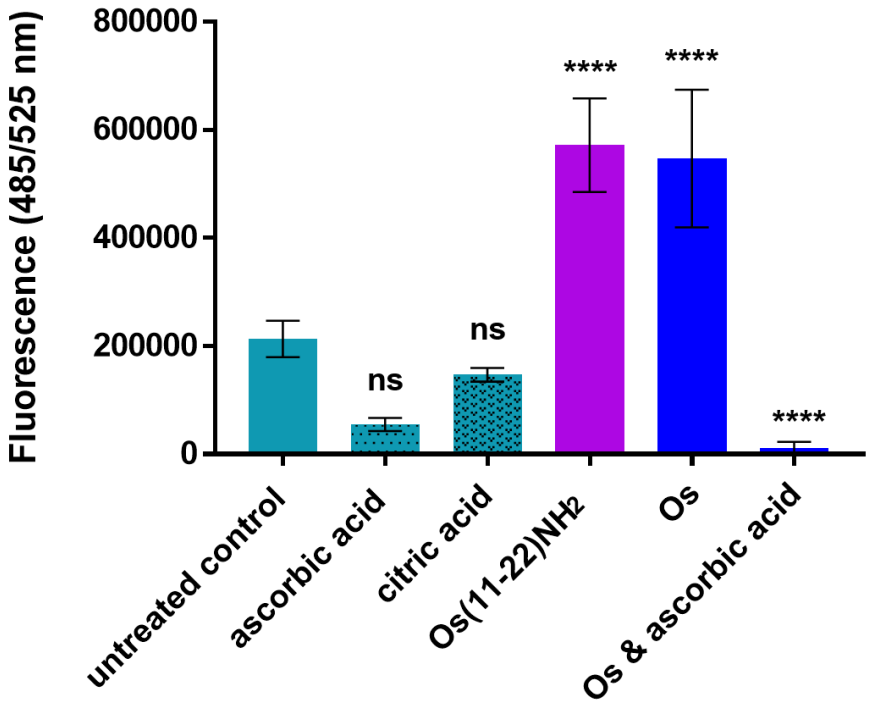

Figure 3.7: ROS production by *C. albicans* biofilms after treatment with Os. Biofilms were grown in the presence of 81 µM Os(11-22)NH_2 (ROS control), citric acid (10 mM; pH control) or ascorbic acid (10 mM), as well as Os (46 µM) on its own and in combination with ascorbic acid (10 mM). Error bars represent the mean ± SEM. Differences compared to the untreated control were not significant (ns) or significant where **** represents $p < 0.0001$. Data is generated from 3 independent experiments, each performed in triplicate.

In order to determine whether ROS formation is a mode of action, the ability of Os to inhibit biofilm formation in the presence of AA was determined. (Figure 3.8). The addition of AA did not decrease the activity of Os, but instead AA significantly enhanced ($p < 0.05$) the activity of Os.

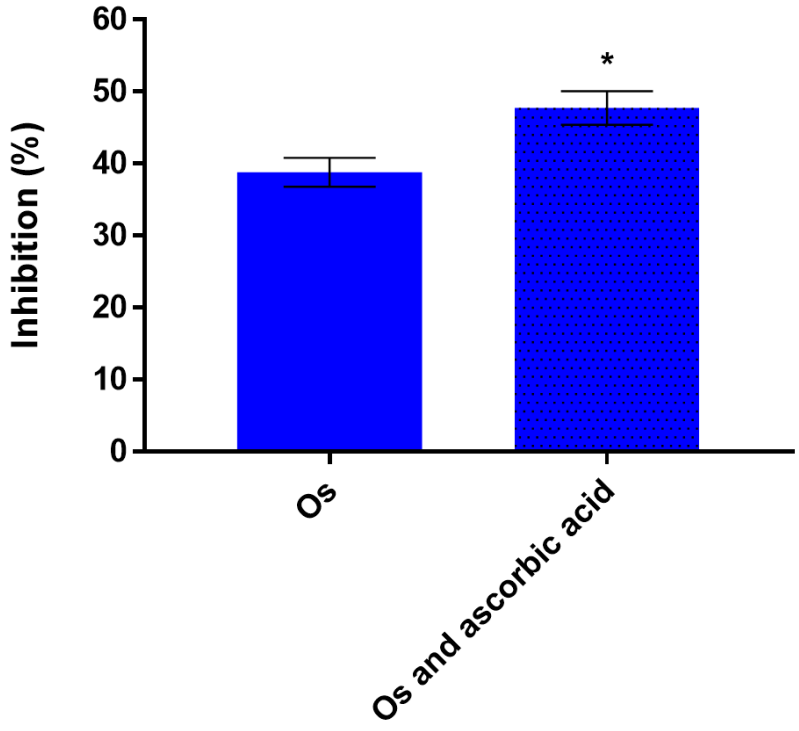

Figure 3.8: Biofilm inhibitory activity of Os and Os in combination with ascorbic acid. Following attachment, *C. albicans* biofilms were allowed to develop in the presence of Os (46 µM) as well as Os (46 µM) in combination with ascorbic acid (10 mM). Data is generated from 3 independent experiments, each performed in triplicate. Error bars represent the mean ± SEM. Compared with Os, the level of significance * is $p < 0.05$.

3.3.3 Os does not inhibit biofilm formation through membrane permeabilisation

The membrane disrupting activity of Os on *C. albicans* biofilms, was determined using PI and DAPI staining (Figure 3.9). PI can only enter cells with damaged plasma membranes, while DAPI will stain all cells with intact and damaged plasma membranes. No PI staining of untreated biofilms was observed. Strong staining was observed, for the positive control, pre-formed biofilms exposed for 30 min to the non-ionic detergent Triton-x 100. Incubation with Os(11-22)NH_2 resulted in a more sparse biofilm with strong PI staining. In contrast, no PI staining was observed for Os treated biofilms. The decreased DAPI staining for Os exposed *C. albicans* biofilms indicates biofilm inhibition.

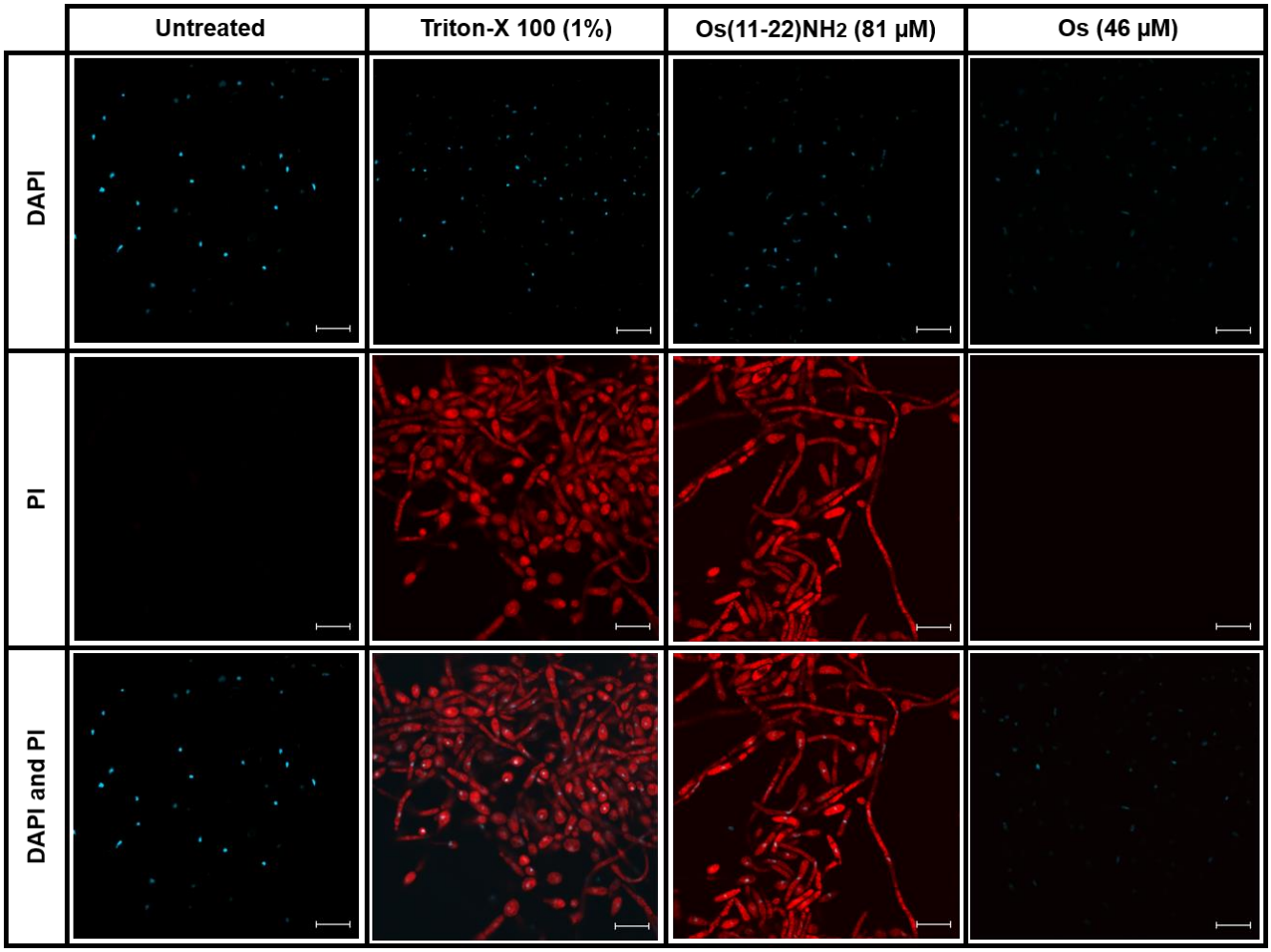

Figure 3.9: Confocal laser scanning microscopy images of untreated and treated biofilms. Following adherence, biofilms were grown in the presence of Os(11-22)NH_2 (81 µM) and Os (46 µM) for 24h. For the positive control, biofilms were grown for 24h and were then treated with Triton-X 100 (1%) for 30 min. Following exposure, all biofilms were first stained with PI (red) and then with DAPI (blue). Red staining indicates a loss of membrane integrity, which leads to an increase in permeability. Scale bars = 10 µm.

3.3.4 Os enters *C. albicans* biofilm cells

In order to determine whether intracellular localisation of Os leads to biofilm inhibition, biofilms were grown in the presence of fluorescently labelled 5FAM-Os, and observed with CLSM (Figure 3.10). 5FAM-penetratin was used as a positive control, and 5FAM-Os(11-22)NH_2 was used for comparison. DAPI served as the nuclear counterstain.

The number of DAPI stained nuclei was reduced for biofilms grown in the presence of 5FAM labelled penetratin, Os(11-22)NH_2 and Os, indicating that labelling with 5FAM did not adversely affect the biofilm inhibitory activity of the peptides.

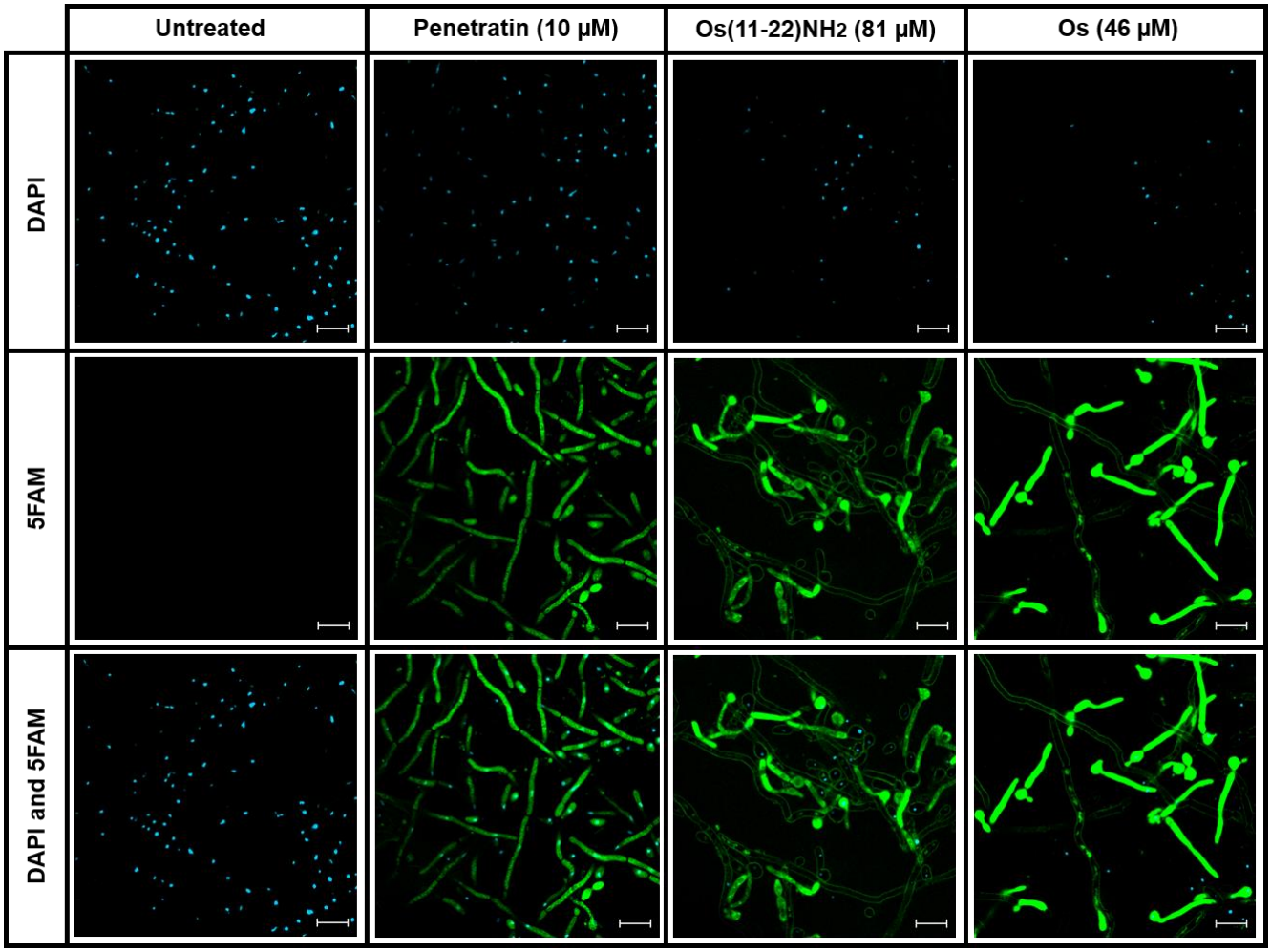

Figure 3.10: Confocal laser scanning microscopy images of *C. albicans* biofilms treated with 5FAM-Os, and subsequently stained with DAPI. Following adherence, biofilms were grown in the presence of 5FAM-penetratin (10 µM), 5FAM-Os(11-22)NH_2 (81 µM) and 5FAM-Os (46 µM) for 24h. This was followed by DAPI staining. Green staining indicates localisation of the peptides whereas blue staining indicates nuclear DNA. Scale bars = 10 µm.

Penetratin is a peptide known to translocate the membrane of cells (Madani *et al.*, 2011). Biofilms treated with 5FAM-penetratin displayed a homogenous distribution of green fluorescence in typical hyphal cells, confirming the ability of penetratin to cross the membranes of *C. albicans* biofilm cells.

In 5FAM-Os(11-22)NH_2 treated biofilms, green fluorescence was associated with the plasma membrane or cell wall and was located intracellularly in predominately hyphae. Likewise 5FAM-Os treated biofilms also displayed green fluorescence staining which was associated with the plasma membrane or cell wall. In contrast, intracellular staining was of greater intensity and was more intense than was observed for 5FAM-Os(11-22)NH_2.

At a higher magnification (Figure 3.11), 5FAM-Os(11-22)NH_2 treated biofilms displayed plasma membrane or cell wall staining of rounded yeast cells and hyphae (white arrows), with pseudohyphal cells displaying low intensity intracellular staining. Some intracellular targets were observed in hyphae

for Os(11-22)NH_2 treated biofilms (red arrow). Plasma membrane or cell wall staining of 5FAM-Os treated biofilms was mostly apparent for the hyphal cells, while budding yeast and pseudohyphal cells displayed intense intracellular fluorescence (white arrows), with specific intracellular targets in hyphae (red arrow). Os(11-22)NH_2 and Os both are associated with the cell wall or plasma membrane, while differences in permeability and intensity of staining with labelled peptides indicates different modes of action.

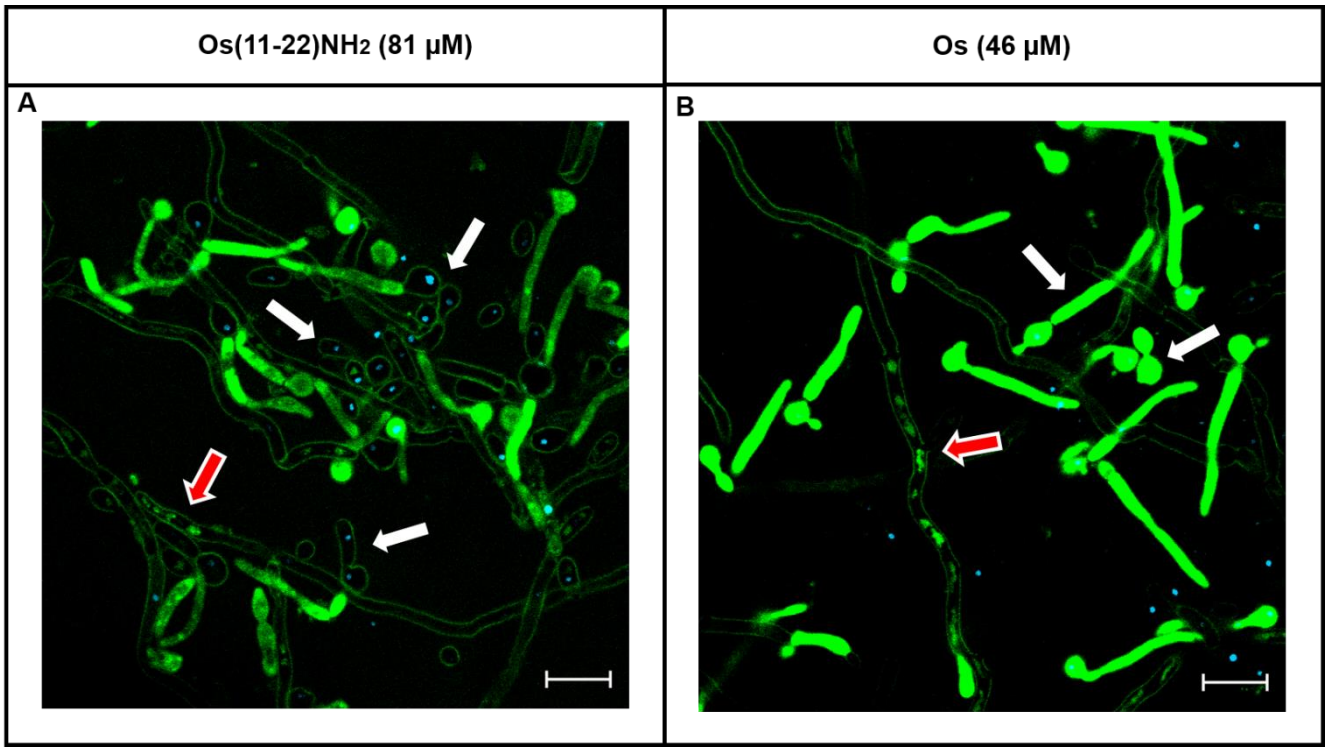

Figure 3.11: Higher magnification of *C. albicans* biofilms treated with 5FAM-Os(11-22)NH_2 and 5FAM-Os (both green), and subsequently stained with DAPI (blue) and analysed with confocal laser scanning microscopy. White arrows indicate planktonic and pseudohyphal staining, while the red arrow shows intracellular accumulation. Scale bars = 10 µm.

3.3.5 Os induces changes to biofilm cell ultrastructure

C. albicans forms complex biofilms composed of various cell types, including round yeast or budding cells, tubular pseudohyphal cells and elongated hyphal cells respectively. Each cell type identified by SEM in the *C. albicans* biofilms established in this study are presented in Figure 3.12. The ECM is absent, due to the solubility of the ECM in the solvents used for sample preparation.

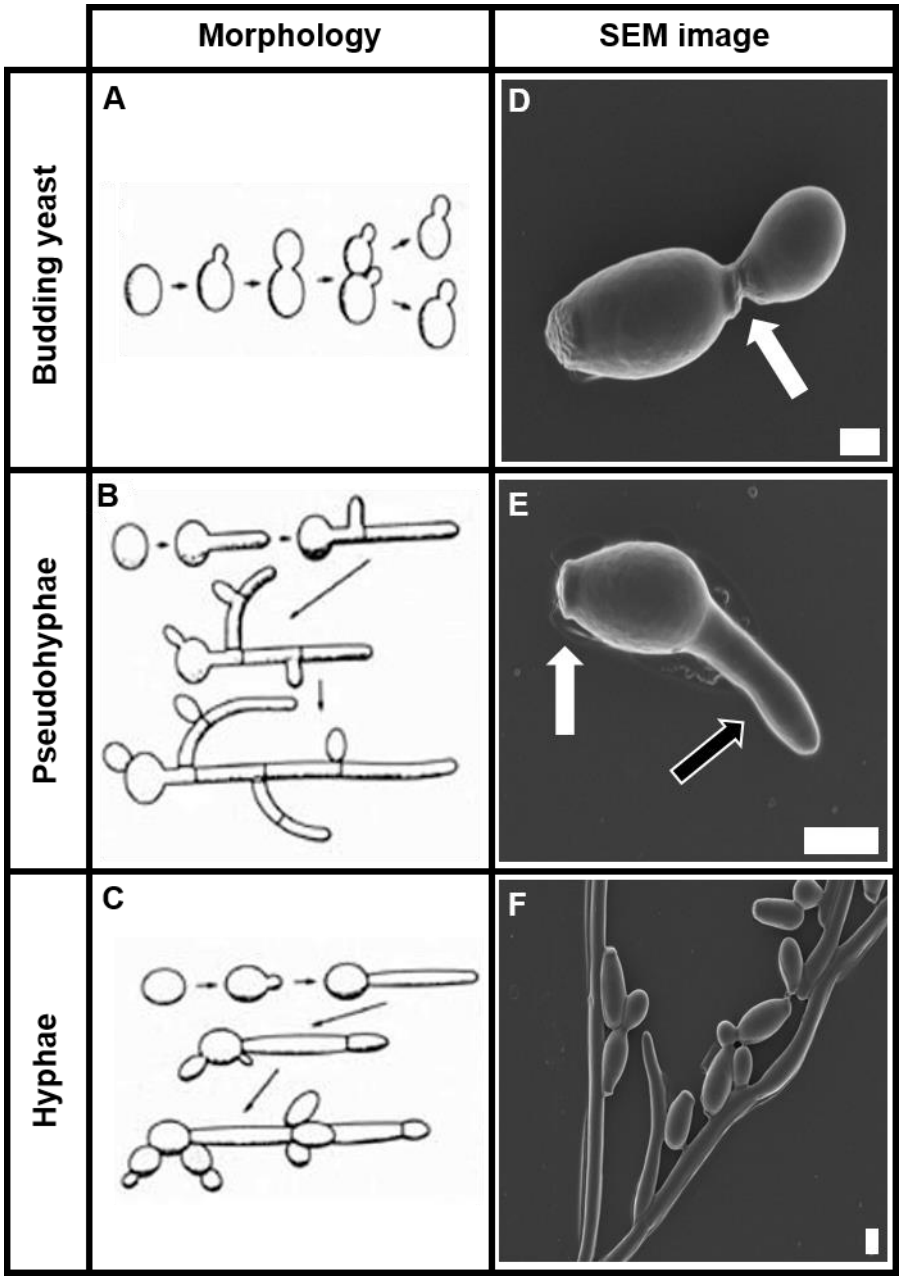

Figure 3.12: Various morphologies of *C. albicans* that occur within a biofilm, along with corresponding SEM images. (A-C) Morphologies, adapted from http://www.med.uvm.edu/mmg/Calbicanscells.jpg and **(D-F)** corresponding SEM images obtained in this study. White arrows indicate bud scars, the black arrow indicates the germ tube. Scale bars D, F = 1 µm, bar E = 2 µm.

Round yeast cells also known as blastospores, produce daughter cells by budding (Figure 3.12 A and D). Initially a small bud (protrusion) forms on the mother cell, and enlarges with cell growth to become the daughter cell. Following duplication of its genetic material, the DNA divides and migrates into the daughter cell. The mature daughter cell separates from the mother cell, leaving behind scar tissue known as a bud scar (Figure 3.12 E white arrow). Hyphal formation involves the formation of a germ tube (Figure 3.12 E black arrow), which develops from pre-existing blastospores. The blastospore with a germ tube is commonly known as pseudohyphae (Figure 3.12 B and E). Cells in the germ tube undergo mitotic division, however cell separation is supressed forming chains of identical cells known as hyphae (Figure 3.12 C and F).

The effects of Os(11-22)NH_2 and Os on biofilm formation was further evaluated with SEM in order to identify specific cellular effects or targets. The major cell type found in biofilms treated with Os(11-22)NH_2 were round yeast cells, localised between elongated and tubular hyphae (Figure 3.13 B). In contrast, biofilms treated with Os, contained fewer round yeast cells, with the hyphae appearing to be less elongated and flattened, rather than tubular (Figure 3.13 C), indicating different effects and confirming the differences in biofilm morphology previously observed using CV staining (Figure 3.6).

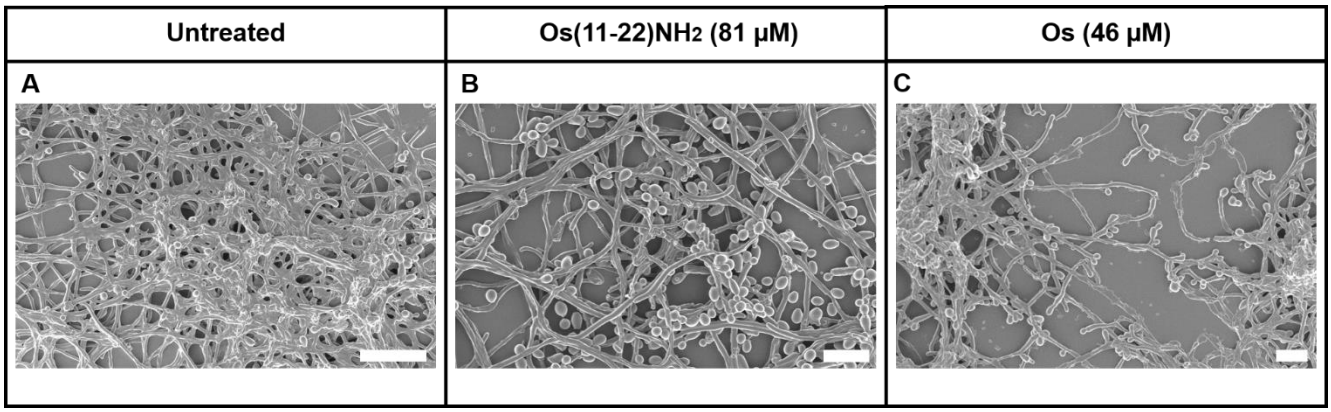

Figure 3.13: *C. albicans* biofilm morphology evaluated using SEM. Untreated **(A)**, treated with **(B)** 81 µM Os(11-22)NH_2 and **(C)** 46 µM Os. Scale bars = 10 µm.

A more detailed study on the effect of these peptides on yeast cells, pseudohyphae and hyphae found in *C. albicans* biofilms was then undertaken. In the untreated cultures, yeast cells generally appeared as spherical or ovoid cells with a smooth cell membrane, with a bud scar usually being present (Figure 3.14 A). Pseudohyphal and hyphal cells are elongated, rod shaped, also with smooth cell walls (Figure 3.14 B and C).

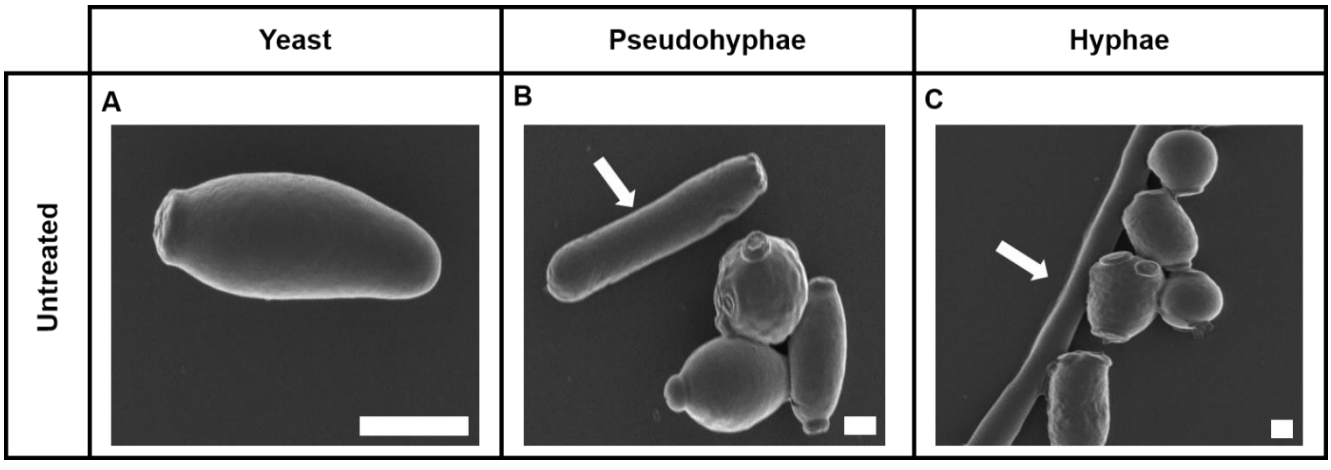

Figure 3.14: Normal morphology of yeast, pseudohyphae, and hyphae of *C. albicans* cells present in biofilms evaluated with SEM. (A) Yeast, **(B)** pseudohyphae, and **(C)** hyphae. Scale bars B, C = 1 µm, bar A = 2 µm.

Evaluation of the morphology of remaining yeast cells after exposure to Os(11-22)NH_2, revealed yeast cells with surface indentations (Figure 3.15 A and B), with some cells displaying a shrivelled morphology (Figure 3.15 C) indicating a loss of intracellular content. Yeast cells in Os treated biofilms were fewer in number (Figure 3.13 C) and some Os treated yeast cells had cracks or tears (Figure 3.15 D and F), displayed a shrivelled or wrinkled appearance (Figure 3.15 E and F) with bud scars still recognisable (Figure 3.15 E).

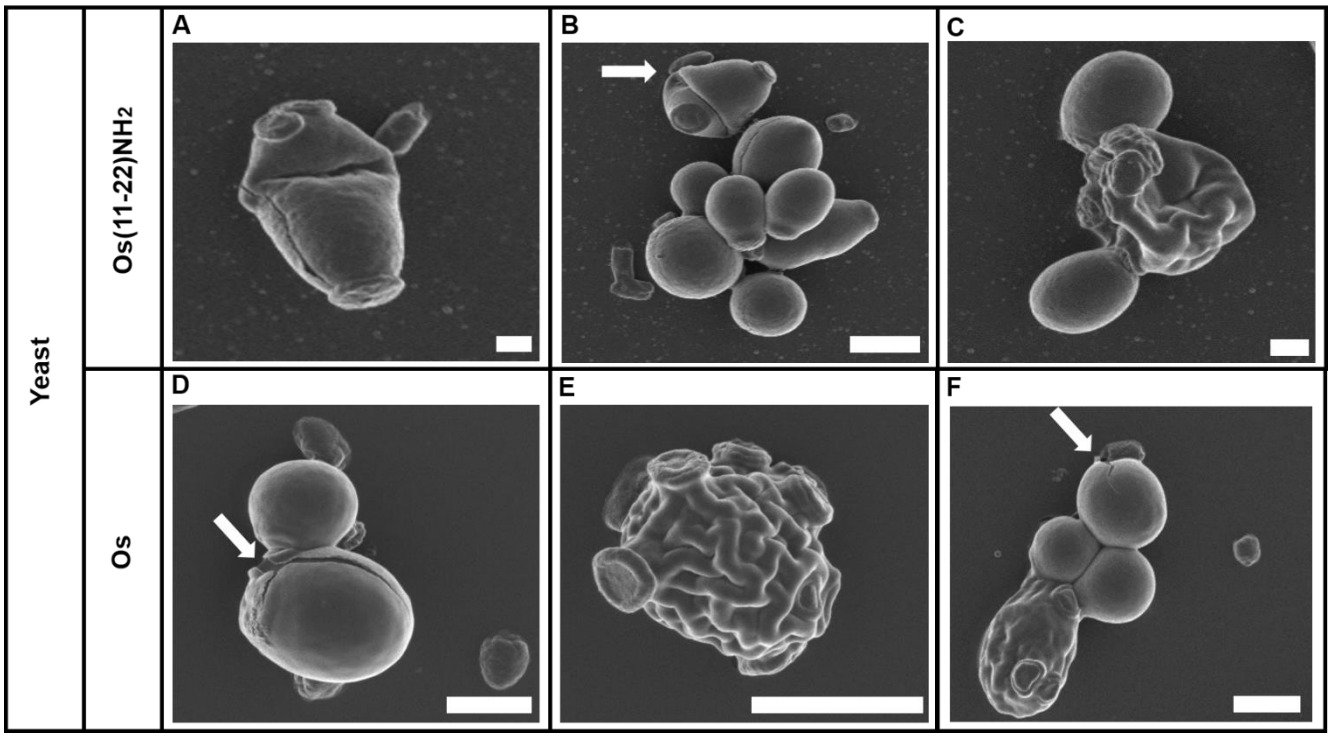

Figure 3.15: Morphology of yeast cells found in *C. albicans* biofilms following treatment with Os(11-22)NH_2 and Os, evaluated with SEM. (A-C) Os(11-22)NH_2 (81 µM), **(D-F)** Os (46 µM). White arrows indicate **(B)** indentation, and **(D and F)** cracking. Scale bars A, D, F = 1 µm, bars B and C, E = 2 µm.

The effects on *C. albicans* pseudohyphal cells were also determined (Figure 3.16). Os(11-22)NH_2 caused changes to the cell membrane with the formation of pits (Figure 3.16 B and C, white arrows). Mother cells appeared to be more circular or rounded, rather than ovoid (Figure 3.16 A - C). Os induced more pseudohyphae reducing membrane smoothness, and these cell types are presented with a shrivelled, shrunken morphology (Figure 3.16 D and E). Mother cells were generally unaffected and ovoid in morphology (Figure 3.16 E and F). Cellular debris surrounding some of the cells was also observed (Figure 3.16 A and F, white arrows).

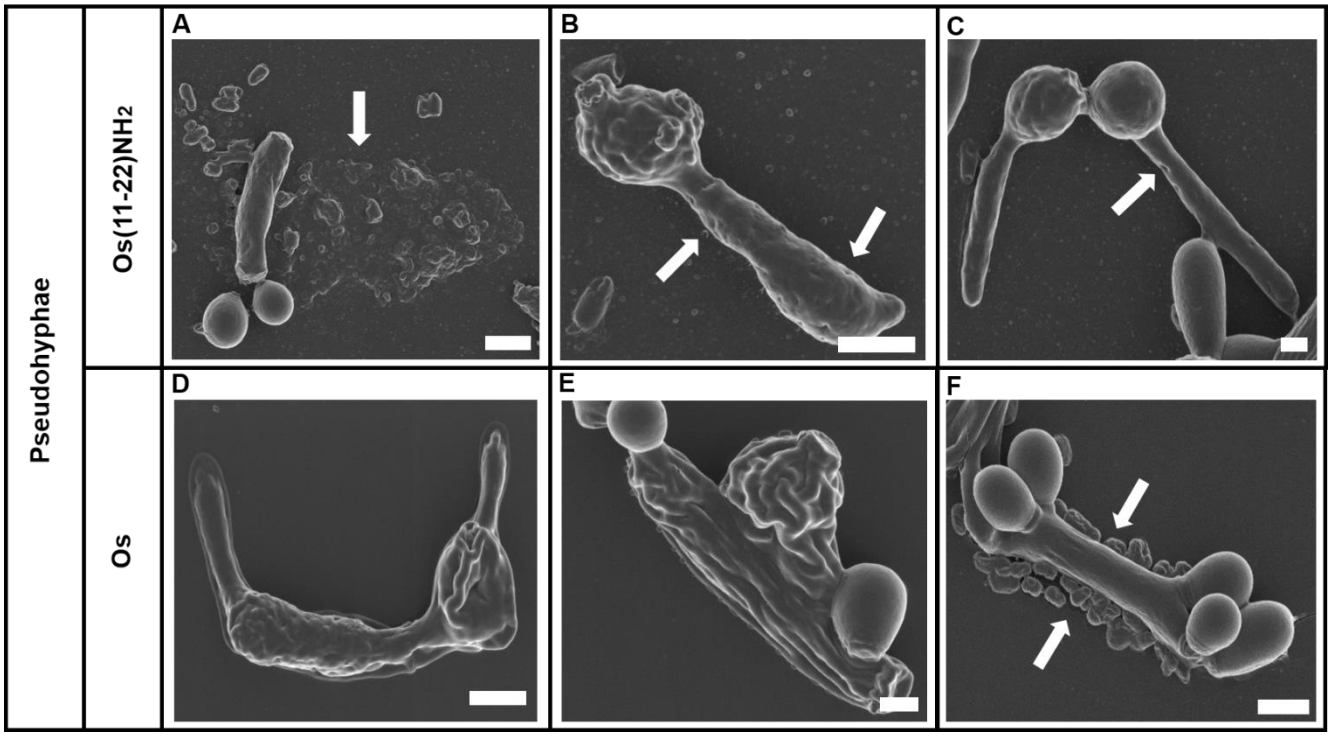

Figure 3.16: Morphology of pseudohyphae found in *C. albicans* biofilms following treatment with Os(11-22)NH_2 and Os, evaluated with SEM. (A-C) Os(11-22)NH_2 (81 µM), **(D-F)** Os (46 µM). White arrows indicate **(A,F)** cellular debris, and **(B – C)** pits. Scale bars A, B, D, F = 2 µm, bars C, E = 1 µm.

The effects on *C. albicans* hyphal cells was lastly determined (Figure 3.17). The hyphae of untreated cells mostly appeared to be elongated with smooth cell membranes (Figure 3.14 C). The hyphae of Os(11-22)NH_2 treated cells appeared mostly unaffected, with minimal changes to cell surface, and confirms the findings in Figure 3.13 B. In contrast, exposure to Os caused a loss of membrane smoothness with an increase in surface roughness (Figure 3.17 D, white arrow), and the formation of small blebs (Figure 3.17 E, white arrows). Cracks and tears were a typical feature, and were present in hyphae and budding cells (Figure 3.17 D - F, black arrows). Changes in the hyphae structure reflect the changes in structure observed in Figure 3.13.

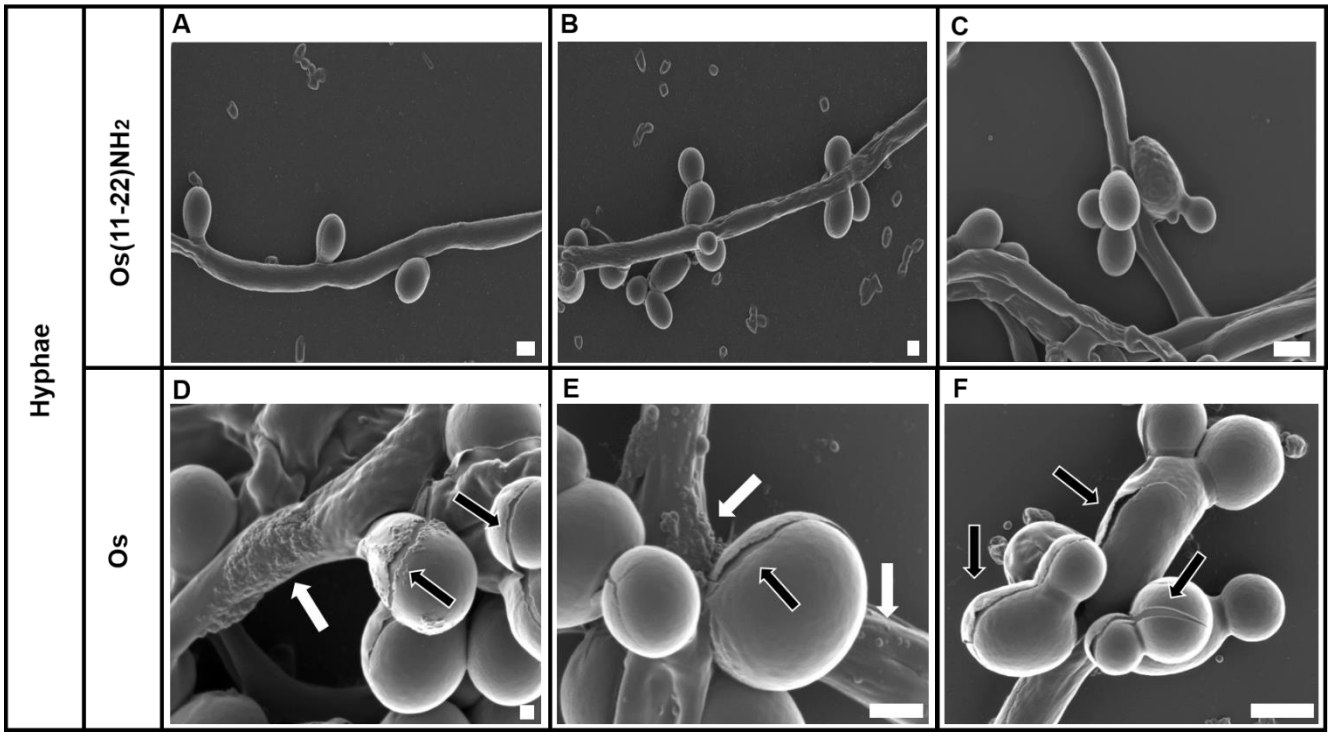

Figure 3.17: Morphology of hyphae found in *C. albicans* biofilms following treatment with Os(11-22)NH_2 and Os, evaluated with SEM. (A-C) Os(11-22)NH_2 (81 µM), **(D-F)** Os (46 µM). White arrows indicate **(D)** surface roughness (white arrow) and **(E)** blebs (white arrows). Black arrows indicate **(D – F)** cracks and tears. Scale bars C, F = 2 µm, bars A, B, D, E = 1 µm.

CHAPTER 4: Discussion

C. albicans is generally harmless, forming part of the normal microbiota of human health, colonising areas such as the GI tract, reproductive tract of females, and the oral cavity. However, infections and the use of antibiotics may alter the immune status of individuals, causing *C. albicans* to rapidly proliferate and cause an infection (Fox & Nobile, 2013). As such, hospital patients are at great risk of contracting hospital-acquired (nosocomial) infections. *Candida* spp are the most common cause of fungal nosocomial infections, with *C. albicans* being the prevalent cause (Ramage *et al.*, 2005). Furthermore, *Candida* is capable of forming disseminated bloodstream infections with mortality rates reaching 47% (Fox & Nobile, 2013). This yeast accounts for 15% of sepsis cases and is the leading cause of 40% of all bloodstream infections in clinical environments (Nobile & Johnson, 2015). Thus, in immunocompromised individuals, including HIV and chemotherapy patients, as well as those with implanted medical devices (Kojic & Darouiche, 2004), *C. albicans* poses an even greater risk in comparison to immunocompetent individuals. Furthermore, *C. albicans* is capable of forming biofilms.

C. albicans biofilms which have the ability to initiate bloodstream infections that may lead to invasive infections of various tissues and organs are highly resistant to antifungal drugs. There are 3 major classes of antifungal agents used to treat fungal infections including the azoles, polyenes and echinocandins. *C. albicans* biofilms have developed resistance to the majority of these drugs (Gulati & Nobile, 2016), and this further limits the number of antifungal agents available for treatment. This highlights the need for the development of novel antifungal therapies against *C. albicans* biofilms. AMPs are small, cationic, amphipathic peptides that serve as the first line of defence against invading pathogens. They inhibit a broad spectrum of microorganisms with minimal toxicity to the host (Matejuk *et al.*, 2010). Therefore, AMPs and their derivatives may serve as a source of novel antifungal agents.

In this study, the antimicrobial peptide Os was investigated for its ability to inhibit biofilm formation and its mode of action was further explored. Initially, a time based study was performed in order to confirm the presence of a mature *C. albicans* biofilm at 24h. After 24h no increase in biofilm biomass (Figure 3.2) was observed, and light microscopy revealed the formation of dense hyphae after 24h (Figure 3.3), typical of biofilms, similar to that described by Nobile and Johnson (2015) as well as Gulati and Nobile (2016). *C. albicans* forms complex biofilms composed of various cell types, including round yeast cells, tubular pseudohyphal cells and elongated hyphal cells respectively. The formation of *C. albicans* biofilms begins with the adherence of round yeast cells (blastospores), (Sardi *et al.*, 2013a) to a solid surface, and typically occurs within 30 min to 1.5h (Gulati & Nobile, 2016). In this study, the adherence phase was set at 1.5h. Following the adherence period, tubular pseudohyphal cells can be seen (Figure 3.3 indicated as 0h). Following adherence, subsequent steps in biofilm formation involve cell proliferation and early stage filamentation of the adhered cells. Hyphal development involves the formation of an outgrowth known as a germ tube (young hyphae), which develops from pre-existing

blastospores, as is observed at 0h. The absence of isolated blastospores at 0h indicates that early cell proliferation has already begun. These tubular pseudohyphal cells form the anchoring basal layer for the biofilm. This observation is line with *C. albicans* biofilms grown *in-vitro*, which often comprise of a foundation of yeast cells, from which a hyphal layer emerges (Douglas, 2003). The switch from yeast to hyphal morphology is a pivotal step in biofilm development, as well a major determinant for virulence. Hyphal growth and elongation appears to increase substantially between 2h and 24h (Figure 3.3), where all germ tubes appear to have increased in length. This result is confirmed (Figure 3.2) where a significant increase in biofilm biomass between 2h and 24h is observed. Moreover, biofilm maturation involves the formation several layers of hyphal cells, as well as the addition of the ECM. After 24h of biofilm growth (Figure 3.3), the cells appear to have substantially elongated, with a thicker density being apparent. Biofilms grown for 24h versus 48h appear to be similar. This result is confirmed (Figure 3.2), where no significant difference in biofilm biomass occurred between 24h and 48h respectively. Therefore, a mature biofilm appears to have formed after 24h. Maturation also involves the addition of the ECM, however cryo-SEM is required to confirm the presence of the ECM.

Fungal hyphae result from anisotropic growth, which is the occurrence when growth rates are not equal in all directions, thus cells grow quicker in one direction than in another. Notably, cell shape may also be anisotropic. In fungi, anisotropic growth as hyphae plays vital roles in mating, colonisation as well as nutrient acquisition. In *C. albicans*, hyphal development is important for pathogenesis, as seen in the decrease in virulence in hyphal-defect mutants for mucosal infections. Hyphal initiation begins with the development of a polarity axis for anisotropic growth to occur (Desai, 2018). Moreover, hyphal formation involves the formation of a germ tube. The germ tube subsequently extends, with growth occurring only at the tip. The hyphae of fungi only grow at their tips, and this is termed apical growth (Figure 4.1). Throughout apical growth, there is a continuous movement of protoplasm from the older regions of the hyphae to the newer hyphal tip. Older areas behind the tip may eventually be broken down by autolysis. The extreme tip of all growing hyphae contain large amounts of Golgi-derived, membrane-bound vesicles, collectively termed the apical vesicle cluster (AVC) or the spitzenkorper (“apical body”). Furthermore, the cell wall at the hyphal tip is thinner in comparison to the cell wall behind the tip.

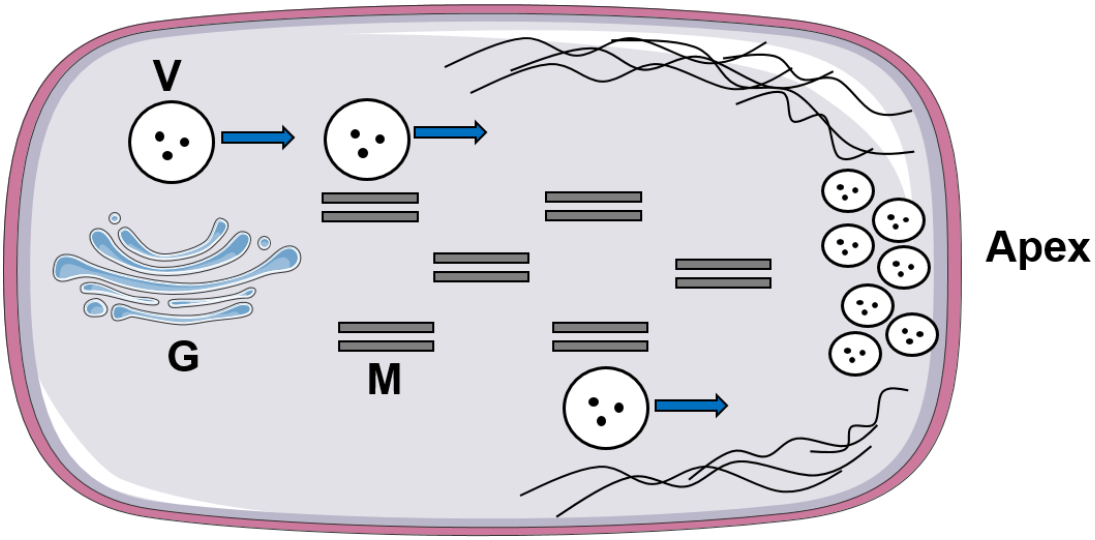

Figure 4.1 Schematic representation of the apical growth of hyphae in *C. albicans*. Secretory vesicles **(V)** derived from the golgi **(G)** are transported by cytoskeleton tracks, such as microtubules **(M)** to the apex of the hyphae, where the vesicles carrying cell wall material fuse with the plasma membrane and release their contents. Adapted from http://archive.bio.ed.ac.uk/jdeacon/microbes/apical.htm with modifications.

Within the centre of this structure no vesicles occur. The spitzenkorper may be observed as a dark body with light microscopy. Secretory vesicles carrying material required for cell wall synthesis (including the enzyme chitin synthase) are delivered to the tip by tracks formed by the cytoskeleton, where they first fuse with a structure known as the exocyst, followed by fusion to the plasma membrane (Sudbery, 2008). The region behind the extreme hyphal tip, is rich in mitochondria, and important for nutrient uptake at the hyphal tip. Parallel to tip-expansion, cells of the germ tube undergo mitotic division, however, cell separation is supressed (Sudbery, 2011). Thus, hyphae are chains of identical cell types. However, the presence of septa suggests hyphae are chains of interconnected compartments rather than cells. Furthermore, several nuclei may also be found in the apical compartment. However, under certain environmental conditions, the nuclei may traverse septal pores (Roper *et al.*, 2011).

Before testing Os for biofilm inhibitory activity, Os was first screened for antifungal activity against planktonic *C. albicans* cells. Os had no activity against planktonic *C. albicans* cells. The positive control AmpB, displayed anti-planktonic activity characterised by an MIC_{50} value of 0.49 ± 0.06 µM (Figure 3.1) and was comparable to 0.26 ± 0.01 µM reported by Troskie *et al.* (2014). Os(11-22)NH_2 was used for comparison, with the MIC_{50} (Table 3.1) previously established as 47 ± 0.30 µM (Chiramba, 2018). Physicochemical properties should be considered when investigating the lack of antifungal activity of Os, in comparison to Os(11-22)NH_2. Os is a relatively short peptide with 22 residues, 6 hydrophobic residues, and a net charge of +6 (Table 1.3). Positive charges drive peptide binding to negatively charged lipid bilayers through electrostatic interaction (Matsuzaki *et al.*, 1991). Os(11-2)NH_2 is smaller in size, comprises the C-terminal end of Os, and contains in its sequence the 3 Cys residues present in Os. Moreover, Os(11-22)NH_2 is less positively charged than Os, with a net charge of +4 (Table 1.3). Previously, Os and Os(11-22)NH_2 were both shown to have activity in sodium phosphate buffer (NaPB),

a low salt environment (Mbuayama, 2016). Moreover, in the same medium both peptides were able to cause membrane permeabilisation in planktonic *C. albicans* cells, with Os showing increased activity over Os(11-22)NH_2. This suggests that Os relies more on electrostatic interactions, and therefore binds more strongly to the plasma membrane of planktonic *C. albicans* cells. The majority of AMPs show a reduction in their activity in the presence of salts (Marr *et al.*, 2006). RPMI-160 is a high salt and high amino acid medium. Increased salt concentrations may compete for binding sites on microbial cells (Bellamy *et al.*, 1992). This may explain the lack of antifungal activity of Os in RPMI-1640 against *C. albicans* biofilms. The activity of Os(11-22)NH_2 appears to be less affected by salt, and thus Os(11-22)NH_2 retains its antifungal activity in RPMI-1640 against *C. albicans* biofilms, suggesting other interactions besides electrostatic interactions may be involved. The smaller peptide is amidated, known to increase peptide stability towards proteolytic degradation (Kim & Seong, 2001) and associated increased helix stability at the plasma membrane results in enhanced activity (Mura *et al.*, 2016).

To evaluate the anti-biofilm activity of Os, AmpB was used as a control. AmpB is the first significant and most effective antifungal agent available (Gallis *et al.*, 1990). The BIC_{50} determined using the CTB assay was 0.28 ± 0.03 µM (Figure 3.4) which was comparable to the reported BIC_{50} of 0.32 µM (Chiramba, 2018). In this study, Os was found to possess anti-biofilm activity, with maximum activity at higher concentrations. Os exhibited anti-biofilm activity against *C. albicans* biofilms, characterized by a BIC_{50} of 46 µM (Figure 3.5). A possible explanation for the profile of the Os curve, is the barrel-stave model of AMP membrane interaction. In this model, a certain threshold concentration of AMPs is required before the AMPs insert themselves into the membrane and exert their effect (Nguyen *et al.*, 2011). As such, at lower Os concentrations, the peptides are aggregating on the membrane surface, exerting a minimal effect, and once the peptides have reached their threshold concentration, they are able to exert their effect, displaying a steep gradient as indicated in Figure 3.5.

Previously, Os(11-22)NH_2 was investigated for its ability to inhibit *C. albicans* biofilm formation, and a BIC_{50} of 81 µM was reported (Chiramba, 2018) (Table 3.2). Since ergosterol is constitutively expressed, AmpB displays anti-planktonic and anti-biofilm activity. The fact that Os only has anti-biofilm activity, suggests that perhaps Os has a target specific for biofilms, other than the plasma membrane as is the case for planktonic *C. albicans* cells. Other peptides have also been found to possess only anti-biofilm activity against *C. albicans*, including the human cathelicidn LL-37, which has almost no activity against planktonic *P. aeruginosa*, with mostly biofilm targeted activity (Andrea *et al.*, 2018). Based on the concentration required to inhibit biofilm formation, peptides can be divided into two groups (Batoni *et al.*, 2016). The first group includes peptides with anti-biofilm activity at concentrations equal to or higher than the MIC against planktonic cells. These peptides inhibit biofilm formation by killing planktonic biofilm forming cells as well as cells detaching from the biofilm. Os(11-22)NH_2 had a BIC_{50} approximately 2 fold higher than the MIC_{50}. The higher proportion of planktonic cells in Os(11-22)NH_2 treated biofilms (Figure 3.6) suggests that this peptide was targeting the planktonic cells and inhibiting the formation of hyphae, and subsequently biofilm development. In contrast, peptides with anti-biofilm

activity at concentrations lower than the MIC, including the LL-37 peptide, displayed anti-biofilm activity through gene dysregulation involved in biofilm formation (Overhage *et al.*, 2008). Other peptides that fall within this class displayed anti-biofilm activity by interfering with the expression of the extracellular polysaccharide-intercellular-adhesion (PIA) synthesis genes (Zhu *et al.*, 2013), direct interaction with intracellular nucleotide ppGpp (De la Fuente-Núñez *et al.*, 2014) and targeting intracellular nucleotides guanosine pentaphosphate (p) ppGpp (de la Fuente-Núñez *et al.*, 2015). Most of these targets appear to be intracellular. Os displayed no anti-planktonic activity at the tested concentrations with only anti-biofilm activity, suggesting that Os may fall within the second class of peptides.

AFPs have different modes of action, including ROS production, membrane permeabilisation, inhibition of nucleic acid and protein synthesis, inhibition of cell wall synthesis, and apoptosis to name a few (Bondaryk *et al.*, 2017). As ROS formation and membrane acting effects are the most common modes of action, these effects of Os were compared to Os(11-22)NH_2.

Free radicals derived from oxygen (ROS), form in the mitochondria under normal physiological conditions, contributing to important cellular processes. However, increased ROS may adversely affect cell macromolecules, leading to cellular damage or death (Mesa-Arango *et al.*, 2014). ROS include peroxides, superoxides and hydroxyl radicals. In *C. albicans* there are 6 superoxide dismutase (SOD) enzymes located within the cytoplasm, mitochondria and cell surface (Frohner *et al.*, 2009) that convert superoxides into unreactive species containing oxygen. Certain antifungal agents, are known to induce the production of ROS in susceptible fungi, including the azole miconazole, inducing ROS production in planktonic and sessile cells (Francois *et al.*, 2006), through the inhibition of enzymes responsible for the breakdown of peroxide radicals (Francois *et al.*, 2006). In contrast, the azole fluconazole has been reported not to induce ROS production within *C. albicans* (Bink *et al.*, 2011). Various peptides have also been shown to induce ROS production. Plant defensins *Pv*D1 and *Rs*AFP2 have both been shown to inhibit *C. albicans* through ROS production (Neves de Medeiros *et al.*, 2014) and Aerts *et al.* (2007). In this study, in order to establish whether Os lead to the production of ROS within *C. albicans* biofilms, the DCFH-DA assay was used. Os(11-22)NH_2 was previously shown to induce ROS production within *C. albicans* biofilms (Chiramba, 2018). Therefore, Os(11-22)NH_2 was used as the positive control in this assay. Treatment of *C. albicans* biofilms with Os(11-22)NH_2 and Os led to a significant increase in the production of ROS, compared to the untreated growth control (Figure 3.7). In order to link ROS production to killing as a mode of action, the inhibitory activity of Os in the presence of AA was further investigated (Figure 3.8). In the presence of AA, Os retained antifungal activity, indicating that this peptide does produce ROS in *C. albicans* biofilms, but that this is not the mode of killing. Furthermore, it was found that AA potentiates the antifungal activity of Os (Figure 3.8). AA has previously been shown to potentiate the effects of AmpB on *C. albicans* (Ojha *et al.*, 2009). Although AA is a known antioxidant, many of its other functions remain unclear (Ojha *et al.*, 2009). One study found that in *C. albicans*, AA binds $Fe^{3+,}$ enhancing the yeasts sensitivity to antifungal agents, since Fe^{3+} homeostasis is important for fungal survival (Li *et al.*, 2018).

The plasma membrane of *C. albicans* is an important location for many reactions (Prasad, 1991), as well as an important interface between the yeast and its host. The lipid bilayer making up the membrane contains important proteins mediating various functions within the cell. Enzymes involved in cell wall synthesis are located within the membrane. A previous study aimed to employ various strategies, in order to obtain the largest number of plasma membranes proteins and GPI-anchored membrane proteins of *C. albicans*. Bioinformatic analysis of this particular study found that most of the identified plasma proteins were involved in biopolymer synthesis or transport processes. Furthermore, the GPI-anchored proteins were determined to be involved in β-(1,3)-glucan synthesis and virulence factors (Cabezon *et al.*, 2009). The plasma membrane is a major target for some conventional antifungal agents, as well as various AFPs. Host defence peptide C4 causes membrane permeabilisation in *C. albicans (*Menzel *et al.,* 2017*).* Plant defensin HsAFP1 in combination with CAS caused membrane permeabilisation in *C. albicans* (Cools *et al.*, 2017). Likewise, in comparison to Os(11-22)NH_2, this study aimed to determine whether the antimicrobial peptide Os targets the plasma membrane of *C. albicans*. Triton-X 100 was used as a detergent control. As Triton-X 100 (0.0001%) was found to inhibit growth of *C. albicans* biofilms grown in RPMI-1640 for 24h (data not shown) biofilms were exposed to Triton-X 100 (1%) for only 30 minutes (Figure 3.9). In the untreated biofilms, only nuclear staining with DAPI was detected, indicating no membrane permeabilisation. Triton-X 100 (1%) treated biofilms displayed a high intensity PI fluorescence, due to DNA and RNA binding indicating membrane permeabilisation. The ability of Os(11-22)NH_2 to cause membrane permeabilsation has previously been confirmed (Chiramba, 2018). In Os treated biofilms, only DAPI fluorescence is visible, indicating lack of membrane permeabilisation indicating a mode of action different from Os(11-22)NH_2.

In order to determine whether Os enters *C. albicans* biofilm cells, biofilms were treated with 5FAM labelled Os, and subsequently visualised using CLSM (Figure 3.10). As a control 5FAM-penetratin a known cell-penetrating peptide (CPP) was used. CPPs are a class of peptides, capable of crossing cellular membranes (Nielsen *et al.*, 2015). CPPs are also known to transport cargo such as proteins and nucleic acids into living cells, and thus serve as good candidates for drug delivery vehicles (Gong & Karlsson, 2017). Certain bioactive compounds have already been successfully conjugated to CPPs, and transported intracellularly. Studies involving CPPs and *C. albicans* are limited, with penetratin only being tested on planktonic *C. albicans* cells. Only a single study could be found that investigated the translocation of 1 µM to 50 µM 5FAM-penetratin into planktonic *C. albicans* cells (Gong & Karlsson, 2017). The antifungal activity of penetratin against planktonic *C. albicans* cells, was investigated using a concentration range of 12.5 µM to 200 µM (Masman *et al.*, 2009). Concentrations of 25 µM and above caused > 90% inhibition of biofilm formation. Therefore, in this study 5FAM-penetratin was initially tested at concentrations of 1 µM, 10 µM and 25 µM (data not shown). 5FAM-penetratin (10 µM) was chosen as the control, as 1 µM showed no translocation and 25 µM appeared to inhibit biofilm formation. Biofilms treated with 5FAM-penetratin displayed green fluorescence of all cells. In contrast, biofilms treated with 5FAM-Os(11-22)NH_2 showed fluorescence along the circumference of most cells (Figure

3.11) indicating that Os(11-22)NH_2 binds or acts on the plasma membrane of *C. albicans* during biofilm inhibition. Furthermore, 5FAM-Os(11-22)NH_2 treated biofilms displayed little to no intensity in planktonic and pseudohyphal cells (Figure 3.11). In contrast, biofilms treated with 5FAM-Os displayed more intense intracellular staining (Figure 3.11) and the observed fluorescence appears to be localised within the yeast and pseudohyphal cells, and along the cell wall or plasma membranes of long hyphal cells (Figure 3.11). Moreover, 5FAM-Os treated biofilms appear to have intracellular targets in the long hyphal cells (Figure 3.11). Taute *et al.* (2015) have shown that Os binds plasmid DNA and therefore in an intracellular environment, may also bind DNA. Indications are that both peptides to different degrees bind to the plasma membrane and then accumulate intracellularly or target intracellular organelles or macromolecules. Permeabilisation, allows large macromolecules to freely move across the cell wall, however processes that involve active uptake will result in the intracellular accumulation, and more intense staining as was observed for Os.

The mode of action of Os is not due to ROS formation or membrane permeabilisation, although Os does translocate into the cytoplasm of *C. albicans* cells in biofilms. Electron microscopy, can provide detailed information on the effects of peptides on cell morphology and can be used to identify potential targets and may also provide a better understanding on the mode of action. Crystal violet and SEM analysis were used to observe changes to the overall biofilm morphology after treatment with Os. Os(11-22)NH_2 was used for comparison in order to elucidate the mode of action of Os. In Os(11-22)NH_2 treated biofilms, a higher proportion of yeast cells are visible (Figure 3.6 and Figure 3.13) with little effect on hyphal cells (Figure 3.13). This indicates that Os(11-22)NH_2 potentially targets the yeast cells, inhibiting the transition from yeast to hyphal cells with minimal effect on the hyphal cells. On the other hand, Os treated biofilms have relatively fewer yeast cells (Figure 3.6 and Figure 3.13) with a clear change in hyphal structure (Figure 3.13). This indicates a different mode of action of Os, with Os affecting hyphal cells.

AFPs can target different *C. albicans* cell types based on the composition of the cell wall and plasma membrane (Table 1.1). Therefore, the yeast cells, pseudohyphae and hyphae may differ in their susceptibility to the effects of Os and Os(11-22)NH_2.

Using SEM the various cell types that occur within a *C. albicans* biofilm were identified (Figure 3.12). *C. albicans* begins as round/ovoid yeast cells, and the subsequent outgrowth of a germ tube allows for the formation of tubular pseudohyphal cells. Cells within this germ tube undergo mitosis, without cell separation, in order to form elongated hyphae.

In this study SEM was also used to investigate possible changes to *C. albicans* cell surface, after treatment with Os and Os(11-22)NH_2. Untreated yeast cells showed a smooth cell surface (Figure 3.14), while Os(11-22)NH_2 and Os treated yeast cells showed surface changes (Figure 3.15). Both peptides appeared to cause cell shrinkage. Other studies suggest that this wrinkled and shrivelled appearance

is due to membrane disruption and further cell collapse (Leng *et al.*, 2017). Results from this study indicate that Os(11-22)NH_2 causes membrane permeabilisation, and could thus be a cause of the observed cell collapse. However, Os displayed no membrane permeabilisation, but is able to translocate into cells suggesting that changes to the cell surface could be a secondary effect. Surface indentations were only observed in Os(11-22)NH_2 treated cells (Figure 3.15 A – B), while surface cracks or tears were only observed in Os treated cells (Figure 3.15 D and F). Cracks on of *Candida* yeast cell surfaces have been previously observed, and were described resulting from the disruption of membrane integrity (Setiawati *et al.*, 2017). Previous studies on *C. albicans* cells described the cracks as slits/ruptures, and as a result of both cell wall and membrane damage (Xiong *et al.*, 2010). Therefore, Os may cause cell surface changes to the yeast cells of *C. albicans* biofilms.

The effect of Os on pseudohyphal cells was also observed. Untreated pseudohyphal cells appeared smooth and tubular (Figure 3.14). Similarly, a wrinkled and shrivelled appearance was also shown (Figure 3.16) for pseudohyphal treated cells. Cellular debris among the cells was observed with SEM. This debris could possibly be the intracellular contents from cells with compromised or collapsed membranes. In comparison to untreated pseudohyphal cells, it can be concluded that Os has an effect on the pseudohyphal cells of *C. albicans* biofilms.

Lastly, untreated hyphal cells appear smooth and elongated cells (Figure 3.14), whereas, Os(11-22)NH_2 appears to have minimal to no effect on *C. albicans* hyphae (Figure 3.17 A - C). This observation is further supported by Figure 3.13 where the hyphae appear smooth and elongated, similar to the untreated hyphae. Moreover, a higher proportion of yeast cells appear to be present in the Os(11-22)NH_2 treated biofilms (Figure 3.13). This further indicates that Os(11-22)NH_2 not only targets the non-hyphal cells, but is potentially affecting the yeast to hyphal transition. As a result those cells affected by the peptide were prevented from transitioning to hyphae, and thus more yeast cells are present. This is an important observation, since one of the main virulence determinants of *C. albicans*, is its ability to undergo a dimorphic switch, from the yeast to the hyphal phase. On the other hand Os appears to have a clear effect on the cell surface of hyphal cells (Figure 3.17 D - F). Roughening of the surface (Figure 3.17 D) and the formation of surface protuberances or blebs were observed (Figure 3.18 E). Previously, 5 cathelicidin peptides were investigated for their fungicidal effect on planktonic *C. albicans* cells (Benincasa *et al.*, 2006), with similar SEM observations being made. This study stated that the observations were consistent with a cell membrane targeting mode of action, with the various changes to membrane morphology, merely being different consequences of membrane damage. Once again, surface cracks/slits were observed in Os treated hyphae (Figure 3.17 D - F), indicating cell wall or plasma membrane damage.

CHAPTER 5: Conclusions and Future Perspectives

This study aimed to determine the mode of action of Os on *C. albicans* biofilm formation. A summary of the main findings is presented in Table 5.1.

Table 5.1: Summary of the main findings of this study

Os		Summary of observed effects
ANTIFUNGAL ACTIVITY		
Planktonic	x	No activity at the tested concentrations
Biofilm	✓	BIC_{50} = 46 µM, with maximum activity at higher concentrations
MODE OF ACTION		
ROS mediated killing	x	No ROS killing, killing enhanced with AA
Membrane permeabilisation	x	No observed PI staining
Intracellular localisation and targets	✓	Cell wall or plasma membrane, possible nuclear DNA binding and accumulation
Changes to yeast ultrastructure	✓	Cell shrinkage and plasma membrane/cell wall cracks or tears
Changes to pseudohyphal ultrastructure	✓	Cell shrinkage and formation of pits
Changes to hyphal ultrastructure	✓	Cracks or tears and surface protuberances

✓ Effect observed, x effect not observed

Os displayed no activity against planktonic *C. albicans* cells, but retained the ability to inhibit biofilm formation in the presence of RPMI-1640, indicating this peptides sensitivity to high salt environments. Although the inhibition of biofilm formation is of value, clinically the eradication of mature biofilms is of the utmost importance and thus the ability of Os to eradicate mature biofilms, as described by Troskie *et al.* (2014) should be investigated in future studies.

Os targets the growth and development of adhered cells. The presence of pseudohyphal cells in the CV images of biofilms treated with Os indicate that this peptide possibly impairs the development of hyphae which is essential for the development of candidemia where the hyphae penetrates surrounding membranes and tissues (Koh *et al.*, 2008). In a more detailed study the effects of Os on the growth and development of *C. albicans* hyphal cells should be investigated, focussing on the effects on hyphal wall protein 1 (Hwp1), and agglutin-like sequence 3 (Als3) expression. This can be achieved with using real-time PCR as described by Nailis *et al.* (2010).

Os induced ROS is not the mode of action, although Os did increase ROS production in *C. albicans* biofilms. AA treatment did not decrease Os biofilm inhibition, but rather increased biofilm inhibition, a phenomenon which has previously been observed in tyrocidine AFPs (Troskie *et al.*, 2014). AA has

previously also been shown to potentiate the effects of AmpB on *C. albicans* (Ojha *et al.*, 2009). Combination studies could therefore be conducted to fully determine the effect of AA on peptide activity. Assays such as the checkerboard assay, as described by Vriens *et al.* (2015) could determine the type of interaction, if any between Os and AA. In addition, AA binds Fe^{3+} and this comprises haemostasis, possibly making *C. albicans* more susceptible to the effects of AFPs such as Os and Os(11-22)NH_2 (Li *et al.*, 2018). This is an important aspect to investigate further, as AFPs are expensive to synthesise, and synergistic effects will reduce the required concentration for biofilm inhibition.

The mode of action identified for certain tyrocidines, was not ROS production, but as a result of osmotic stress or from the binding to GlcCer lipid rafts within fungal membranes, including plant defensin *Pv*D1, which resulted in the disarrangement of the plasma membrane (Neves de Medeiros *et al.*, 2014). As such, Os induced ROS may also be as a result of lipid binding within *C. albicans* plasma membrane, and may explain any observed morphological defects with *C. albicans* cell structure. Therefore, it is important to determine whether Os binds to lipids within *C. albicans* plasma membrane. Previously, AMP-lipid binding was investigated using surface pressure measurements, neutron reflectivity and external reflection-fourier transform infrared spectroscopy respectively (Lad *et al.*, 2007). The AMPs mellitin, magainin and cecropin P1 were all shown to bind various lipids, and may be used as positive controls for such techniques.

Os does not inhibit biofilm formation through membrane permeabilisation, notwithstanding the cell wall is a major target for AFPs. The chitin binding AFP NP-1 has been shown to induce various morphological defects (Cabib & Arroyo, 2013) as well as a loss of membrane integrity (Endo *et al.*, 1997) without causing membrane permeabilisation. Therefore, it will be necessary to investigate the effect of Os on cell wall components, which may explain any observed morphological defects within *C. albicans* cell structure. In order to determine whether Os interacts with the cell wall, the effect of representative fungal cell wall polysaccharides, such as laminarin and mannan on the anti-biofilm activity of Os could be investigated, as described by Wang *et al.* (2015).

Fungal membranes contain various membrane proteins, and the ability of Os to bind the most common of these proteins, including the GPI-anchored proteins, can be evaluated using a sub-proteomic approach to obtain an overview of the protein composition of *C. albicans* plasma membrane. Protein extraction methods include formation of *C. albicans* protoplast, mechanical disruption, and ultracentrifugation in sucrose gradients to name a few (Moreau, 1987). Moreover, to get a better understanding of the direct effect of Os on the plasma membrane and its ability to affect membrane integrity, model membranes including liposomes could be utilised (Lee *et al.*, 2003).

Os enters *C. albicans* biofilm cells without compromising the integrity of the cell wall or plasma membrane, while increased intracellular localisation is observed. Uptake of AFPs can be through active transport such as endocytosis, as has been observed for plant defensin NaD1 (Hayes *et al.*, 2018) and

can be investigated using 5FAM-Os, sodium azide (inhibits production of ATP synthesis) and evaluated using CLSM.

5FAM-Os does appear to bind intracellular targets. Future research should focus on the more specific identification of these targets. To achieve this 5FAM-Os and CLSM could be further employed in conjunction with dyes targeting specific organelles, including MitoTracker for the mitochondria and Cell Tracker Blue for vacuoles, since these organelles have been known to be targeted by various AFPs. Previously, *C. albicans* co-incubated with low concentrations of the peptide FAM labelled pVEC bound to the yeast vacuole stain Cell Tracker Blue, displayed co-localisation. However, at higher peptide concentrations the vacuoles had disappeared with the peptide fluorescence located within the cytoplasm (Gong & Karlsson, 2017), possibly indicating membrane targeting effects. Thus, CLSM will provide a better understanding of the relationship between Os and *C. albicans* organelles.

SEM was used to observe ultrastructural changes to *C. albicans* after treatment with Os. This study focussed on the different cell types found in the *C. albicans* biofilms. Os treatment caused cell shrinkage, and cracks to cell surfaces as a result of membrane disruption. Moreover, cellular debris surrounding the cells was observed, indicating potential leakage of intracellular contents. All the observed effects may be either due to the direct effects of the peptides or a secondary effects due to the disruption of cellular pathways. To determine if this is a primary or secondary effect, Au labelled peptides with transmission electron microscopy (TEM) can be used to localise the labelled Os, where a primary target will be the cell wall and secondary targets will be intracellular organelles and associated biochemical pathways (De Alteriis *et al.*, 2018).

CHAPTER 6: References

Abbott, J. 1995. Clinical and microscopic diagnosis of vaginal yeast infection: a prospective analysis. *Annals of Emergency Medicine,* 25(5):587-591.

Aerts, A.M., François, I.E., Meert, E.M., Li, Q.-T., Cammue, B.P. & Thevissen, K. 2007. The antifungal activity of RsAFP2, a plant defensin from Raphanus sativus, involves the induction of reactive oxygen species in *Candida albicans*. *Journal of Molecular Microbiology and Biotechnology,* 13(4):243-247.

Alberts, B., Johnson, A., Lewis, J., Walter, P., Raff, M. & Roberts, K. 2002. *Molecular Biology of the Cell 4th Edition: International Student Edition*.

Andes, D.R., Safdar, N., Baddley, J.W., Playford, G., Reboli, A.C., Rex, J.H., Sobel, J.D., Pappas, P.G. & Kullberg, B.J. 2012. Impact of treatment strategy on outcomes in patients with candidemia and other forms of invasive candidiasis: a patient-level quantitative review of randomized trials. *Clinical Infectious Diseases,* 54(8):1110-1122.

Andrea, A., Molchanova, N. & Jenssen, H. 2018. Antibiofilm peptides and peptidomimetics with focus on surface immobilization. *Biomolecules,* 8(2):27.

Andrews, J.M. 2001. Determination of minimum inhibitory concentrations. *Journal of Aantimicrobial Chemotherapy,* 48(suppl 1):5-16.

Bahar, A.A. & Ren, D. 2013. Antimicrobial peptides. *Pharmaceuticals,* 6(12):1543-1575.

Barker, K.S. & Rogers, P.D. 2006. Recent insights into the mechanisms of antifungal resistance. *Current Infectious Disease Reports,* 8(6):449-456.

Batoni, G., Maisetta, G. & Esin, S. 2016. Antimicrobial peptides and their interaction with biofilms of medically relevant bacteria. *Biochimica et Biophysica Acta (BBA)-Biomembranes,* 1858(5):1044-1060.

Bellamy, W., Takase, M., Wakabayashi, H., Kawase, K. & Tomita, M. 1992. Antibacterial spectrum of lactoferricin B, a potent bactericidal peptide derived from the N-terminal region of bovine lactoferrin. *Journal of Applied Bacteriology,* 73(6):472-479.

Benincasa, M., Scocchi, M., Pacor, S., Tossi, A., Nobili, D., Basaglia, G., Busetti, M. & Gennaro, R. 2006. Fungicidal activity of five cathelicidin peptides against clinically isolated yeasts. *Journal of Antimicrobial Chemotherapy,* 58(5):950-959.

Bink, A., Vandenbosch, D., Coenye, T., Nelis, H., Cammue, B.P. & Thevissen, K. 2011. Superoxide dismutases are involved in *Candida albicans* biofilm persistence to miconazole. *Antimicrobial Agents and Chemotherapy*:AAC. 00280-00211.

Bondaryk, M., Staniszewska, M., Zielińska, P. & Urbańczyk-Lipkowska, Z. 2017. Natural antimicrobial peptides as inspiration for design of a new generation antifungal compounds. *Journal of Fungi,* 3(3):46.

Buranasompob, A. 2005. Kinetics of the inactivation of microorganisms by water insoluble polymers with antimicrobial activity./handle/11303/1346.

Cabezon, V., Llama-Palacios, A., Nombela, C., Monteoliva, L. & Gil, C. 2009. Analysis of *Candida albicans* plasma membrane proteome. *Proteomics,* 9(20):4770-4786.

Cabib, E. & Arroyo, J. 2013. How carbohydrates sculpt cells: chemical control of morphogenesis in the yeast cell wall. *Nature Reviews Microbiology,* 11(9):648.

Cannon, R.D., Lamping, E., Holmes, A.R., Niimi, K., Baret, P.V., Keniya, M.V., Tanabe, K., Niimi, M., Goffeau, A. & Monk, B.C. 2009. Efflux-mediated antifungal drug resistance. *Clinical Microbiology Reviews,* 22(2):291-321.

Carter, M. 2015. *Guide to research techniques in neuroscience.* Academic Press.

Chandra, J., Kuhn, D.M., Mukherjee, P.K., Hoyer, L.L., Mccormick, T. & Ghannoum, M.A. 2001. Biofilm formation by the fungal pathogen *Candida albicans*: development, architecture, and drug resistance. *Journal of Bacteriology,* 183(18):5385-5394.

Chen, S.C. & Sorrell, T.C. 2007. Antifungal agents. *Medical Journal of Australia,* 187(7):404.

Chiramba. 2018. *Anti-biofilm activity of the tick derived antimicrobial peptide Os(11-22)NH_2 against Candida albicans (ATCC 90028).* University of Pretoria

Cimpan, M.R., Matre, R., Skaug, N., Lie, S.A. & Lygre, H. 2005. The coinitiator DMABEE induces death by apoptosis and necrosis in human monoblastoid cells. *Clinical Oral Investigations,* 9(3):168-172.

Cools, T.L., Struyfs, C., Drijfhout, J.W., Kucharíková, S., Lobo Romero, C., Van Dijck, P., Ramada, M.H., Bloch Jr, C., Cammue, B. & Thevissen, K. 2017. A linear 19-mer plant defensin-derived peptide acts synergistically with caspofungin against *Candida albicans* biofilms. *Frontiers in Microbiology,* 8:2051.

Coste, A.T. 2015. *Antifungals.* Caister Academic Press.

Daum, G., Lees, N.D., Bard, M. & Dickson, R. 1998. Biochemistry, cell biology and molecular biology of lipids of *Saccharomyces cerevisiae*. *Yeast,* 14(16):1471-1510.

De Alteriis, E., Maselli, V., Falanga, A., Galdiero, S., Di Lella, F.M., Gesuele, R., Guida, M. & Galdiero, E. 2018. Efficiency of gold nanoparticles coated with the antimicrobial peptide indolicidin against biofilm formation and development of *Candida* spp. clinical isolates. *Infection and Drug Resistance,* 11:915.

De Brucker, K., Delattin, N., Robijns, S., Steenackers, H., Verstraeten, N., Landuyt, B., Luyten, W., Schoofs, L., Dovgan, B. & Fröhlich, M. 2014. Derivatives of the mouse cathelicidin-related antimicrobial peptide (CRAMP) inhibit fungal and bacterial biofilm formation. *Antimicrobial Agents and Chemotherapy,* 58(9):5395-5404.

De La Fuente-Núñez, C., Reffuveille, F., Haney, E.F., Straus, S.K. & Hancock, R.E. 2014. Broad-spectrum anti-biofilm peptide that targets a cellular stress response. *PLoS Pathogens,* 10(5):e1004152.

De La Fuente-Núñez, C., Reffuveille, F., Mansour, S.C., Reckseidler-Zenteno, S.L., Hernández, D., Brackman, G., Coenye, T. & Hancock, R.E. 2015. D-enantiomeric peptides that eradicate wild-type and multidrug-resistant biofilms and protect against lethal *Pseudomonas aeruginosa* infections. *Chemistry & Biology,* 22(2):196-205.

De Lucca, A., Bland, J., Jacks, T., Grimm, C. & Walsh, T. 1998. Fungicidal and binding properties of the natural peptides cecropin B and dermaseptin. *Medical Mycology,* 36(5):291-298.

De Lucca, A.J. & Walsh, T.J. 1999. Antifungal peptides: novel therapeutic compounds against emerging pathogens. *Antimicrobial Agents and Chemotherapy,* 43(1):1-11.

De Pauw, B., Walsh, T.J., Donnelly, J.P., Stevens, D.A., Edwards, J.E., Calandra, T., Pappas, P.G., Maertens, J., Lortholary, O. & Kauffman, C.A. 2008. Revised definitions of invasive fungal disease from the European organization for research and treatment of cancer/invasive fungal infections cooperative group and the national institute of allergy and infectious diseases mycoses study group (EORTC/MSG) consensus group. *Clinical Infectious Diseases,* 46(12):1813-1821.

Delattin, N., De Brucker, K., Craik, D.J., Cheneval, O., Fröhlich, M., Veber, M., Girandon, L., Davis, T.R., Weeks, A.E. & Kumamoto, C.A. 2014. Plant-derived decapeptide OSIP108 interferes with *Candida albicans* biofilm formation without affecting cell viability. *Antimicrobial Agents and Chemotherapy,* 58(5):2647-2656.

Den Hertog, A.L., Van Marle, J., Bolscher, J.G., Veerman, E.C. & Arie, V. 2005. Candidacidal effects of two antimicrobial peptides: histatin 5 causes small membrane defects, but LL-37 causes massive disruption of the cell membrane. *Biochemical Journal,* 388(2):689-695.

Desai, J.V. 2018. *Candida albicans* Hyphae: From Growth Initiation to Invasion. *Journal of Fungi,* 4(1):10.

Dixon, D.M. & Walsh, T.J. 1996. Antifungal agents.

Dos Santos Abrantes, P.M., Mcarthur, C.P. & Africa, C.W.J. 2014. Multi-drug resistant oral *Candida* species isolated from HIV-positive patients in South Africa and Cameroon. *Diagnostic Microbiology and Infectious Disease,* 79(2):222-227.

Douglas, L.J. 2003. *Candida* biofilms and their role in infection. *Trends in Microbiology,* 11(1):30-36.

Endo, M., Takesako, K., Kato, I. & Yamaguchi, H. 1997. Fungicidal action of aureobasidin A, a cyclic depsipeptide antifungal antibiotic, against *Saccharomyces cerevisiae*. *Antimicrobial Agents and Chemotherapy,* 41(3):672-676.

Fesel, P.H. & Zuccaro, A. 2016. β-glucan: Crucial component of the fungal cell wall and elusive MAMP in plants. *Fungal Genetics and Biology,* 90:53-60.

Fesharaki, S.H., Aghili, S.R., Shokohi, T. & Boroumand, M.A. 2018. Catheter-related candidemia and identification of causative *Candida* species in patients with cardiovascular disorder. *Current Medical Mycology,* 4(2):7.

Finkel, J.S. & Mitchell, A.P. 2011. Genetic control of *Candida albicans* biofilm development. *Nature Reviews Microbiology,* 9(2):109.

Fox, E.P. & Nobile, C.J. 2013. The role of *Candida albicans* biofilms in human disease. *Candida albicans Symptoms, Causes and Treatment Options. Nova Science Publishers*:1-24.

Fox, E.P., Singh-Babak, S.D., Hartooni, N. & Nobile, C.J. 2015. Biofilms and antifungal resistance. *Antifungals: From Genomics to Resistance and the Development of Novel Agents; Caister Academic Press: Poole, UK*:71-90.

Francois, I.E., Cammue, B., Borgers, M., Ausma, J., Dispersyn, G.D. & Thevissen, K. 2006. Azoles: mode of antifungal action and resistance development. Effect of miconazole on endogenous reactive oxygen species production in *Candida albicans*. *Anti-Infective Agents in Medicinal Chemistry (Formerly Current Medicinal Chemistry-Anti-Infective Agents),* 5(1):3-13.

Frohner, I.E., Bourgeois, C., Yatsyk, K., Majer, O. & Kuchler, K. 2009. *Candida albicans* cell surface superoxide dismutases degrade host-derived reactive oxygen species to escape innate immune surveillance. *Molecular Microbiology,* 71(1):240-252.

Gallis, H.A., Drew, R.H. & Pickard, W.W. 1990. Amphotericin B: 30 years of clinical experience. *Reviews of Infectious Diseases,* 12(2):308-329.

Georgopapadakou, N.H. & Walsh, T.J. 1996. Antifungal agents: chemotherapeutic targets and immunologic strategies. *Antimicrobial Agents and Chemotherapy,* 40(2):279.

Ghannoum, M.A. & Elewski, B. 1999. Successful treatment of fluconazole-resistant oropharyngeal candidiasis by a combination of fluconazole and terbinafine. *Clinical and Diagnostic Laboratory Immunology,* 6(6):921-923.

Ghannoum, M.A. & Rice, L.B. 1999. Antifungal agents: mode of action, mechanisms of resistance, and correlation of these mechanisms with bacterial resistance. *Clinical Microbiology Reviews,* 12(4):501-517.

Gong, Z. & Karlsson, A.J. 2017. Translocation of cell-penetrating peptides into *Candida* fungal pathogens. *Protein Science,* 26(9):1714-1725.

Gonzalez, R. & Tarloff, J. 2001. Evaluation of hepatic subcellular fractions for Alamar blue and MTT reductase activity. *Toxicology In Vitro,* 15(3):257-259.

Granger, B.L. 2012. Insight into the antiadhesive effect of yeast wall protein 1 of *Candida albicans*. *Eukaryotic Cell,* 11(6):795-805.

Groll, A.H. & Walsh, T.J. 2001. Caspofungin: pharmacology, safety and therapeutic potential in superficial and invasive fungal infections. *Expert Opinion on Investigational Drugs,* 10(8):1545-1558.

Grover, N.D. 2010. Echinocandins: A ray of hope in antifungal drug therapy. *Indian Journal of Pharmacology,* 42(1):9.

Gulati, M. & Nobile, C.J. 2016. *Candida albicans* biofilms: development, regulation, and molecular mechanisms. *Microbes and Infection,* 18(5):310-321.

Hall-Stoodley, L., Costerton, J.W. & Stoodley, P. 2004. Bacterial biofilms: from the natural environment to infectious diseases. *Nature Reviews Microbiology,* 2(2):95.

Halliwell, B. & Gutteridge, J.M. 2015. *Free Radicals in Biology and Medicine.* Oxford University Press, USA.

Hancock, R.E. 2001. Cationic peptides: effectors in innate immunity and novel antimicrobials. *The Lancet Infectious Diseases,* 1(3):156-164.

Hartung, R. 1987. Dose—Response Relationships. *Toxic Substances and Human Risk*: Springer.

Hayes, B., Bleackley, M., Anderson, M. & Van Der Weerden, N. 2018. The plant defensin NaD1 enters the cytoplasm of *Candida albicans* via endocytosis. *Journal of Fungi,* 4(1):20.

Hobson, R. 2003. The global epidemiology of invasive *Candida* infections—is the tide turning? *Journal of Hospital Infection,* 55(3):159-168.

Hsieh, M.H., Chen, M.Y., Victor, L.Y. & Chow, J.W. 1993. Synergy assessed by checkerboard a critical analysis. *Diagnostic Microbiology and Infectious Disease,* 16(4):343-349.

Hwang, P.M. & Vogel, H.J. 1998. Structure-function relationships of antimicrobial peptides. *Biochemistry and Cell Biology,* 76(2-3):235-246.

Ishitsuka, Y., Pham, D.S., Waring, A.J., Lehrer, R.I. & Lee, K.Y.C. 2006. Insertion selectivity of antimicrobial peptide protegrin-1 into lipid monolayers: effect of head group electrostatics and tail group packing. *Biochimica et Biophysica Acta (BBA)-Biomembranes,* 1758(9):1450-1460.

Jacobsen, I.D., Wilson, D., Wächtler, B., Brunke, S., Naglik, J.R. & Hube, B. 2012. *Candida albicans* dimorphism as a therapeutic target. *Expert Review of Anti-Infective Therapy,* 10(1):85-93.

John, H., Maronde, E., Forssmann, W., Meyer, M. & Adermann, K. 2008. N-terminal acetylation protects glucagon-like peptide GLP-1-(7-34)-amide from DPP-IV-mediated degradation retaining cAMP-and insulin-releasing capacity. *European Journal of Medical Research,* 13(2):73.

Kathiravan, M.K., Salake, A.B., Chothe, A.S., Dudhe, P.B., Watode, R.P., Mukta, M.S. & Gadhwe, S. 2012. The biology and chemistry of antifungal agents: a review. *Bioorganic & Medicinal Chemistry,* 20(19):5678-5698.

Kelly, J. & Kavanagh, K. 2011. Caspofungin primes the immune response of the larvae of Galleria mellonella and induces a non-specific antimicrobial response. *Journal of Medical Microbiology,* 60(2):189-196.

Khaksa, G., D'souza, R., Lewis, S. & Udupa, N. 2000. Pharmacokinetic study of niosome encapsulated insulin.

Kim, K.-H. & Seong, B.L. 2001. Peptide amidation: Production of peptide hormones *in vivo* and *in vitro*. *Biotechnology and Bioprocess Engineering,* 6(4):244-251.

Koh, A.Y., Köhler, J.R., Coggshall, K.T., Van Rooijen, N. & Pier, G.B. 2008. Mucosal damage and neutropenia are required for *Candida albicans* dissemination. *PLoS Pathogens,* 4(2):e35.

Kojic, E.M. & Darouiche, R.O. 2004. *Candida* infections of medical devices. *Clinical Microbiology Reviews,* 17(2):255-267.

Koltin, Y. & Hitchcock, C.A. 1997. The search for new triazole antifungal agents. *Current Opinion in Chemical Biology,* 1(2):176-182.

Koo, H.B. & Seo, J. 2019. Antimicrobial peptides under clinical investigation. *Peptide Science*:e24122.

Lad, M.D., Birembaut, F., Clifton, L.A., Frazier, R.A., Webster, J.R. & Green, R.J. 2007. Antimicrobial peptide-lipid binding interactions and binding selectivity. *Biophysical Journal,* 92(10):3575-3586.

Lamichhane, T.N., Abeydeera, N.D., Duc, A.-C.E., Cunningham, P.R. & Chow, C.S. 2011. Selection of peptides targeting helix 31 of bacterial 16S ribosomal RNA by screening M13 phage-display libraries. *Molecules,* 16(2):1211-1239.

Landini, P., Antoniani, D., Burgess, J.G. & Nijland, R. 2010. Molecular mechanisms of compounds affecting bacterial biofilm formation and dispersal. *Applied Microbiology and Biotechnology,* 86(3):813-823.

Lau, J.L. & Dunn, M.K. 2018. Therapeutic peptides: Historical perspectives, current development trends, and future directions. *Bioorganic & Medicinal Chemistry,* 26(10):2700-2707.

Laupland, K.B., Gregson, D.B., Church, D.L., Ross, T. & Elsayed, S. 2005. Invasive *Candida* species infections: a 5 year population-based assessment. *Journal of Antimicrobial Chemotherapy,* 56(3):532-537.

Lee, D.G., Kim, H.K., Am Kim, S., Park, Y., Park, S.-C., Jang, S.-H. & Hahm, K.-S. 2003. Fungicidal effect of indolicidin and its interaction with phospholipid membranes. *Biochemical and Biophysical Research Communications,* 305(2):305-310.

Lee, S., Pagoria, D., Raigrodski, A. & Geurtsen, W. 2007. Effects of combinations of ROS scavengers on oxidative DNA damage caused by visible-light-activated camphorquinone/N, N-dimethyl-p-toluidine. *Journal of Biomedical Materials Research Part B: Applied Biomaterials: An Official Journal of The Society for Biomaterials, The Japanese Society for Biomaterials, and The Australian Society for Biomaterials and the Korean Society for Biomaterials,* 83(2):391-399.

Leng, K.M., Vijayarathna, S., Jothy, S.L., Sasidharan, S. & Kanwar, J.R. 2017. *In vitro* and *in vivo* anticandidal activities of alginate-enclosed chitosan–calcium phosphate-loaded Fe-bovine lactoferrin nanocapsules. *Future Science OA,* 4(2):FSO257.

Levitz, S.M., Selsted, M.E., Ganz, T., Lehrer, R.I. & Diamond, R.D. 1986. In vitro killing of spores and hyphae of *Aspergillus fumigatus* and *Rhizopus oryzae* by rabbit neutrophil cationic peptides and bronchoalveolar macrophages. *Journal of Infectious Diseases,* 154(3):483-489.

Lewis, K. 2010. Persister cells. *Annual review of microbiology,* 64:357-372.

Li, J. & Wang, N. 2011. Genome-wide mutagenesis of Xanthomonas axonopodis pv. citri reveals novel genetic determinants and regulation mechanisms of biofilm formation. *PLoS One,* 6(7):e21804.

Li, X.S., Reddy, M.S., Baev, D. & Edgerton, M. 2003. *Candida albicans* Ssa1/2p is the cell envelope binding protein for human salivary histatin 5. *Journal of Biological Chemistry,* 278(31):28553-28561.

Li, Y., Sun, L., Lu, C., Gong, Y., Li, M. & Sun, S. 2018. Promising antifungal targets against *Candida albicans* based on ion homeostasis. *Frontiers in Cellular and Infection Microbiology,* 8.

Lupetti, A., Danesi, R., Campa, M., Del Tacca, M. & Kelly, S. 2002. Molecular basis of resistance to azole antifungals. *Trends in Molecular Medicine,* 8(2):76-81.

Madani, F., Lindberg, S., Langel, Ü., Futaki, S. & Gräslund, A. 2011. Mechanisms of cellular uptake of cell-penetrating peptides. *Journal of Biophysics,* 2011.

Marr, A.K., Gooderham, W.J. & Hancock, R.E. 2006. Antibacterial peptides for therapeutic use: obstacles and realistic outlook. *Current Opinion in Pharmacology,* 6(5):468-472.

Masman, M.F., Rodríguez, A.M., Raimondi, M., Zacchino, S.A., Luiten, P.G., Somlai, C., Kortvelyesi, T., Penke, B. & Enriz, R.D. 2009. Penetratin and derivatives acting as antifungal agents. *European Journal of Medicinal Chemistry,* 44(1):212-228.

Matejuk, A., Leng, Q., Begum, M., Woodle, M., Scaria, P., Chou, S. & Mixson, A. 2010. Peptide-based antifungal therapies against emerging infections. *Drugs of the Future,* 35(3):197.

Matsuzaki, K., Harada, M., Funakoshi, S., Fujii, N. & Miyajima, K. 1991. Physicochemical determinants for the interactions of magainins 1 and 2 with acidic lipid bilayers. *Biochimica et Biophysica Acta (BBA)-Biomembranes,* 1063(1):162-170.

Mbuayama. 2016. *Antifungal properties of peptides derived from a defensin from the tick Ornithodoros savignyi.* University of Pretoria

Menzel, L.P., Chowdhury, H.M., Masso-Silva, J.A., Ruddick, W., Falkovsky, K., Vorona, R., Malsbary, A., Cherabuddi, K., Ryan, L.K. & Difranco, K.M. 2017. Potent in vitro and in vivo antifungal activity of a small molecule host defense peptide mimic through a membrane-active mechanism. *Scientific Reports,* 7(1):4353.

Mesa-Arango, A.C., Trevijano-Contador, N., Román, E., Sánchez-Fresneda, R., Casas, C., Herrero, E., Argüelles, J.C., Pla, J., Cuenca-Estrella, M. & Zaragoza, O. 2014. The production of reactive oxygen species is an universal action mechanism of Amphotericin B against pathogenic yeasts and contributes to the fungicidal effect of this drug: AMPHORES study. *Antimicrobial Agents and Chemotherapy*:AAC. 03570-03514.

Moreau, R.A. 1987. Calcium-binding proteins in fungi and higher plants. *Journal of Dairy Science,* 70(7):1504-1512.

Morici, P., Fais, R., Rizzato, C., Tavanti, A. & Lupetti, A. 2016. Inhibition of *Candida albicans* biofilm formation by the synthetic lactoferricin derived peptide hLF1-11. *PloS One,* 11(11):e0167470.

Munro, C.A. 2013. Chitin and glucan, the yin and yang of the fungal cell wall, implications for antifungal drug discovery and therapy. *Advances in Applied Microbiology*: Elsevier.

Mura, M., Wang, J., Zhou, Y., Pinna, M., Zvelindovsky, A.V., Dennison, S.R. & Phoenix, D.A. 2016. The effect of amidation on the behaviour of antimicrobial peptides. *European Biophysics Journal,* 45(3):195-207.

Mwiria. 2017. *Activity of tick antimicrobial peptides against Candida albicans biofilms.* University of Pretoria

Nailis, H., Kucharíková, S., Řičicová, M., Van Dijck, P., Deforce, D., Nelis, H. & Coenye, T. 2010. Real-time PCR expression profiling of genes encoding potential virulence factors in *Candida albicans* biofilms: identification of model-dependent and-independent gene expression. *BMC Microbiology,* 10(1):114.

Nes, W.R. 1974. Role of sterols in membranes. *Lipids,* 9(8):596-612.

Nett, J., Lincoln, L., Marchillo, K., Massey, R., Holoyda, K., Hoff, B., Vanhandel, M. & Andes, D. 2007. Putative role of β-1, 3 glucans in *Candida albicans* biofilm resistance. *Antimicrobial Agents and Chemotherapy,* 51(2):510-520.

Nett, J.E., Zarnowski, R., Cabezas-Olcoz, J., Brooks, E.G., Bernhardt, J., Marchillo, K., Mosher, D.F. & Andes, D.R. 2015. Host contributions to construction of three device-associated *Candida albicans* biofilms. *Infection and Immunity,* 83(12):4630-4638.

Neves De Medeiros, L., Domitrovic, T., Cavalcante De Andrade, P., Faria, J., Barreto Bergter, E., Weissmüller, G. & Kurtenbach, E. 2014. Psd1 binding affinity toward fungal membrane components as assessed by SPR: the role of glucosylceramide in fungal recognition and entry. *Peptide Science,* 102(6):456-464.

Nguyen, L.T., Haney, E.F. & Vogel, H.J. 2011. The expanding scope of antimicrobial peptide structures and their modes of action. *Trends in Biotechnology,* 29(9):464-472.

Nguyen, M.H., Peacock Jr, J.E. & Morris, J. 1995. Therapeutic Approaches in Patients. *Arch Intern Med,* 155:2429-2435.

Nielsen, E.J.B., Kamei, N. & Takeda-Morishita, M. 2015. Safety of the cell-penetrating peptide penetratin as an oral absorption enhancer. *Biological and Pharmaceutical Bulletin,* 38(1):144-146.

Niimi, K., Maki, K., Ikeda, F., Holmes, A., Lamping, E., Niimi, M., Monk, B. & Cannon, R. 2006. Overexpression of *Candida albicans* CDR1, CDR2, or MDR1 does not produce significant changes in echinocandin susceptibility. *Antimicrobial Agents and Chemotherapy,* 50(4):1148-1155.

Nobile, C.J. & Johnson, A.D. 2015. Candida albicans biofilms and human disease. *Annual Review of Microbiology,* 69:71-92.

Obiero, C.W., Seale, A.C. & Berkley, J.A. 2015. Empiric treatment of neonatal sepsis in developing countries. *The Pediatric Infectious Disease Journal,* 34(6):659-661.

Ojha, R., Manzoor, N. & Khan, L. 2009. Ascorbic acid modulates pathogenecity markers of *Candida albicans. International Journal of Microbiology Research,* 1(1):19.

Oren, Z. & Shai, Y. 1997. Selective lysis of bacteria but not mammalian cells by diastereomers of melittin: structure–function study. *Biochemistry,* 36(7):1826-1835.

Overhage, J., Campisano, A., Bains, M., Torfs, E.C., Rehm, B.H. & Hancock, R.E. 2008. Human host defense peptide LL-37 prevents bacterial biofilm formation. *Infection and Immunity,* 76(9):4176-4182.

Owotade, F.J., Patel, M., Ralephenya, T.R. & Vergotine, G. 2013. Oral *Candida* colonization in HIV-positive women: associated factors and changes following antiretroviral therapy. *Journal of Medical Microbiology,* 62(1):126-132.

Payne, J.A., Bleackley, M.R., Lee, T.-H., Shafee, T.M., Poon, I.K., Hulett, M.D., Aguilar, M.-I., Van Der Weerden, N.L. & Anderson, M.A. 2016. The plant defensin NaD1 introduces membrane disorder through a specific interaction with the lipid, phosphatidylinositol 4, 5 bisphosphate. *Biochimica et Biophysica Acta (BBA)-Biomembranes,* 1858(6):1099-1109.

Perlin, D.S. 2015. *Antifungals: from genomics to resistance and the development of novel agents*.

Peters, B.M., Shirtliff, M.E. & Jabra-Rizk, M.A. 2010. Antimicrobial peptides: primeval molecules or future drugs? *PLoS Pathogens,* 6(10):e1001067.

Pfaller, M. & Diekema, D. 2007. Epidemiology of invasive candidiasis: a persistent public health problem. *Clinical Microbiology Reviews,* 20(1):133-163.

Pierce, C.G., Vila, T., Romo, J.A., Montelongo-Jauregui, D., Wall, G., Ramasubramanian, A. & Lopez-Ribot, J.L. 2017. The *Candida albicans* Biofilm matrix: Composition, structure and function. *Journal of Fungi,* 3(1):14.

Powers, J.-P.S. & Hancock, R.E. 2003. The relationship between peptide structure and antibacterial activity. *Peptides,* 24(11):1681-1691.

Prasad, R. 1991. The plasma membrane of *Candida albicans*: its relevance to transport phenomenon. *Candida albicans*: Springer.

Prasad, R. & Rawal, M.K. 2014. Efflux pump proteins in antifungal resistance. *Frontiers in Pharmacology,* 5:202.

Prinsloo. 2013. *Structural and functional characterization of peptides derived from the carboxy-terminal region of a defensin from the tick Ornithodoros savignyi.* University of Pretoria.

Ramage, G., Saville, S.P., Thomas, D.P. & Lopez-Ribot, J.L. 2005. *Candida* biofilms: an update. *Eukaryotic Cell,* 4(4):633-638.

Rautenbach, M., Troskie, A.M. & Vosloo, J.A. 2016a. Antifungal peptides: to be or not to be membrane active. *Biochimie,* 130:132-145.

Rautenbach, M., Troskie, A.M., Vosloo, J.A. & Dathe, M.E. 2016b. Antifungal membranolytic activity of the tyrocidines against filamentous plant fungi. *Biochimie,* 130:122-131.

Rella, A., Farnoud, A.M. & Del Poeta, M. 2016. Plasma membrane lipids and their role in fungal virulence. *Progress in Lipid Research,* 61:63-72.

Riquelme, M., Aguirre, J., Bartnicki-García, S., Braus, G.H., Feldbrügge, M., Fleig, U., Hansberg, W., Herrera-Estrella, A., Kämper, J. & Kück, U. 2018. Fungal morphogenesis, from the polarized growth of hyphae to complex reproduction and infection structures. *Microbiol. Mol. Biol. Rev.,* 82(2):e00068-00017.

Rodriguez-Tudela, J., Arendrup, M., Barchiesi, F., Bille, J., Chryssanthou, E., Cuenca-Estrella, M., Dannaoui, E., Denning, D., Donnelly, J. & Dromer, F. 2008. EUCAST Definitive Document EDef 7.1: method for the determination of broth dilution MICs of antifungal agents for fermentative yeasts: Subcommittee on Antifungal Susceptibility Testing (AFST) of the ESCMID European Committee for Antimicrobial Susceptibility Testing (EUCAST)∗. *Clinical Microbiology and Infection,* 14(4):398-405.

Roper, M., Ellison, C., Taylor, J.W. & Glass, N.L. 2011. Nuclear and genome dynamics in multinucleate ascomycete fungi. *Current Biology,* 21(18):R786-R793.

Roscetto, E., Contursi, P., Vollaro, A., Fusco, S., Notomista, E. & Catania, M.R. 2018. Antifungal and anti-biofilm activity of the first cryptic antimicrobial peptide from an archaeal protein against *Candida* spp. clinical isolates. *Scientific Reports,* 8(1):17570.

Sandai, D., Tabana, Y.M., El Ouweini, A. & Ayodeji, I.O. 2016. Resistance of *Candida albicans* biofilms to drugs and the host immune system. *Jundishapur Journal of Microbiology,* 9(11).

Sardi, J., Scorzoni, L., Bernardi, T., Fusco-Almeida, A. & Giannini, M.M. 2013a. *Candida* species: current epidemiology, pathogenicity, biofilm formation, natural antifungal products and new therapeutic options. *Journal of Medical Microbiology,* 62(1):10-24.

Sardi, J.D.C.O., Pitangui, N.D.S., Gullo, F.P., Almeida, A.M.F. & Mendes-Giannini, M.J.S. 2013b. A mini review of *Candida* species in hospital infection: epidemiology, virulence factor and drugs resistance and prophylaxis. *Tropical Medicine & Surgery*:1-7.

Schwartz, I.S., Boyles, T.H., Kenyon, C.R., Hoving, J.C., Brown, G.D. & Denning, D.W. 2019. The estimated burden of fungal disease in South Africa. *SAMJ: South African Medical Journal,* 109(11):885-892.

Seo, M.-D., Won, H.-S., Kim, J.-H., Mishig-Ochir, T. & Lee, B.-J. 2012. Antimicrobial peptides for therapeutic applications: a review. *Molecules,* 17(10):12276-12286.

Setiawati, S., Nuryastuti, T., Ngatidjan, N., Mustofa, M., Jumina, J. & Fitriastuti, D. 2017. In vitro antifungal activity of (1)-N-2-Methoxybenzyl-1, 10-phenanthrolinium Bromide against *Candida albicans* and its effects on membrane integrity. *Mycobiology,* 45(1):25-30.

Sevcsik, E., Pabst, G., Jilek, A. & Lohner, K. 2007. How lipids influence the mode of action of membrane-active peptides. *Biochimica et Biophysica Acta (BBA)-Biomembranes,* 1768(10):2586-2595.

Sheehan, D.J., Hitchcock, C.A. & Sibley, C.M. 1999. Current and emerging azole antifungal agents. *Clinical Microbiology Reviews,* 12(1):40-79.

Sood, R., Domanov, Y., Pietiäinen, M., Kontinen, V.P. & Kinnunen, P.K. 2008. Binding of LL-37 to model biomembranes: insight into target vs host cell recognition. *Biochimica et Biophysica Acta (BBA)-Biomembranes,* 1778(4):983-996.

Srinivasan, A., Lopez-Ribot, J.L. & Ramasubramanian, A.K. 2014. Overcoming antifungal resistance. *Drug Discovery Today: Technologies,* 11:65-71.

Steinberg, D.A. & Lehrer, R.I. 1997. Designer assays for antimicrobial peptides: disputing the “one-size-fits-all” theory. *Antibacterial Peptide Protocols*:169-186.

Sudbery, P.E. 2008. Regulation of polarised growth in fungi. *Fungal Biology Reviews,* 22(2):44-55.

Sudbery, P.E. 2011. Growth of *Candida albicans* hyphae. *Nature Reviews Microbiology,* 9(10):737.

Taff, H.T., Mitchell, K.F., Edward, J.A. & Andes, D.R. 2013. Mechanisms of *Candida* biofilm drug resistance. *Future Microbiology,* 8(10):1325-1337.

Tanious, F.A., Veal, J.M., Buczak, H., Ratmeyer, L.S. & Wilson, W.D. 1992. DAPI (4', 6-diamidino-2-phenylindole) binds differently to DNA and RNA: minor-groove binding at AT sites and intercalation at AU sites. *Biochemistry,* 31(12):3103-3112.

Taute, H., Bester, M.J., Neitz, A.W. & Gaspar, A.R. 2015. Investigation into the mechanism of action of the antimicrobial peptides Os and Os-C derived from a tick defensin. *Peptides,* 71:179-187.

Thevissen, K., Terras, F.R. & Broekaert, W.F. 1999. Permeabilization of fungal membranes by plant defensins inhibits fungal growth. *Appl. Environ. Microbiol.,* 65(12):5451-5458.

Thevissen, K., Warnecke, D.C., François, I.E., Leipelt, M., Heinz, E., Ott, C., Zähringer, U., Thomma, B.P., Ferket, K.K. & Cammue, B.P. 2004. Defensins from insects and plants interact with fungal glucosylceramides. *Journal of Biological Chemistry,* 279(6):3900-3905.

Thomma, B.P., Cammue, B.P. & Thevissen, K. 2003. Mode of action of plant defensins suggests therapeutic potential. *Current Drug Targets-Infectious Disorders,* 3(1):1-8.

Tonk, M., Cabezas-Cruz, A., Valdés, J.J., Rego, R.O., Grubhoffer, L., Estrada-Pena, A., Vilcinskas, A., Kotsyfakis, M. & Rahnamaeian, M. 2015. Ixodes ricinus defensins attack distantly-related pathogens. *Developmental & Comparative Immunology,* 53(2):358-365.

Troskie, A.M., Rautenbach, M., Delattin, N., Vosloo, J.A., Dathe, M., Cammue, B.P. & Thevissen, K. 2014. Synergistic activity of the tyrocidines, antimicrobial cyclodecapeptides from Bacillus aneurinolyticus, with amphotericin B and caspofungin against *Candida albicans* biofilms. *Antimicrobial Agents and Chemotherapy,* 58(7):3697-3707.

Uppuluri, P., Chaturvedi, A.K., Srinivasan, A., Banerjee, M., Ramasubramaniam, A.K., Köhler, J.R., Kadosh, D. & Lopez-Ribot, J.L. 2010. Dispersion as an important step in the *Candida albicans* biofilm developmental cycle. *PLoS Pathogens,* 6(3):e1000828.

Van Der Weerden, N.L., Hancock, R.E. & Anderson, M.A. 2010. Permeabilization of fungal hyphae by the plant defensin NaD1 occurs through a cell wall-dependent process. *Journal of Biological Chemistry,* 285(48):37513-37520.

Vandeputte, P., Ferrari, S. & Coste, A.T. 2011. Antifungal resistance and new strategies to control fungal infections. *International Journal of Microbiology,* 2012.

Varki, A., Cummings, R.D., Esko, J.D., Freeze, H.H., Stanley, P., Bertozzi, C.R., Hart, G.W. & Etzler, M.E. 2009. Study Guide.

Vediyappan, G., Rossignol, T. & D'enfert, C. 2010. Interaction of *Candida albicans* biofilms with antifungals: transcriptional response and binding of antifungals to beta-glucans. *Antimicrobial Agents and Chemotherapy,* 54(5):2096-2111.

Vriens, K., Cools, T.L., Harvey, P.J., Craik, D.J., Spincemaille, P., Cassiman, D., Braem, A., Vleugels, J., Nibbering, P.H. & Drijfhout, J.W. 2015. Synergistic activity of the plant defensin HsAFP1 and caspofungin against *Candida albicans* biofilms and planktonic cultures. *PLoS One,* 10(8):e0132701.

Wang, K., Dang, W., Xie, J., Zhu, R., Sun, M., Jia, F., Zhao, Y., An, X., Qiu, S. & Li, X. 2015. Antimicrobial peptide protonectin disturbs the membrane integrity and induces ROS production in yeast cells. *Biochimica et Biophysica Acta (BBA)-Biomembranes,* 1848(10):2365-2373.

Webber, M. & Piddock, L. 2003. The importance of efflux pumps in bacterial antibiotic resistance. *Journal of Antimicrobial Chemotherapy,* 51(1):9-11.

Winter, J. & Wenghoefer, M. 2012. Human defensins: potential tools for clinical applications. *Polymers,* 4(1):691-709.

Xiong, Z., Lu, X., Feng, A., Pan, Y. & Ostrikov, K. 2010. Highly effective fungal inactivation in He+ O 2 atmospheric-pressure non equilibrium plasmas. *Physics of Plasmas,* 17(12):123502.

Yeaman, M.R. & Yount, N.Y. 2003. Mechanisms of antimicrobial peptide action and resistance. *Pharmacological Reviews,* 55(1):27-55.

Zarnowski, R., Westler, W.M., Lacmbouh, G.A., Marita, J.M., Bothe, J.R., Bernhardt, J., Sahraoui, A.L.-H., Fontaine, J., Sanchez, H. & Hatfield, R.D. 2014. Novel entries in a fungal biofilm matrix encyclopedia. *MBio,* 5(4):e01333-01314.

Zhu, C., Tan, H., Cheng, T., Shen, H., Shao, J., Guo, Y., Shi, S. & Zhang, X. 2013. Human β-defensin 3 inhibits antibiotic-resistant Staphylococcus biofilm formation. *Journal of Surgical Research,* 183(1):204-213.

Zhu, F.-Y., Wang, Q.-Q., Zhang, X.-S., Hu, W., Zhao, X. & Zhang, H.-X. 2014. 3D nanostructure reconstruction based on the SEM imaging principle, and applications. *Nanotechnology,* 25(18):185705.

Zimmer, E.A. & Roalson, E. 2005. *Molecular Evolution, Producing the Biochemical Data.* Elsevier.